The Abdus Salam International Centre for Theoretical Physics

United Nations Educational, Scientific and Cultural Organization

IAEA International Atomic Energy Agency

1936-47

Advanced School on Synchrotron and Free Electron Laser Sources and their Multidisciplinary Applications

7 - 25 April 2008

Two-colour and photon correlation spectroscopy

Fulvio Parmigiani
University of Trieste & Sincrotrone Trieste

Strada Costiera 11, 34014 Trieste, Italy - Tel. +39 040 2240 111; Fax +39 040 224 163 - sci_info@ictp.it, www.ictp.it

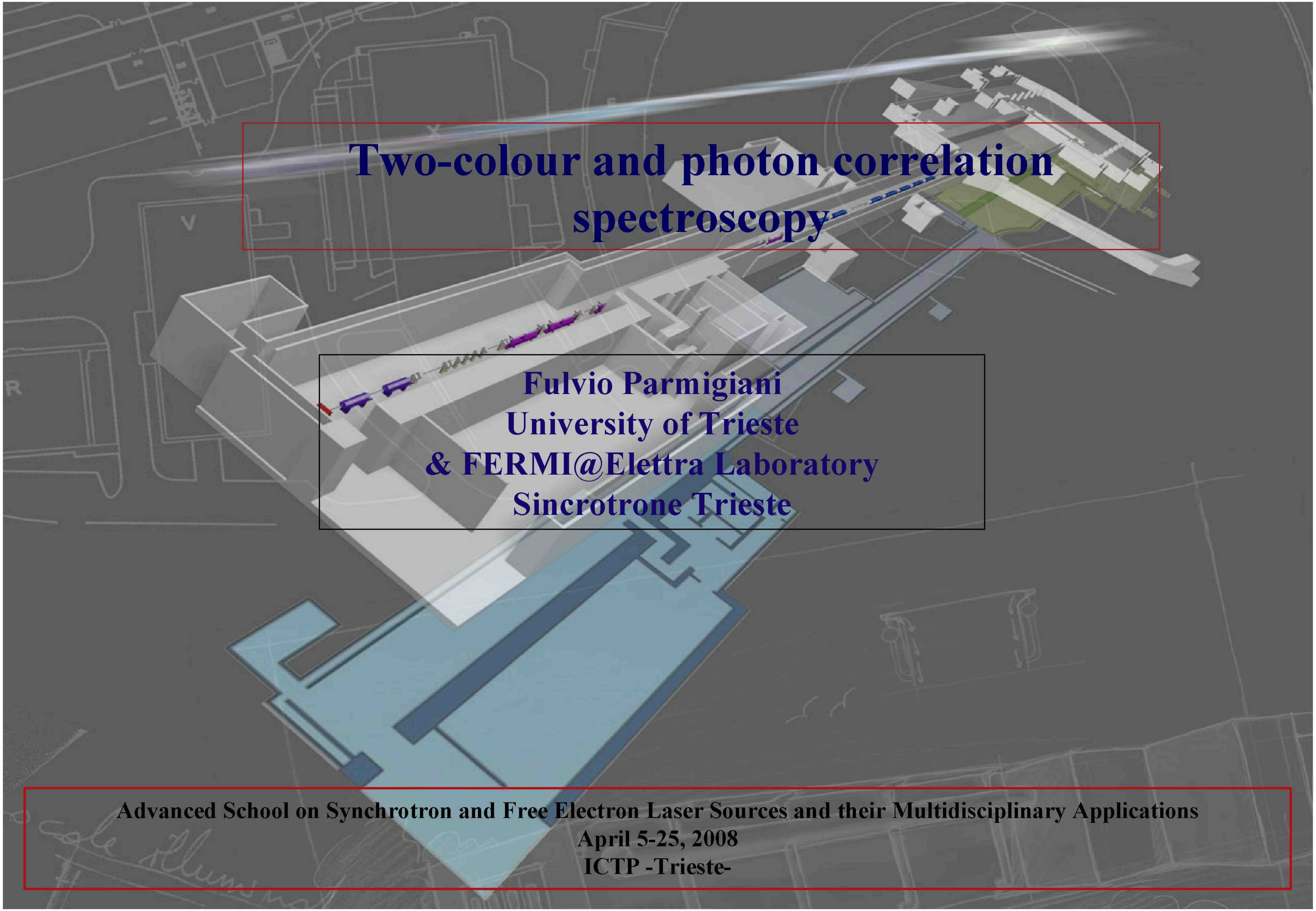

Two-colour and photon correlation spectroscopy

Fulvio Parmigiani
University of Trieste
& FERMI@Elettra Laboratory
Sincrotrone Trieste

Advanced School on Synchrotron and Free Electron Laser Sources and their Multidisciplinary Applications
April 5-25, 2008
ICTP -Trieste-

The VUV, XUV, and soft x-ray regions

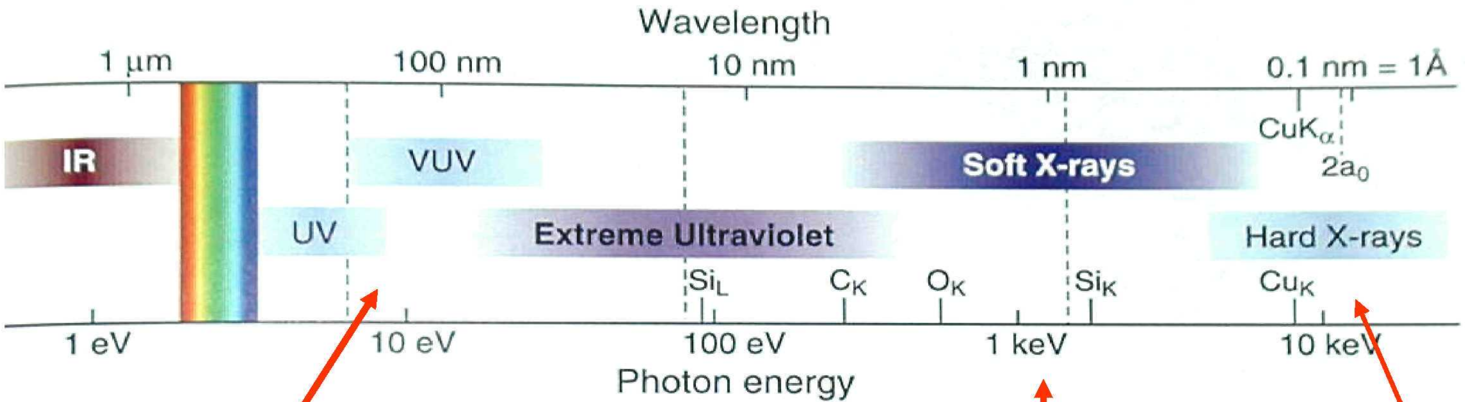

Vacuum-ultraviolet (VUV)
180 nm > l > 50 nm

Absorbed by <<1 mm of air

Ionizing to many materials

Soft x-rays
5 nm > l > 0.5 nm

Strongly interacts with *core electrons* in materials

Extreme-ultraviolet (XUV)
50 nm > l > 5 nm

Ionizing radiation to *all* materials

Hard x-ray

0.5nm> λ> 0.05nm

Scattering from *the lattice* ions

Main parameters to be considered in radiation-matter interaction

- e.m field magnitude (linear processes vs.non-linear)
- time structure of the e.m. field (dynamics)
- transversal and longitudinal coherence (very high resolution spectroscopy and scattering)
- state of polarization (dichroic effects)

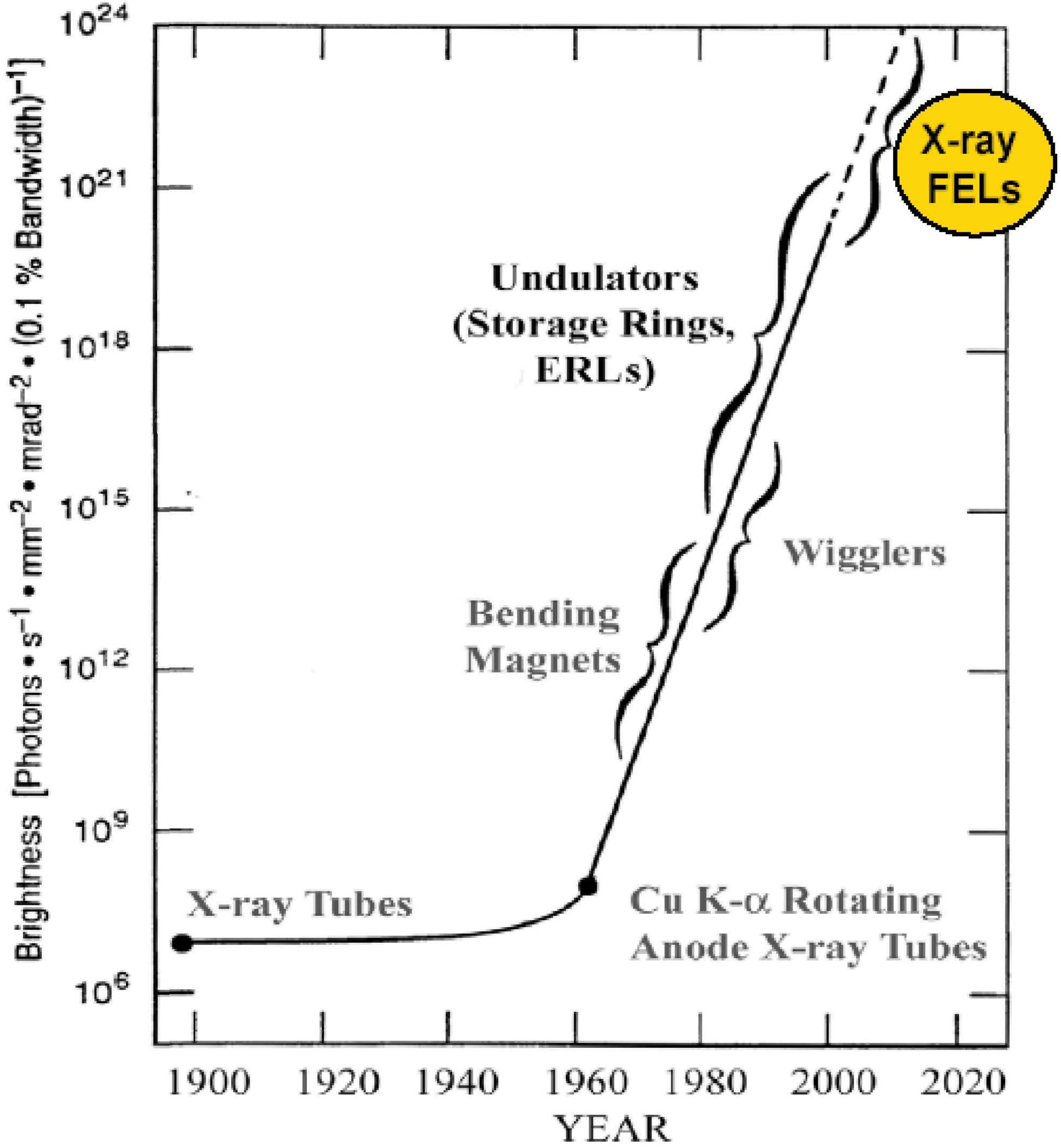

Brightness [Photons • s^{-1} • mm^{-2} • mrad^{-2} • (0.1 % Bandwidth)$^{-1}$]
10^{24}
10^{21}
10^{18}
10^{15}
10^{12}
10^{9}
10^{6}
X-ray FELs
Undulators (Storage Rings, ERLs)
Wigglers
Bending Magnets
X-ray Tubes
Cu K-α Rotating Anode X-ray Tubes
1900
1920
1940
1960
1980
2000
2020
YEAR

- Hot Dense Matter occurs in:
  - Supernova, stellar interiors, accretion disks
  - Plasma devices: laser produced plasmas, Z-pinches
  - Directly driven inertial fusion plasma

- Warm Dense Matter occurs in:
  - Cores of large planets
  - Systems that start solid and end as a plasma
  - X-ray driven inertial fusion implosion

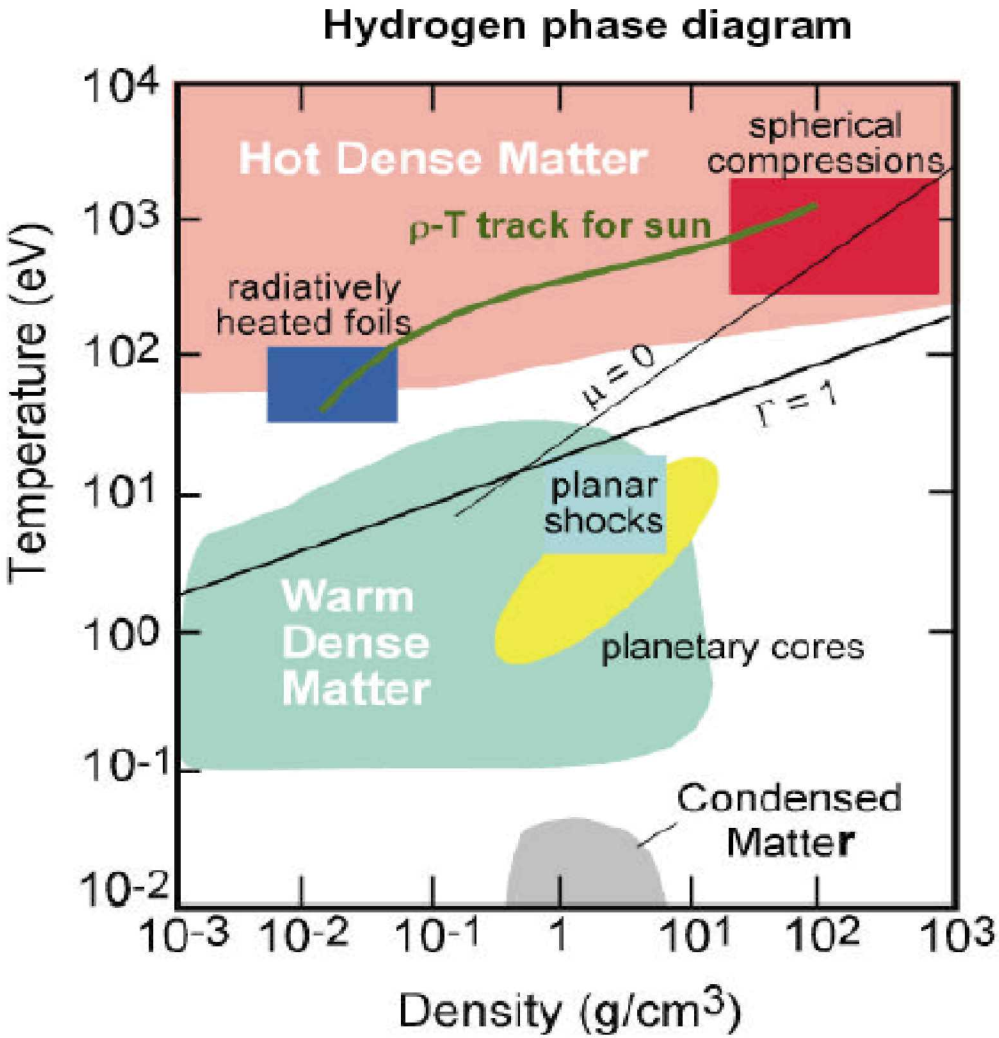

R.W. Lee, LLNL

1. Boiling the Vacuum with Lasers

- **Spontaneous pair creation from vacuum**, induced by an **external field**, was first proposed in the context of e^+e^- **pair creation in static, spatially uniform electric field** [Sauter (1931); Heisenberg,Euler (1936); Schwinger (1951); . . .]

  One of the most intriguing non-linear phenomena in quantum field theory
  - Theoretically important: beyond perturbation theory
  - Eventual experimental observation: probes theory in domain of very strong fields

- Mechanism applied to many problems in contemporary physics:
  - Quantum evaporation of black holes [Hawking (1975); Damour,Ruffini (1976); . . .]
  - e^+e^- creation in vicinity of charged black holes [Damour,Ruffini '75; . . .]
  - Particle production in early universe [Parker (1969); . . .]
  - Particle production in hadronic collisions [Casher, Neuberger, Nussinov (1979); . . .]

Fast phenomena in matter

Time domain scale:

ps (10^{-12} s) *collective processes (ordering) in condensed matter (dynamics of the magnetic* moment...)

fs (10^{-15} s) *phase transitions and VB electron dymanics*

as (10^{-18} s) *electronic dynamics in atoms and molecules*

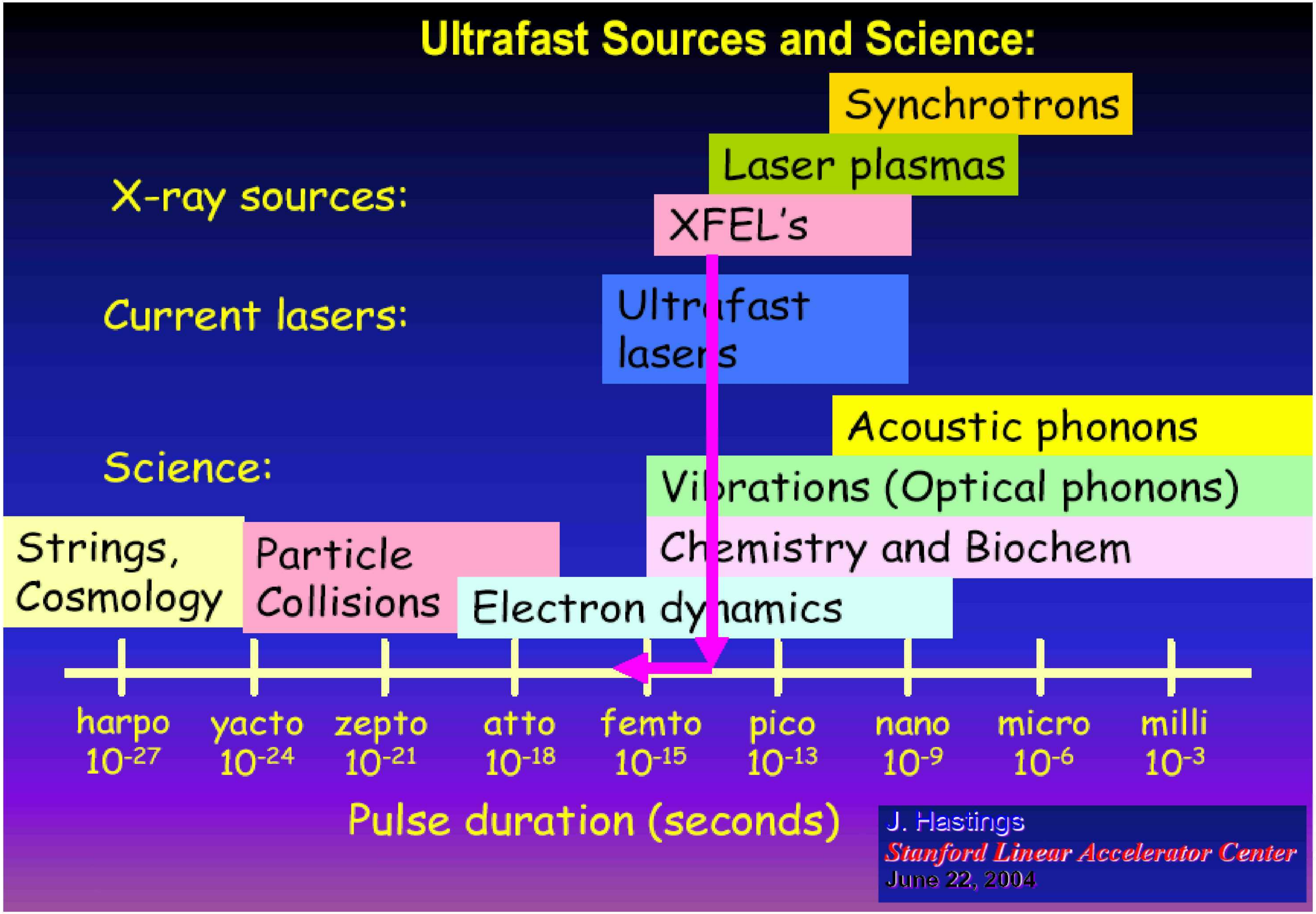

Ultrafast Sources and Science:
Synchrotrons
Laser plasmas
X-ray sources:
XFEL's
Current lasers:
Ultrafast lasers
Acoustic phonons
Science:
Vibrations (Optical phonons)
Chemistry and Biochem
Strings, Cosmology
Particle Collisions
Electron dynamics
harpo 10-27
yacto 10-24
zepto 10-21
atto 10-18
femto 10-15
pico 10-13
nano 10-9
micro 10-6
milli 10-3
Pulse duration (seconds)
J. Hastings
Stanford Linear Accelerator Center
June 22, 2004

Time scales

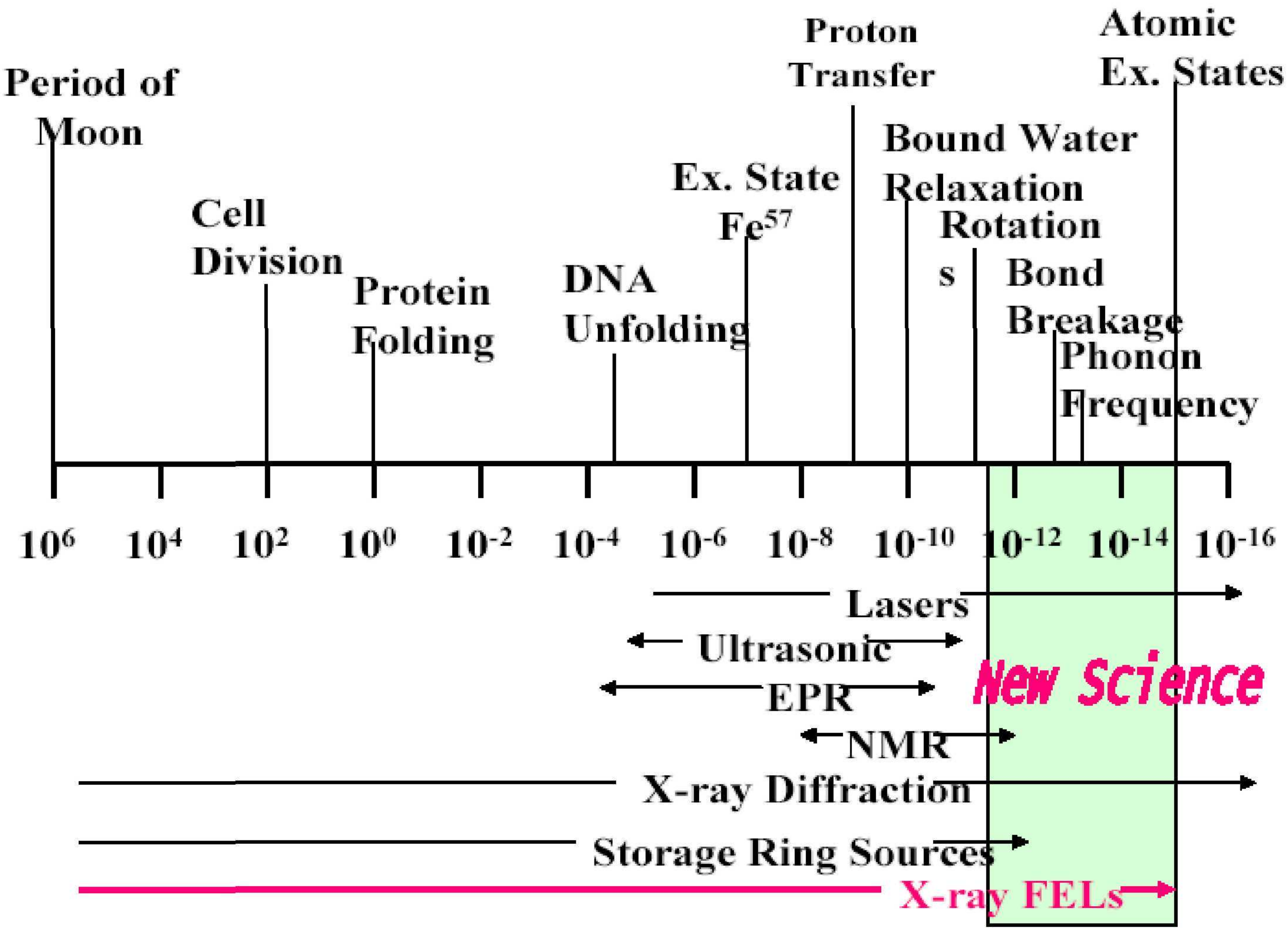

Period of Moon
Cell Division
Protein Folding
DNA Unfolding
Ex. State Fe57
Proton Transfer
Bound Water Relaxation
Rotations
Bond Breakage
Phonon Frequency
Atomic Ex. States
10^6 10^4 10^2 10^0 10^-2 10^-4 10^-6 10^-8 10^-10 10^-12 10^-14 10^-16
Lasers
Ultrasonic
EPR
NMR
X-ray Diffraction
Storage Ring Sources
X-ray FELs
New Science

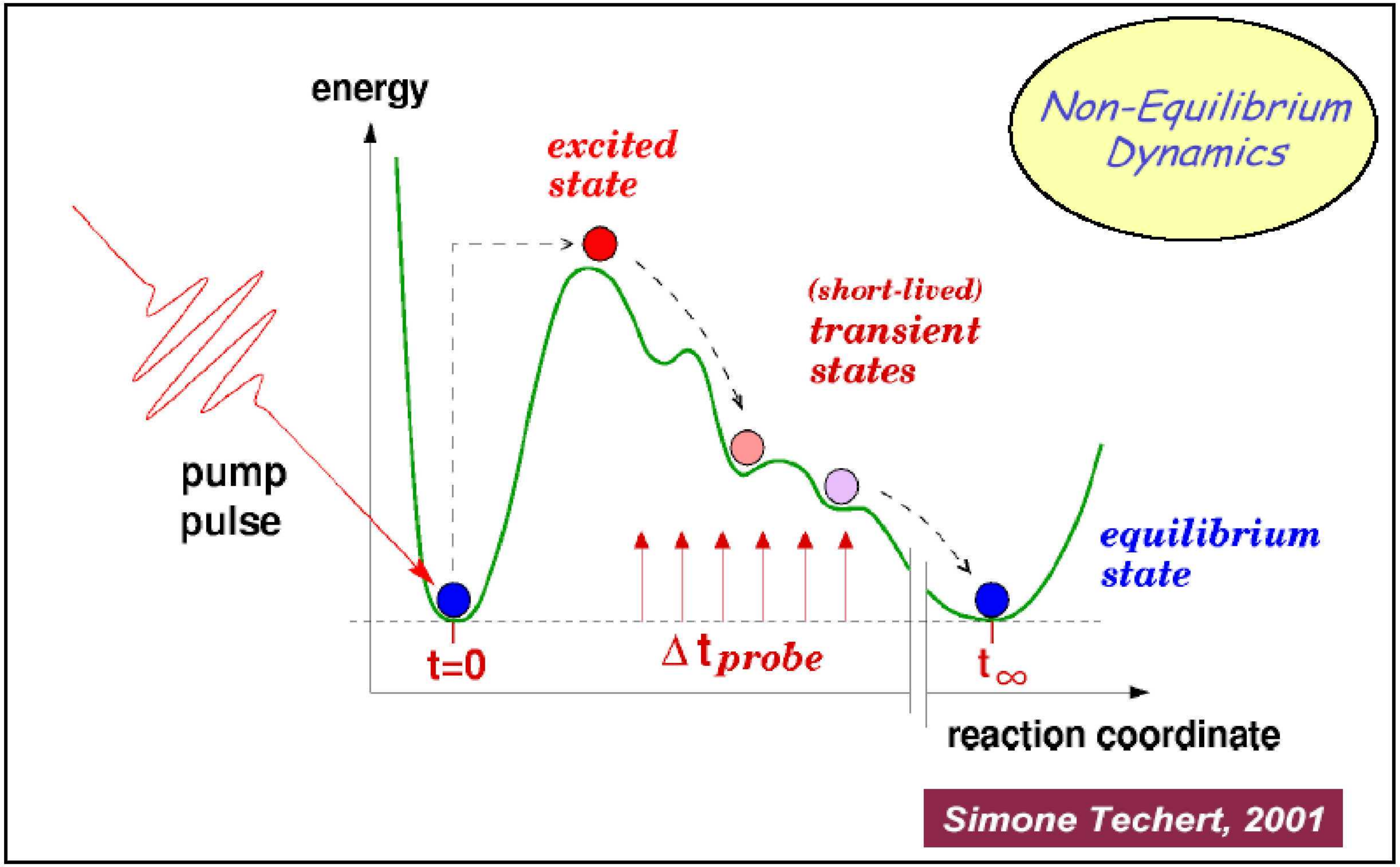
Non-Equilibrium
Dynamics
energy
excited
state
(short-lived)
transient
states
pump
pulse
equilibrium
state
t=0
Δ t probe
t ∞
reaction coordinate
Simone Techert, 2001

Relaxation in Optically excited Solids

Self-amplification
of excited state
K. Nasu (2001)

J. Phys.: Condens. Matter.

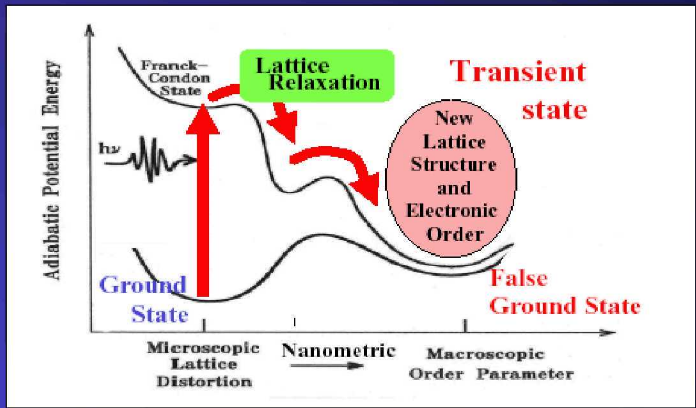

Correlation in solids : lattice play an active role ⇒ COOPERATIVI

Out of equilibrium and multi-scale process in solids

from the electron to the macroscopic transformation.

Depending on the system, different times-scales exist

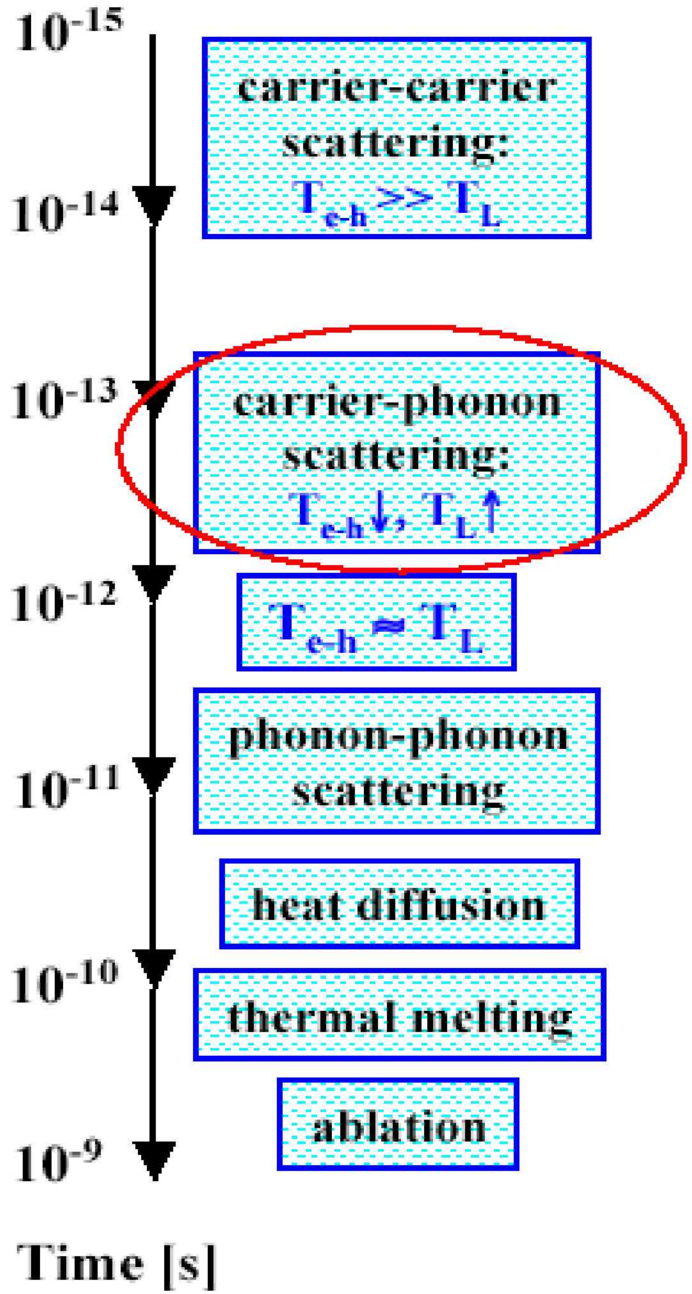

Klaus Sokolowski-Tinten
Institut für Experimentelle Physik

Measuring Atomic Displacements (I): *Transient Debey-Waller Effect*

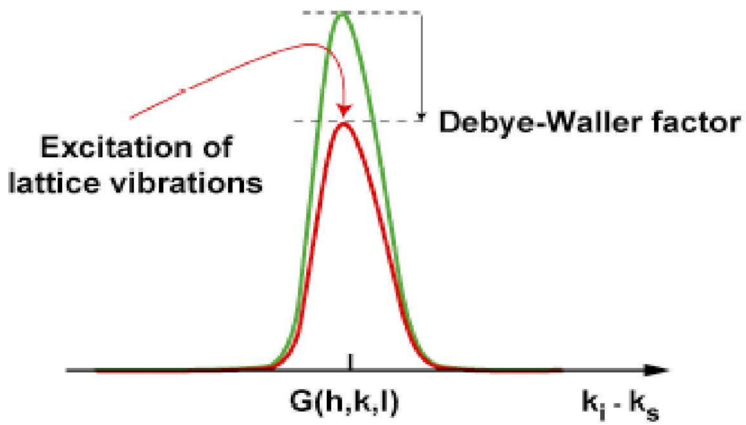

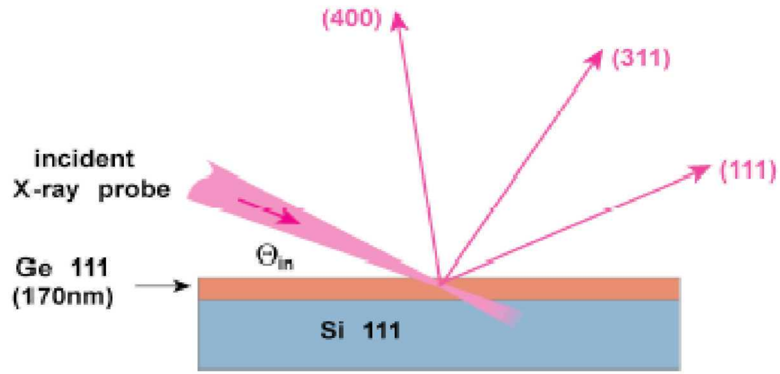

$$DWF = \exp\left(-\frac{4}{3}\pi^2\langle u^2\rangle / d_{hkl}^2\right)$$

mean atomic displacement

111-surface:

111-refl.: $\Rightarrow \Theta_{in} = 24.9^o$; $\Theta_{out} = 24.9^o$

311-refl.: $\Rightarrow \Theta_{in} = 24.2^o$; $\Theta_{out} = 48.8^o$

400-refl.: $\Rightarrow \Theta_{in} = 21.6^o$; $\Theta_{out} = 96.8^o$

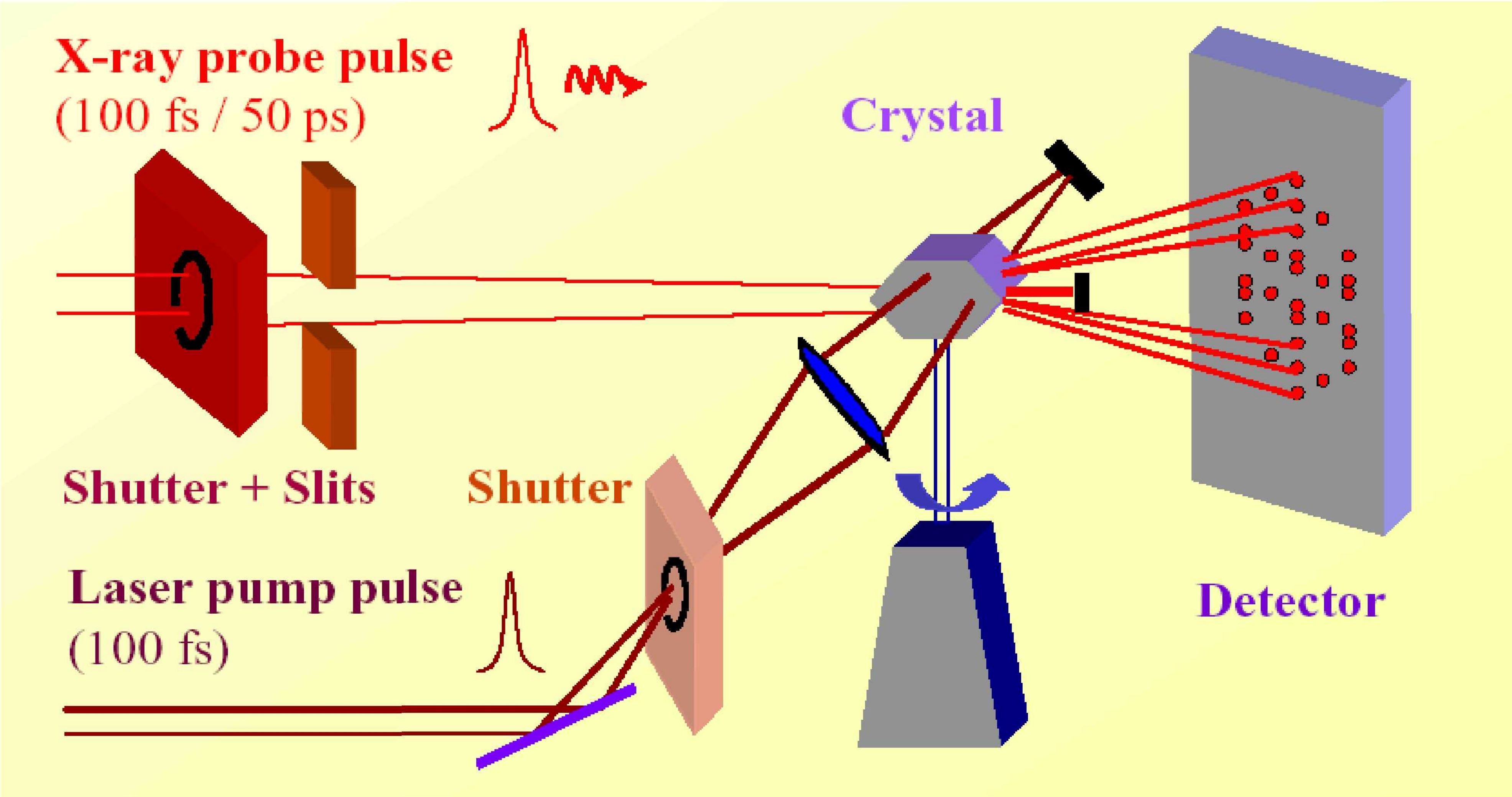

Simone Techert, Max-Planck Institut für biophysikalische Chemie,
Abt. Spektroskopie und Photochemische Kinetik –
Strukturdynamik (bio)chemischer Systeme (Göttingen)

Femtosecond Electron Diffraction Setup

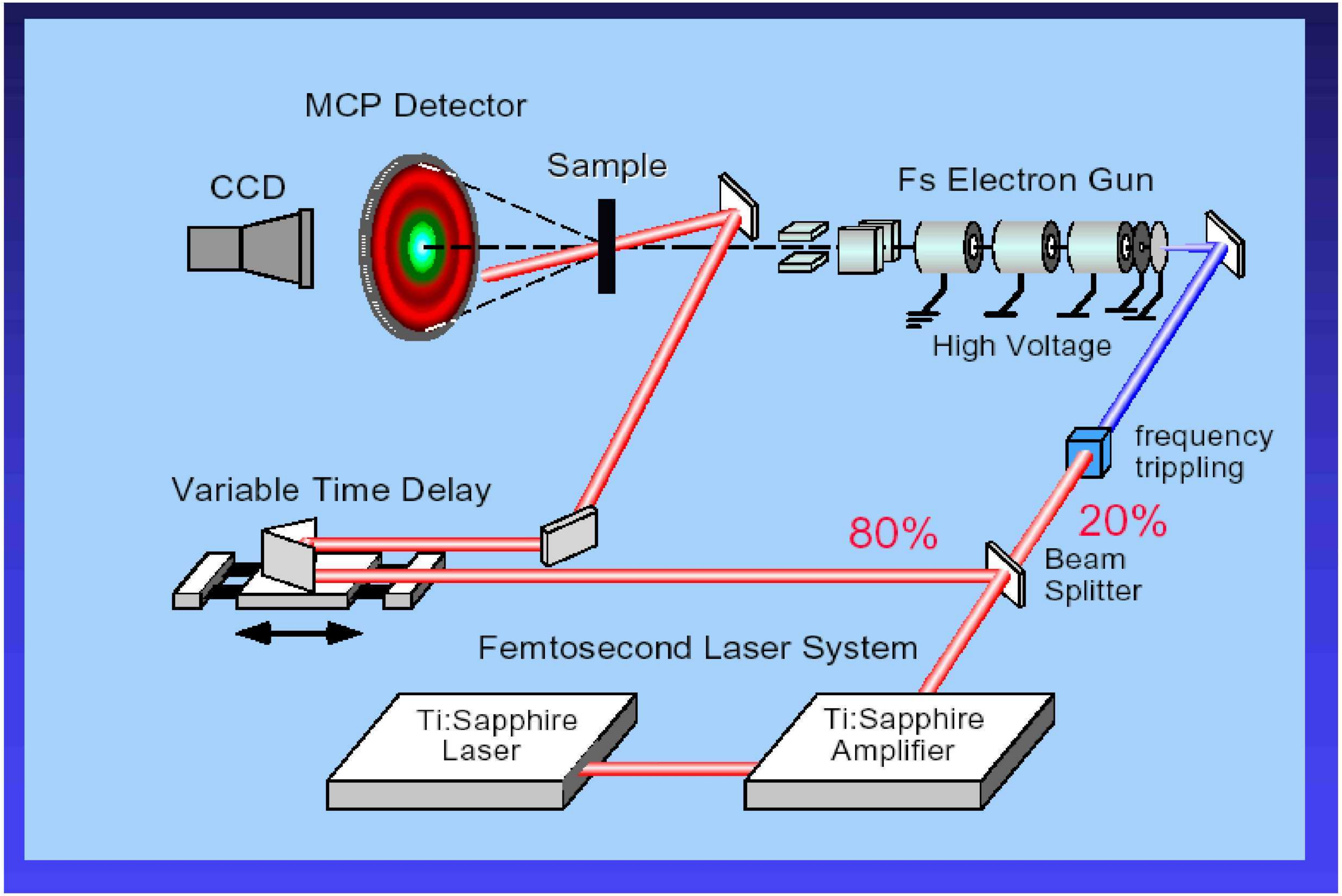

J. Cao, *et al.*, *Appl. Phys. Lett.* **83**, 1044 (2003)

Structural Changes Probed with Diffraction

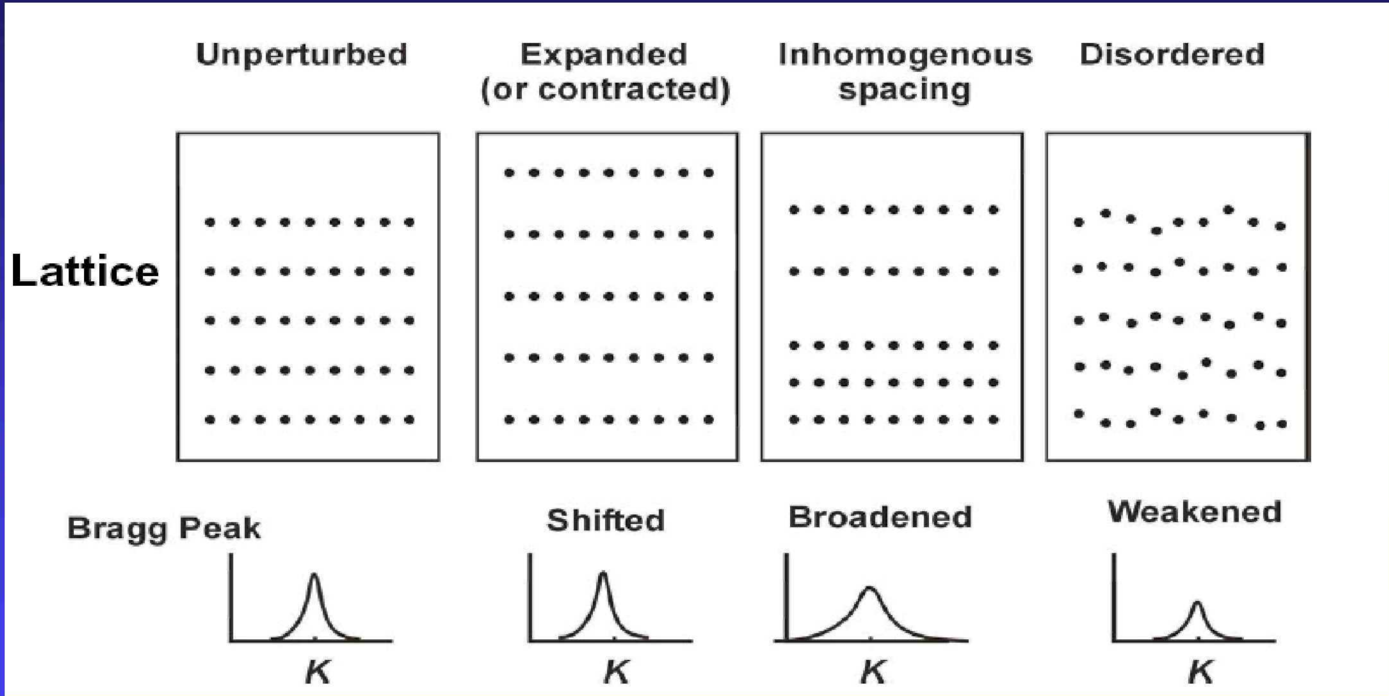

Three aspects of Bragg peak (position, intensity and width) give detailed knowledge of structure change.

Reproduced from: A. Rousse, *et al., Rev. Modern Phys.*, 73, 17(2001)

Strongly-driven thermal melting (superheating)

3.5 ps melting time at laser fluence 70 mJ/cm^2
3.5 ps > 1.5 ps e-ph thermalization (~ 1500K)
predicted by TTM simulation

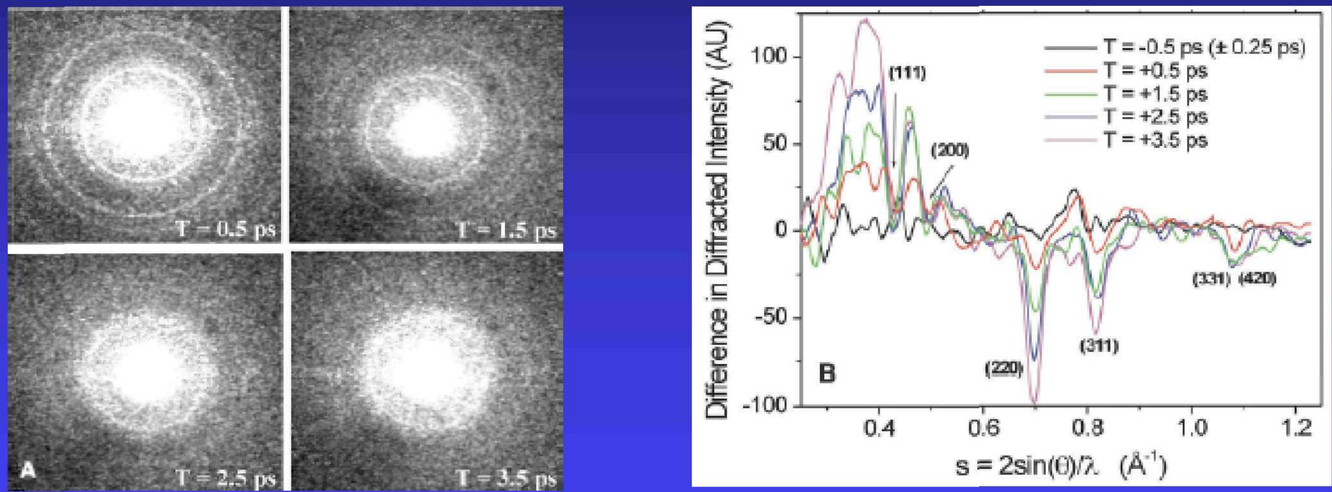

B. J. Siwick, *et al.*, *Science* **302,** 1382 (2003)

Temporal Evolution of Bragg Peaks

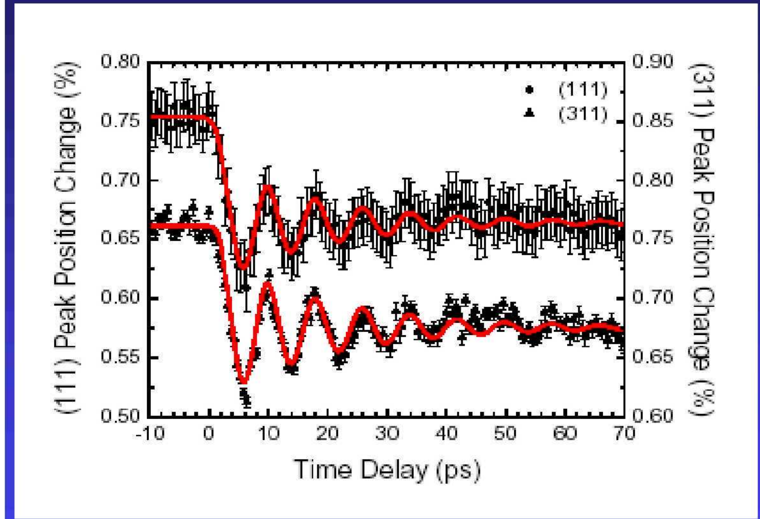

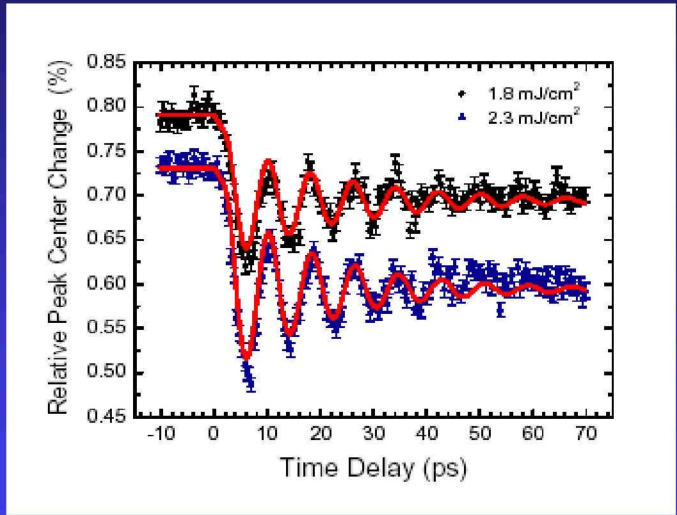

- Coherent and in-phase motions
- Amplitude is proportional the laser fluence
- 8 ps period and damping time constant~ 20 ps

Short pulses radiation sources

- Table-top lasers
- Free electron lasers
- Recirculating LINAC/FELs
- LINAC based sources
- Electron bunch slicing in 3rd generation synchrotrons
- Plasma sources

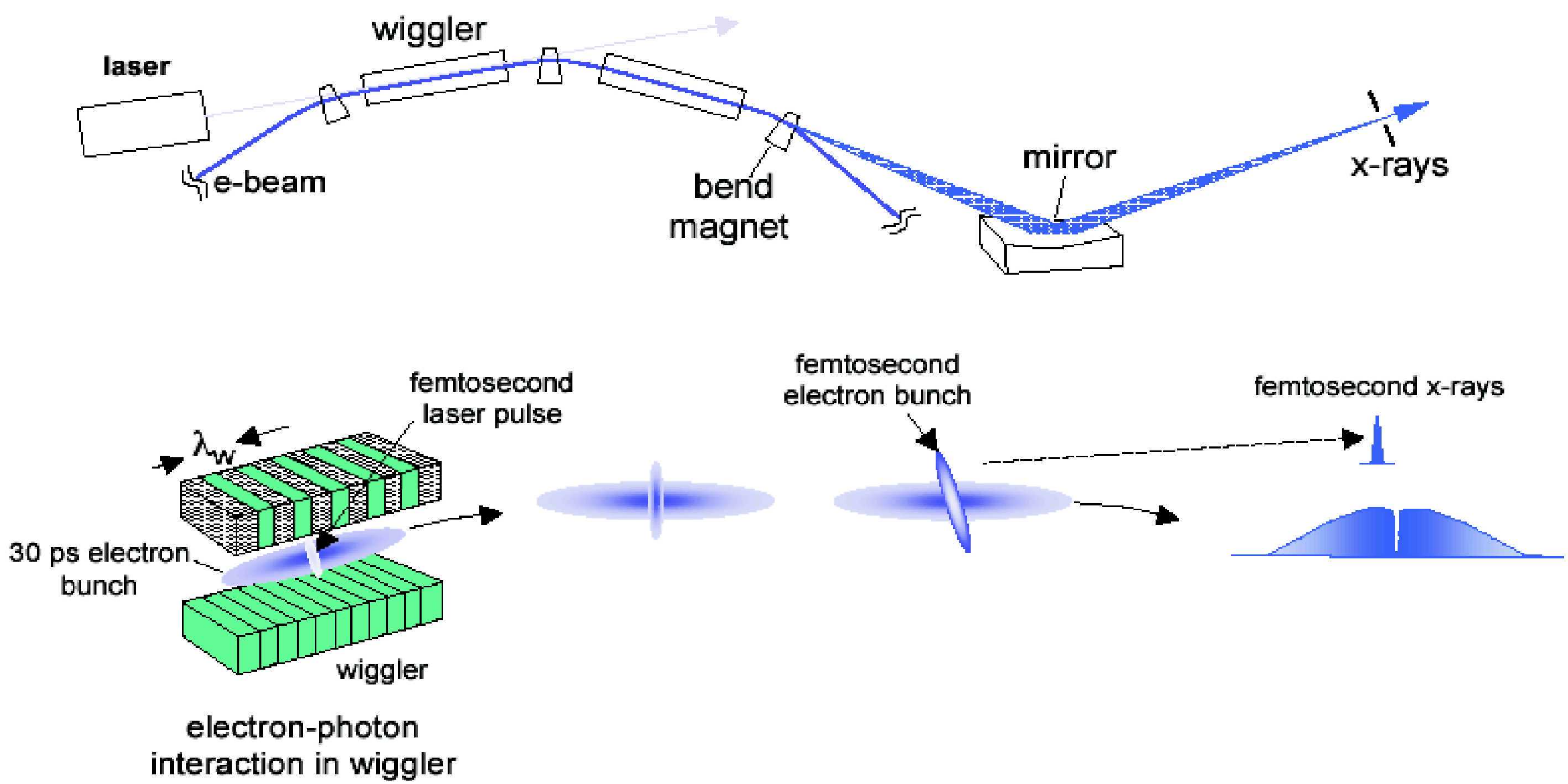

Zholents and Zolotorev, *Phys. Rev. Lett.*, 76, 916,(1996).

Schoenlein et al., *Science,* 287, (2000)

- Coherent EUV light is generated by ionizing a gas with a fs laser
- Broad range of harmonics generated 4.5 up to 550 eV
- "Laser-like" coherent beams in EUV
  - R. Bartels et al, Science 297, 376 (2002), Nature 406, 164 (2000)

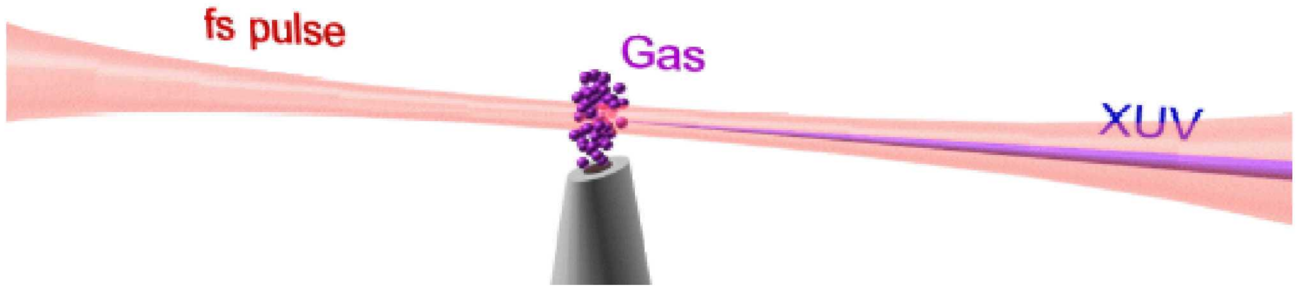

Gas jet

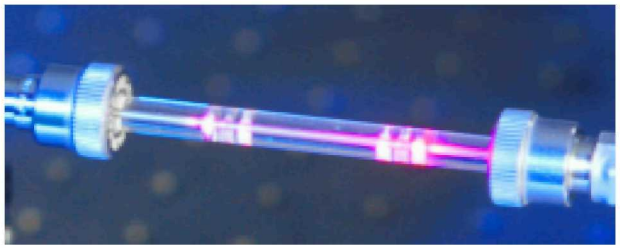

Fiber

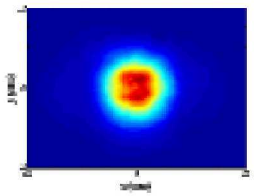

EUV beam

Extreme nonlinear optics: high harmonics (HHG)

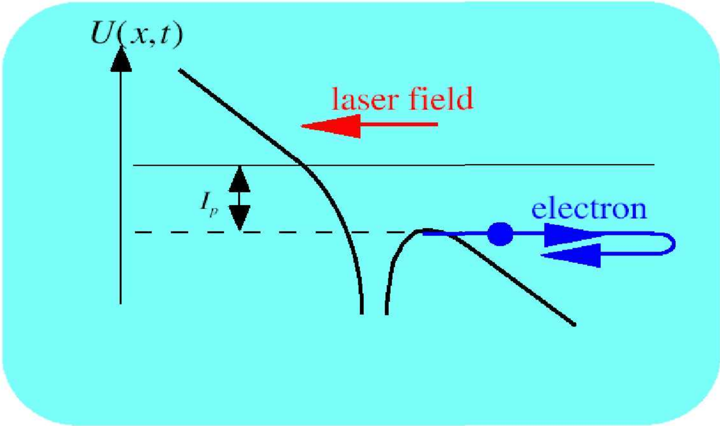

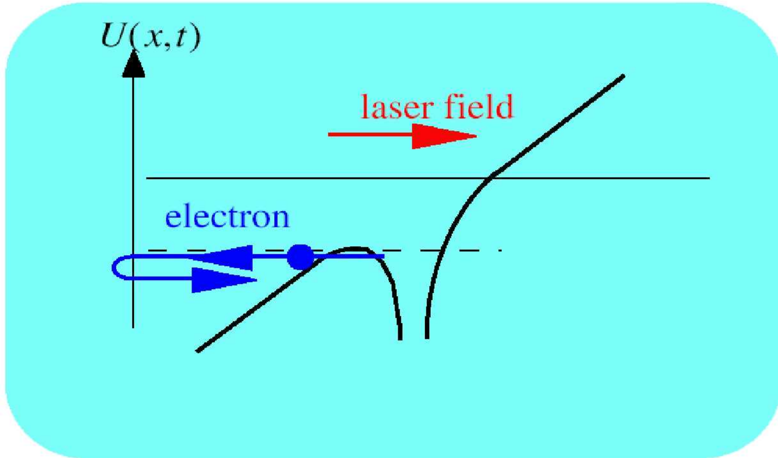

$$h\upsilon_{cutoff} = I_p + 3.2U_p$$

ionization potential of atom

$U_p \approx I_L \lambda^2$ quiver energy of e^-

$$\varphi_{x\text{-}ray} \approx \varphi_{Laser} \text{ and } I_{Laser}$$

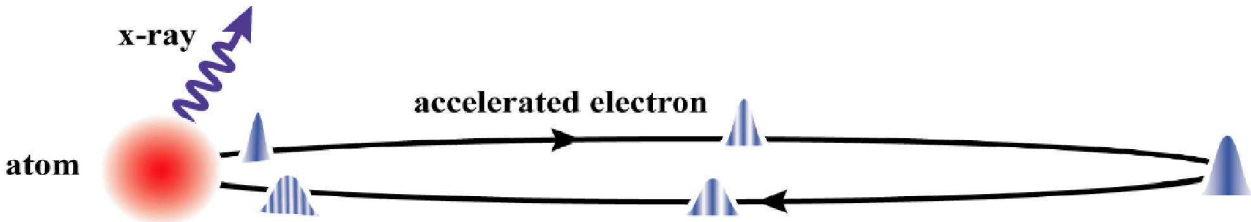

time

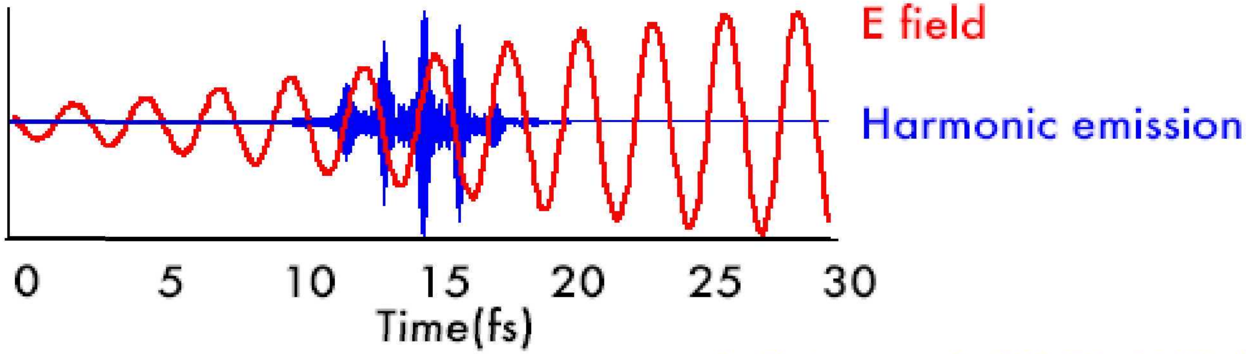

I. Christov et al, PRL 78, 1251, (1997)

frequency

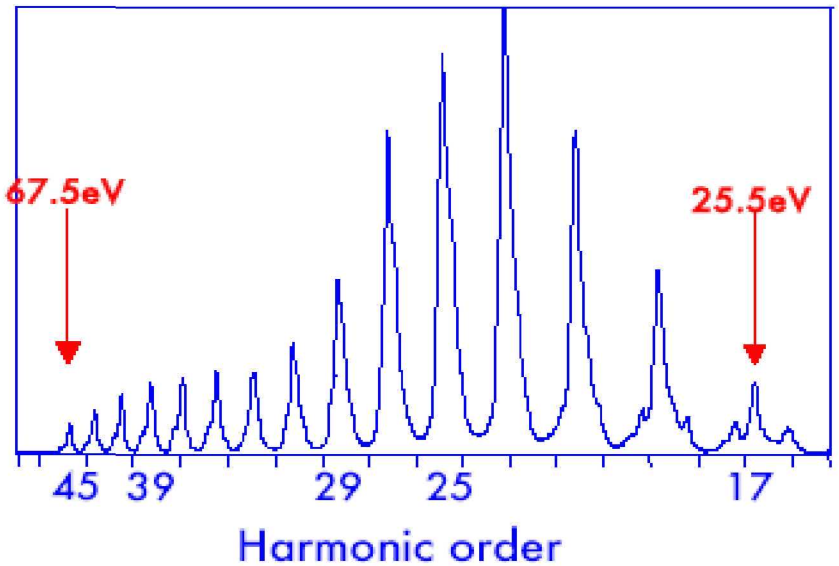

J. Zhou et al, PRL 76(5), 752-755 (1996)

$$\overline{E}(\overline{r},t) \sim e^{-i(\omega_i t - k_i z)} \quad , \; I_{HHG} \propto \frac{\sin^2(\Delta k L/2)}{(\Delta k L/2)^2} \quad where \;\; \Delta k = k_{hhg} - q k_{vis}$$

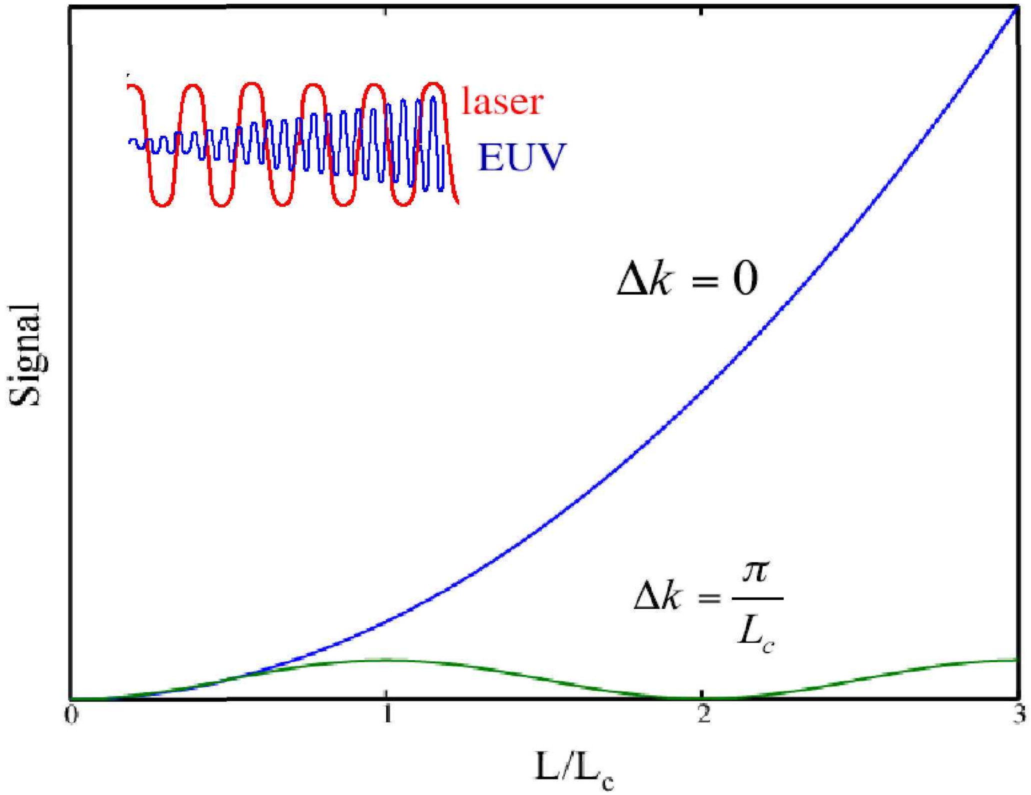

- **Use phase matching (Δk=0) for efficient EUV generation**
- ***If Δk ≠ 0, adjust or restrict emission from regions that are out of phase***
- **Coherence lengths for HHG in the presence of high levels of ionization are μm - mm**

Phase-matched frequency conversion in waveguides:

C. Durfee et al., Optics Letters 22, 1565 (1997)
A. Rundquist, et al, Science, vol. 280, pp. 1412-1415 (1998)

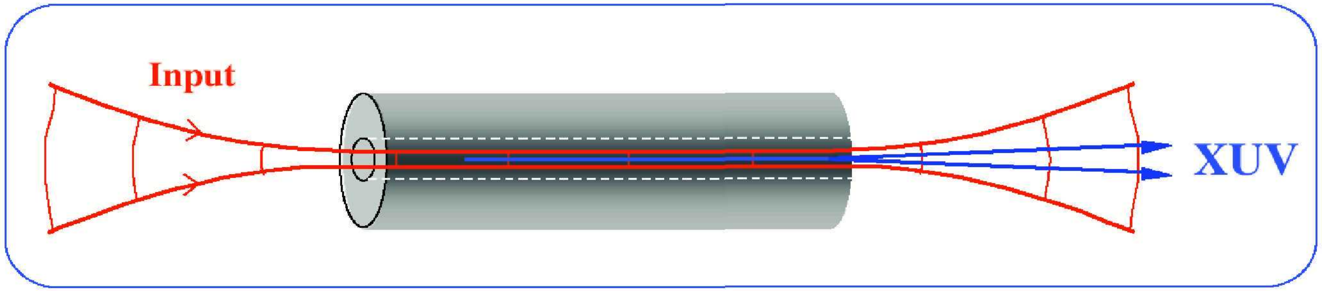

- Waveguide creates plane-wave geometry
- Waveguide can control the phase velocity ($v_p = \omega/k$)

$$k = \frac{2\pi}{\lambda}\left(1 + P\delta(\lambda) - \frac{1}{2}\left[\frac{u\lambda}{2\pi a}\right]^2 - \frac{1}{2}\frac{N_e r_e \lambda^2}{\pi}\right)$$

vacuum gas waveguide ionization

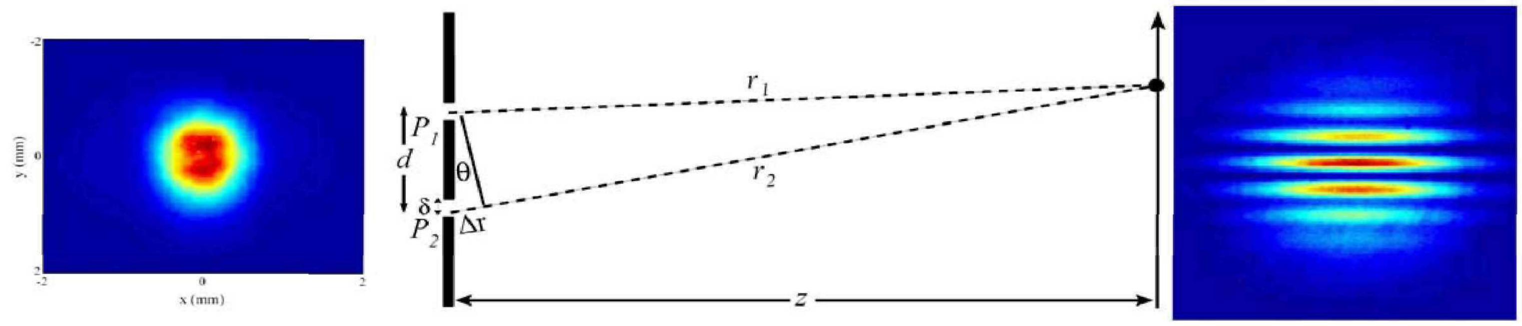

EUV beam **EUV interference pattern**

- Repeat 200 year old experiment – Young's Double Slit
  - Young, Philos. Trans. R. Soc. XCII 12, 387 (1802).
  - E. Wolf et al., JOSA 46, 895 (1957; Opt. Lett. 6, 168 (1981).

Double-slit diffraction patterns from 1mm EUV beam

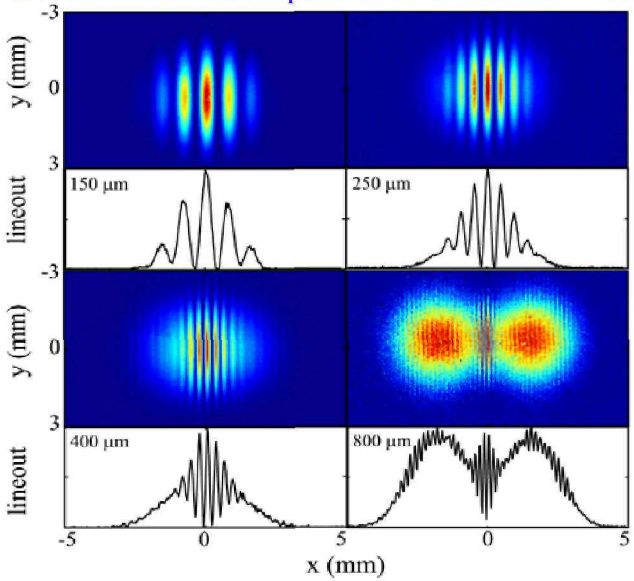

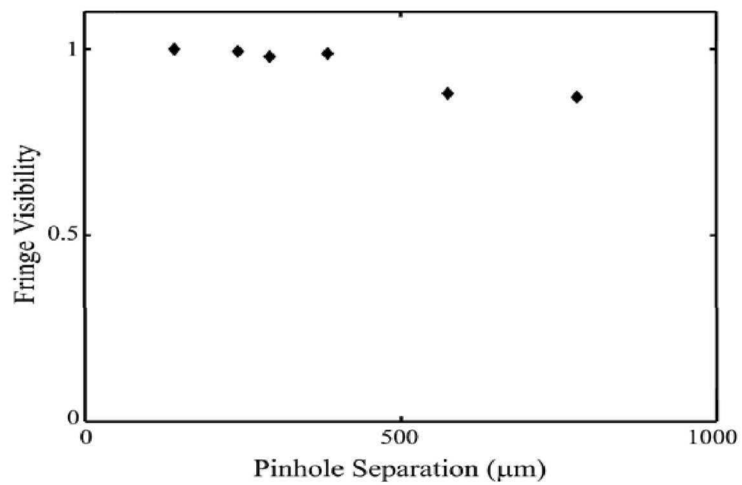

- R. Bartels et al, Science 297, 376 (2002)
- R. Bartels et al, Opt. Lett. 27, 707 (2002)

Generation of Laser-Like EUV Beams using X-Ray Fiber Optics

High spatial coherence demonstrated

R. Bartels et al., Science 297, 376 (2002)

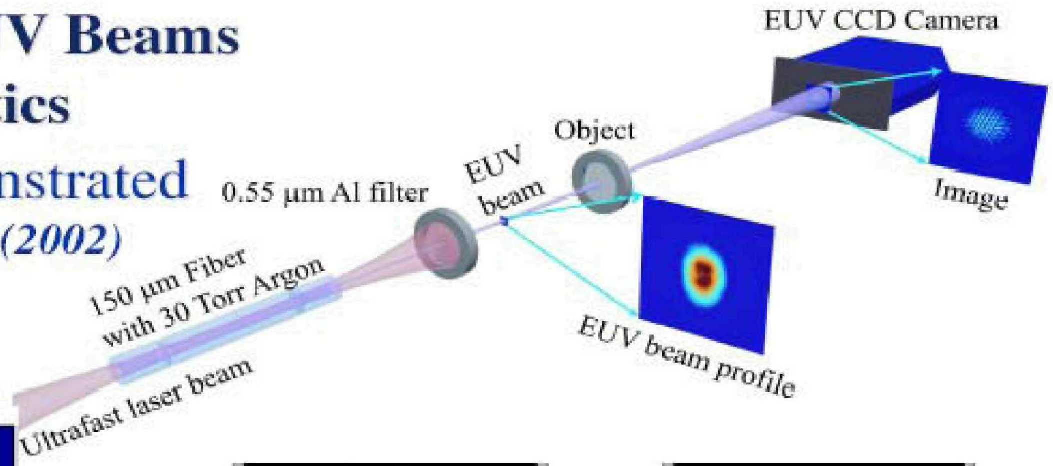

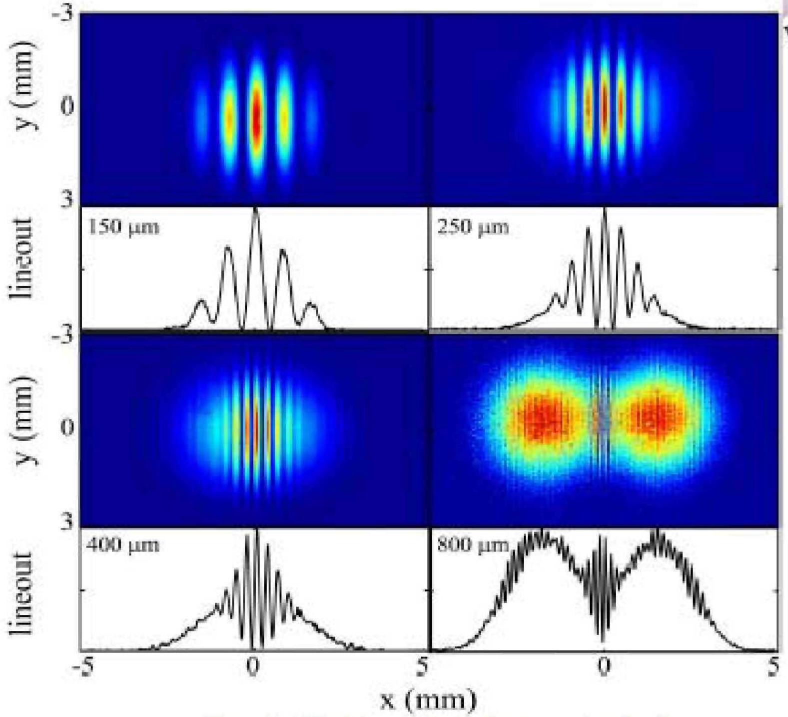

Laser-like EUV beams exhibit high-quality interference patterns

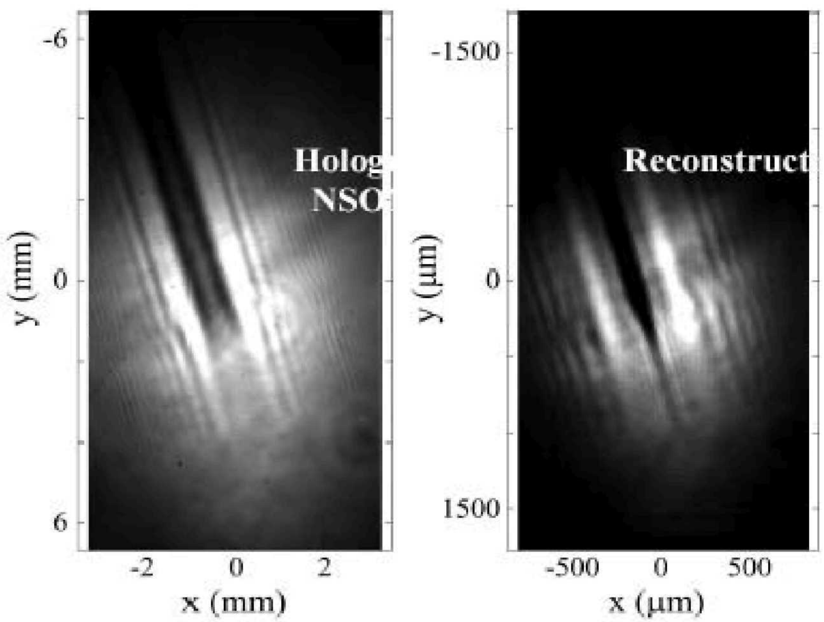

First demonstration of holography at EUV wavelengths using a compact EUV source

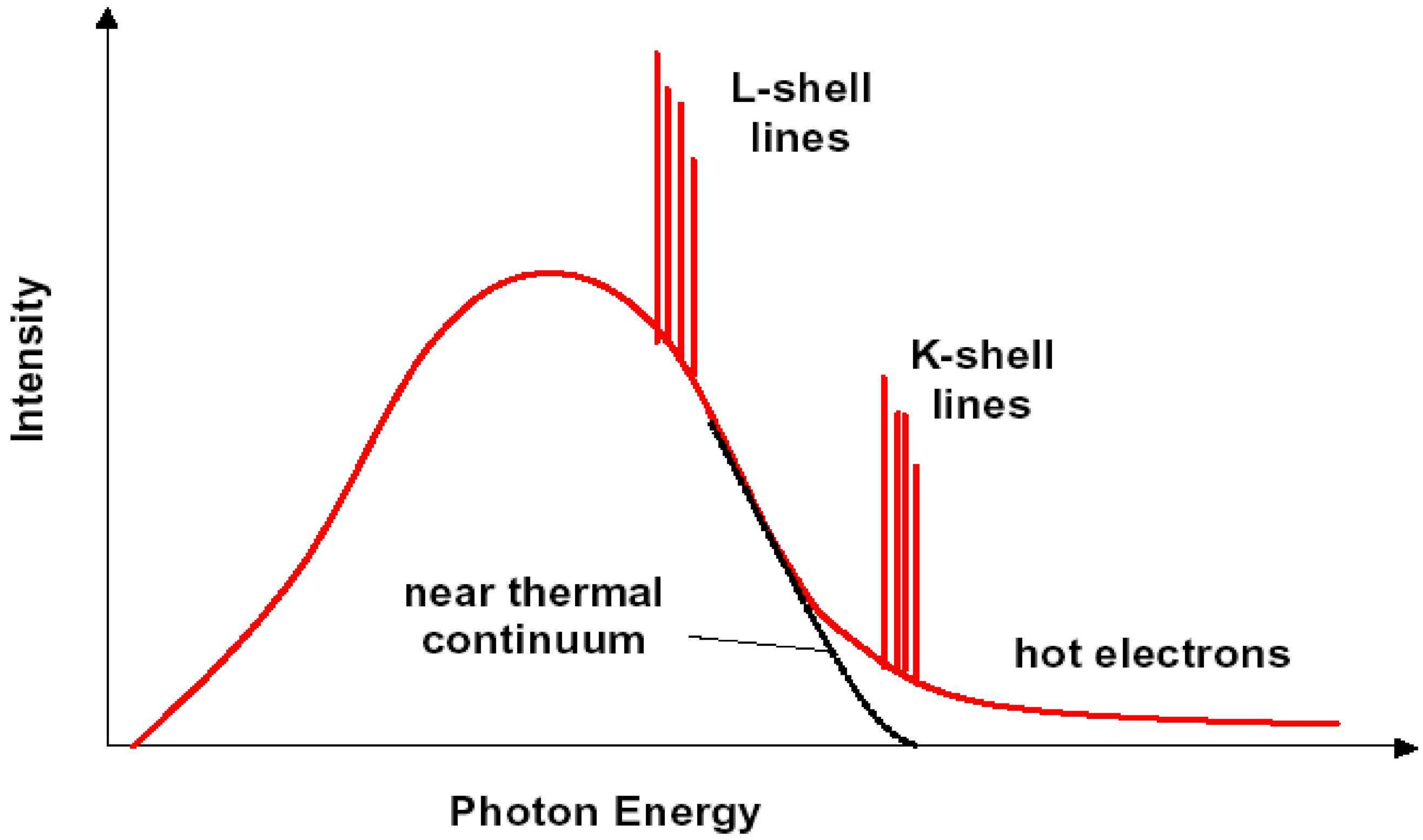

Klaus Sokolowski-Tinten
Institut für Experimentelle Physik

Klaus Sokolowski-Tinten
Institut für Experimentelle Physik

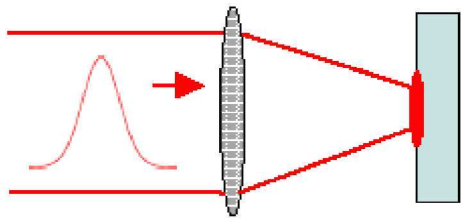

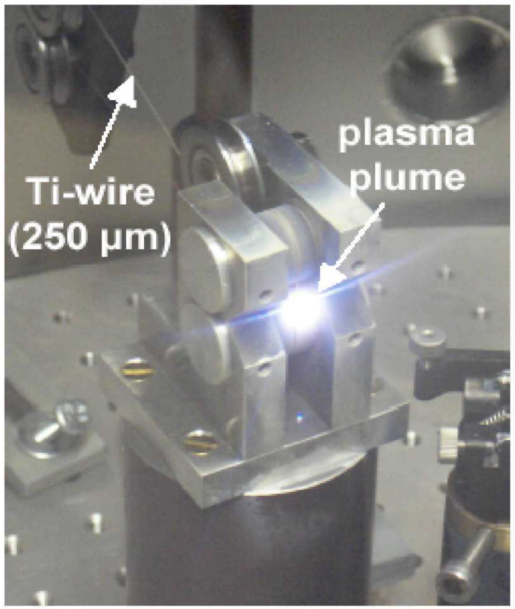

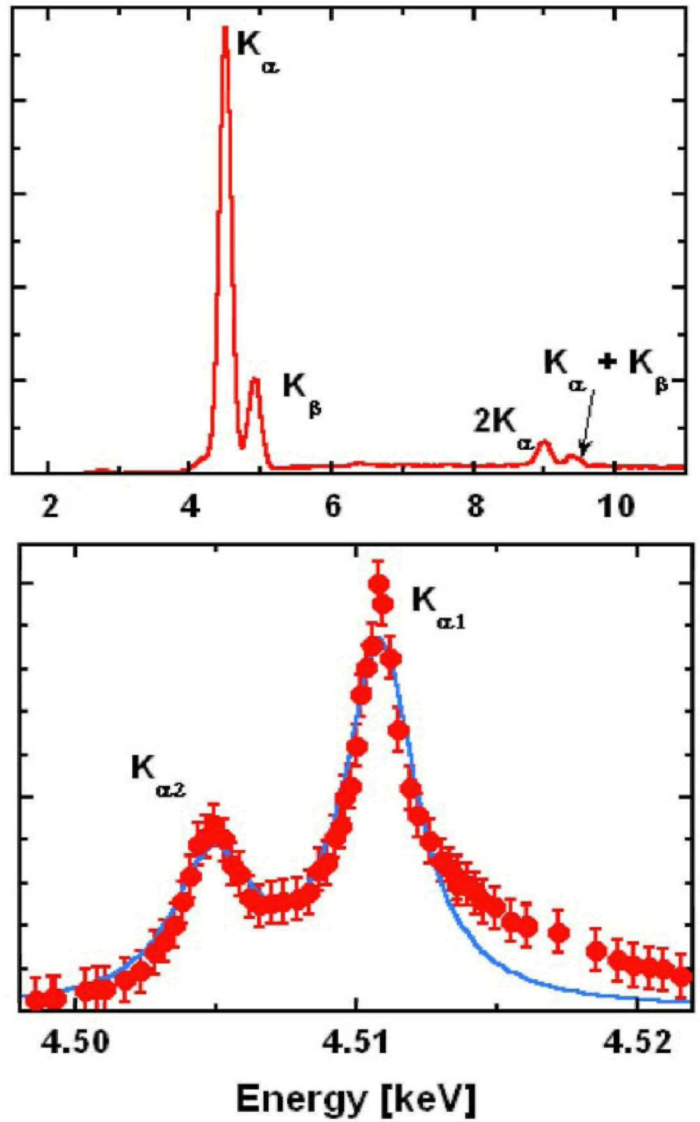

Max Born Institute
Berlin

Matias Bargheer,
N. Zhavoronkov, Y. Gritsai,
M. Wörner, T. Elsaesser

K_α line radiation:

	K_α energy/ eV	K_α flux / 4π*s
Ga	9.2	4.5×10^{10}
Cu	8.2	3.9×10^{10}
Ni	7.5	6.7×10^{10}

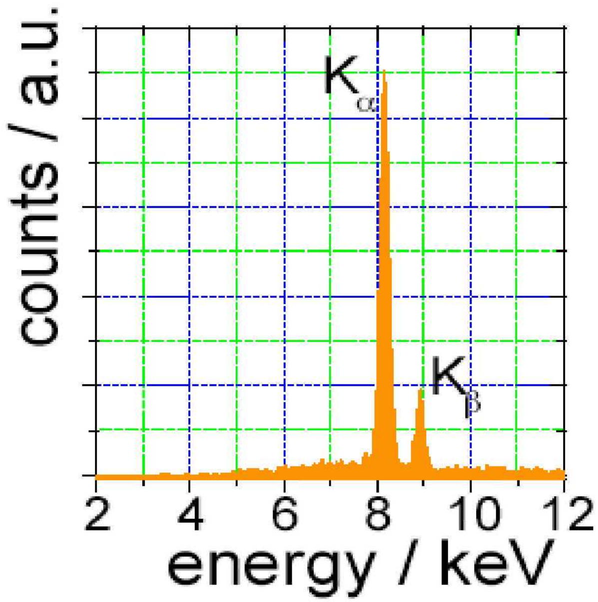

- Plasma generated in 15 μm copper
- X-ray focus 15 μm
- Estimated pulse duration: 200 fs

Brilliance = 4 x 10^7 / (mrad²*mm²s*0.1%BW)

According to specs	Flux on sample / s	Focus / μm
Multilayer mirror (Osmic)	1.4×10^6	30
HOPG reflector (IfG)	5×10^7	200

Klaus Sokolowski-Tinten
Institut für Experimentelle Physik

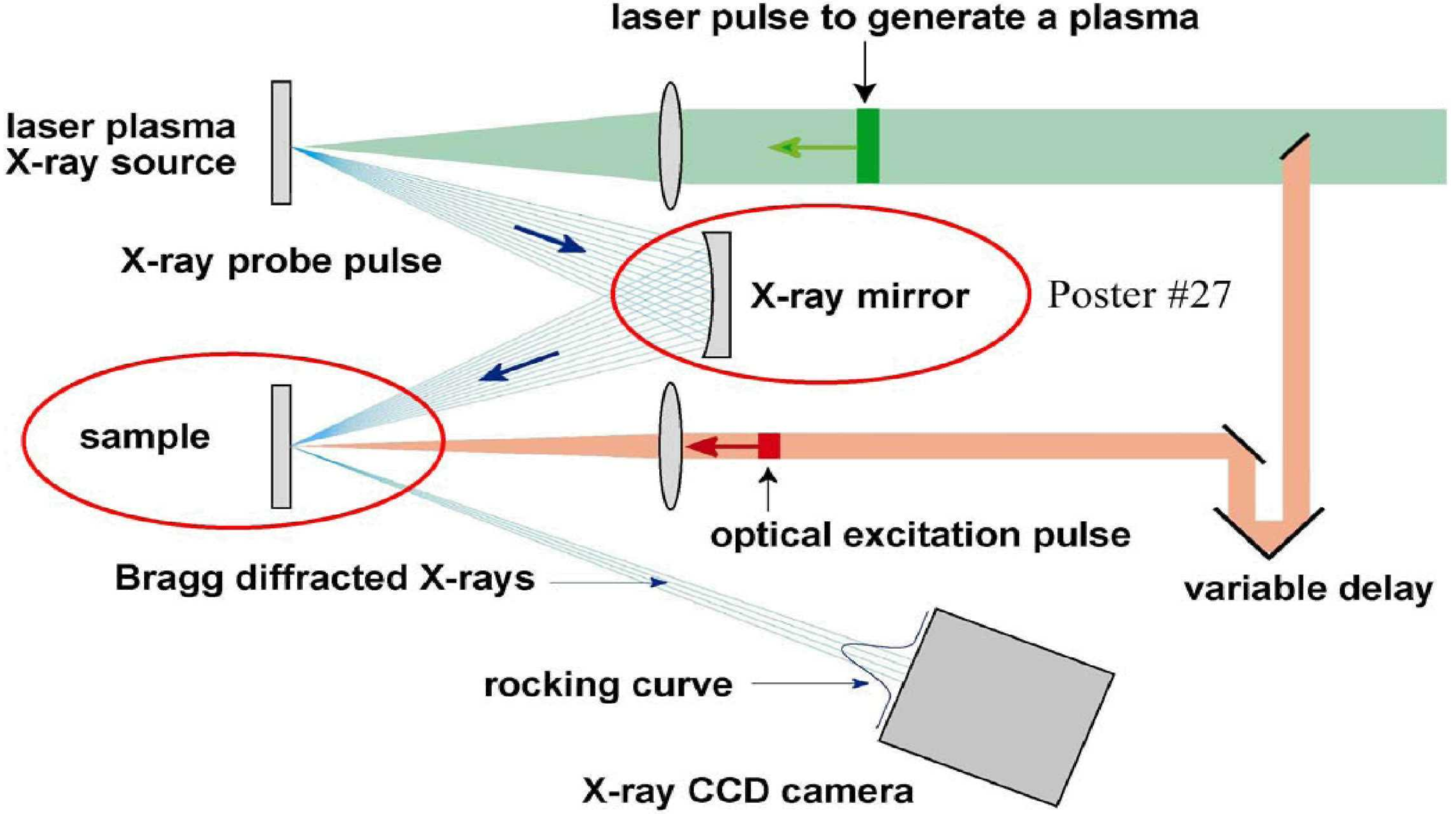

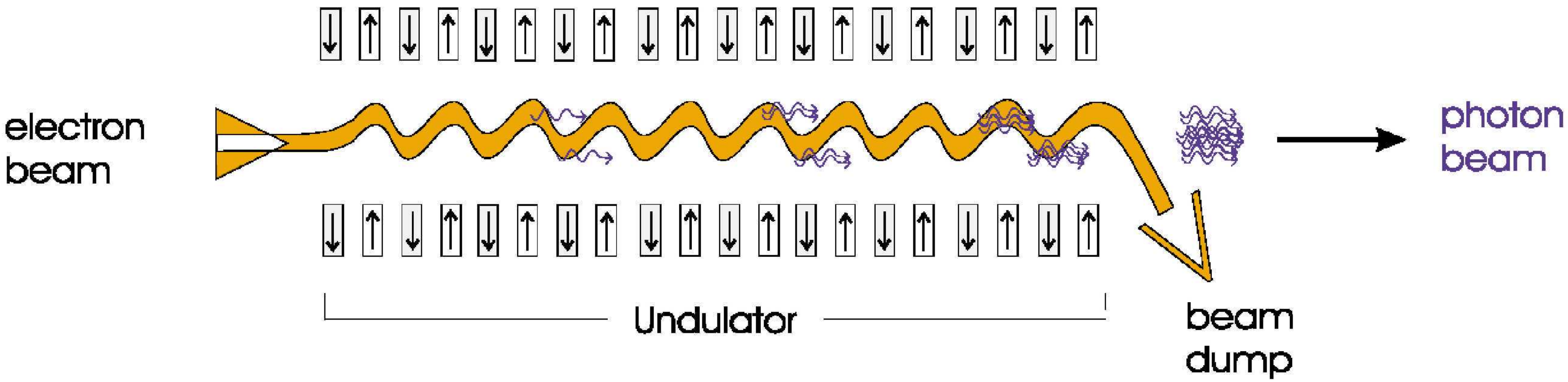
electron
beam
photon
beam
Undulator
beam
dump

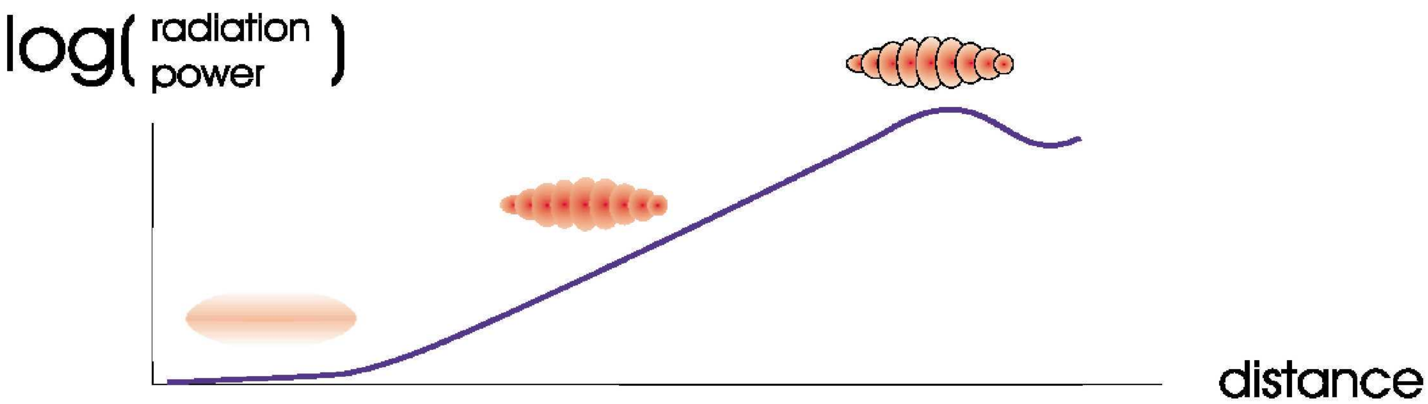
log(radiation power)
distance

Spontaneous Undulator Radiation

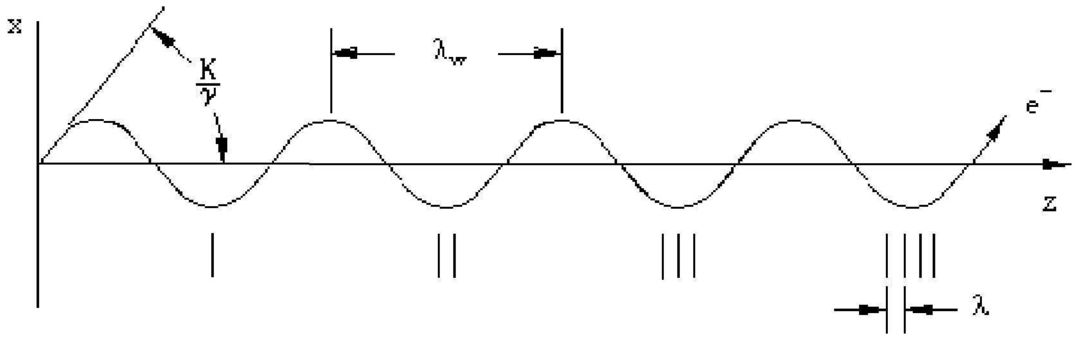

$$\lambda = \frac{\lambda_w}{2\gamma^2}(1 + K^2/2) \qquad K \cong 0.93\, B_w(T)\,\lambda_w(cm)$$

$$\frac{\Delta\lambda}{\lambda_s} = \frac{1}{N_w}$$

Amplification of External Wave

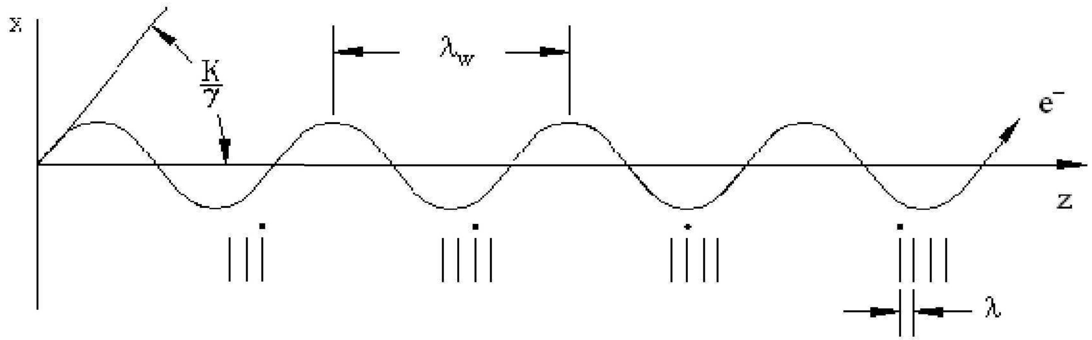

At resonance, while traversing one period of the undulator, the electron falls one radiation wavelength behind the EM-wave

The BESSY Soft X-Ray SASE FEL (Free Electron Laser)

OSCILLATOR

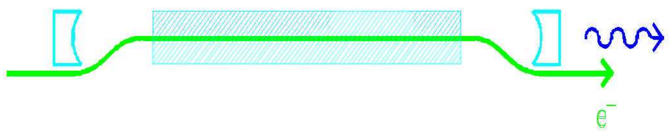

SINGLE PASS FEL

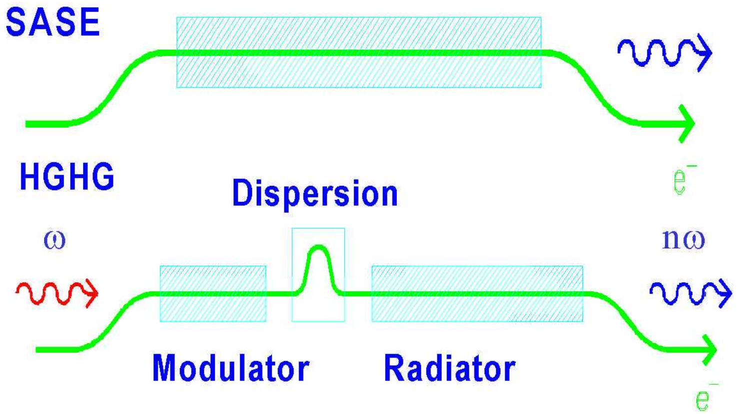

Classical FEL Scheme

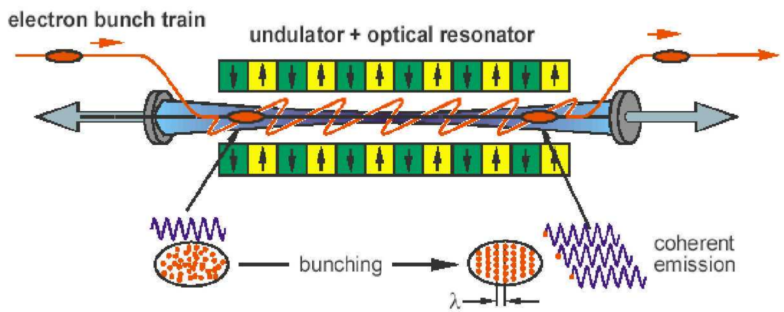

SASE FEL Scheme

(Self Amplified Spontaneous Emission)

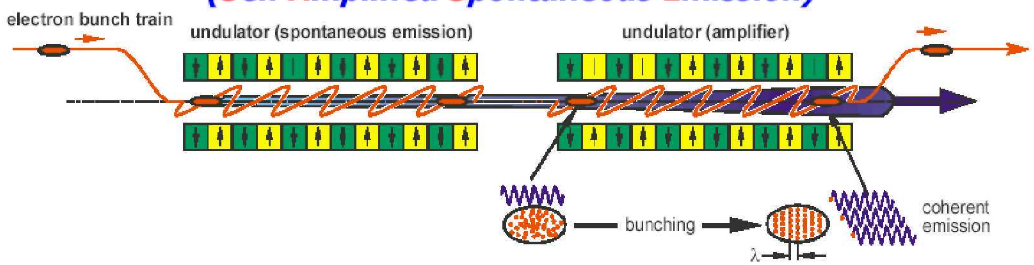

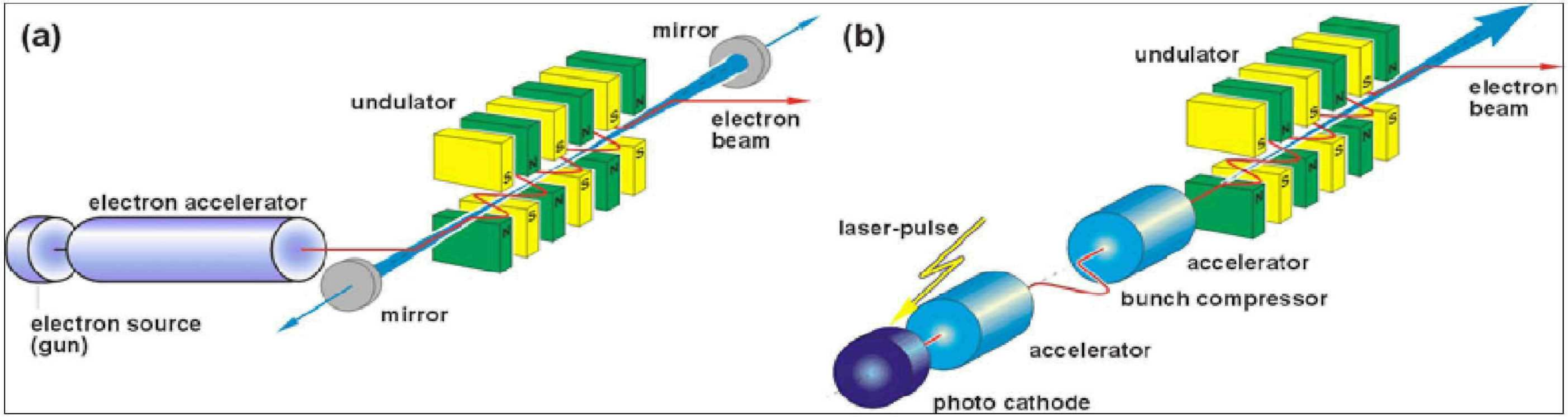
(a)
mirror
undulator
electron beam
electron accelerator
electron source (gun)
mirror
(b)
undulator
electron beam
laser-pulse
accelerator
bunch compressor
accelerator
photo cathode

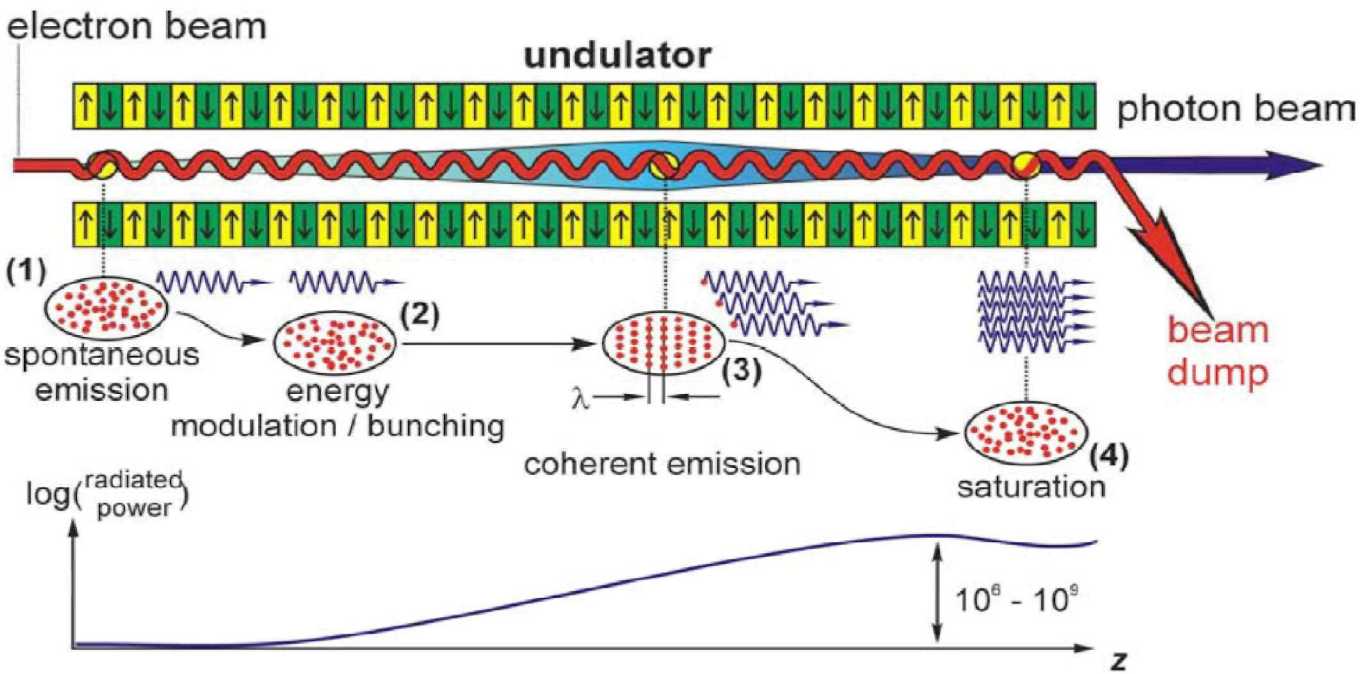
electron beam
undulator
photon beam
(1)
spontaneous emission
(2)
energy modulation / bunching
λ
(3)
coherent emission
(4)
saturation
beam dump
log(radiated power)
10^6 - 10^9
z

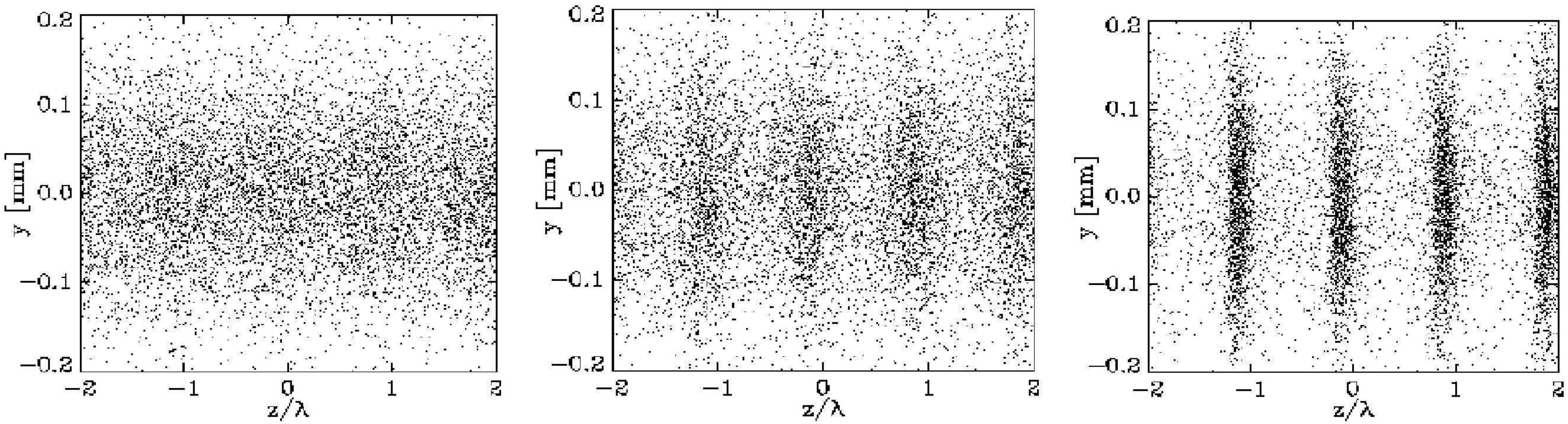

y [mm]
z/λ
0.2
0.1
0.0
−0.1
−0.2
−2
−1
0
1
2

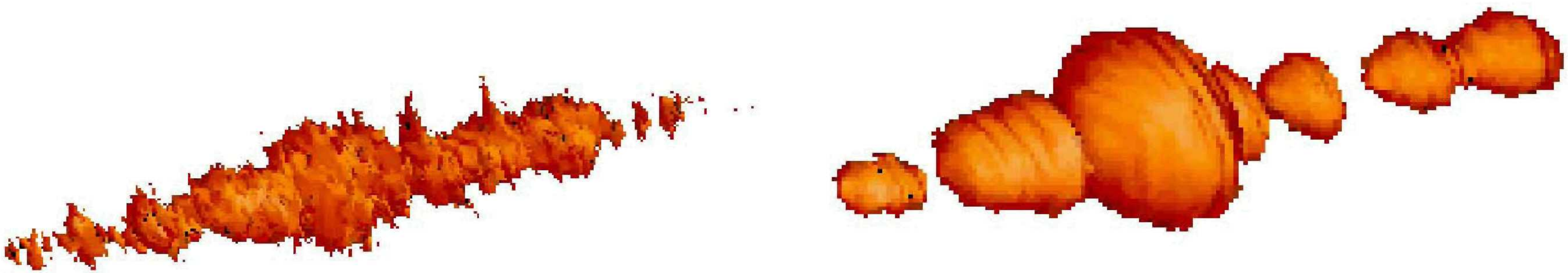

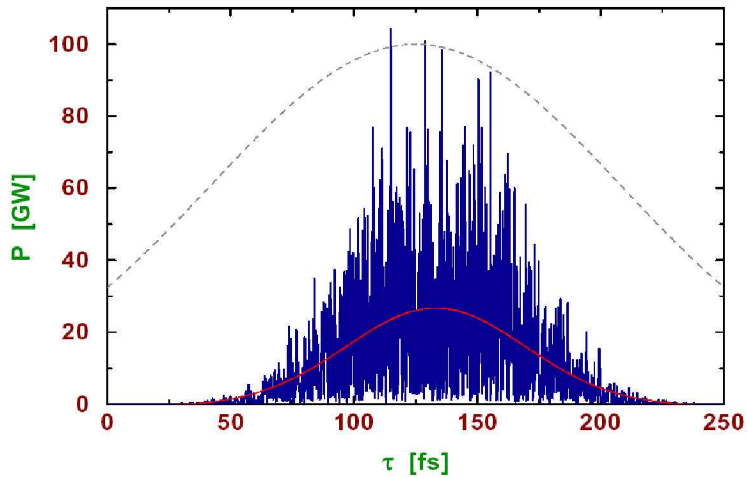

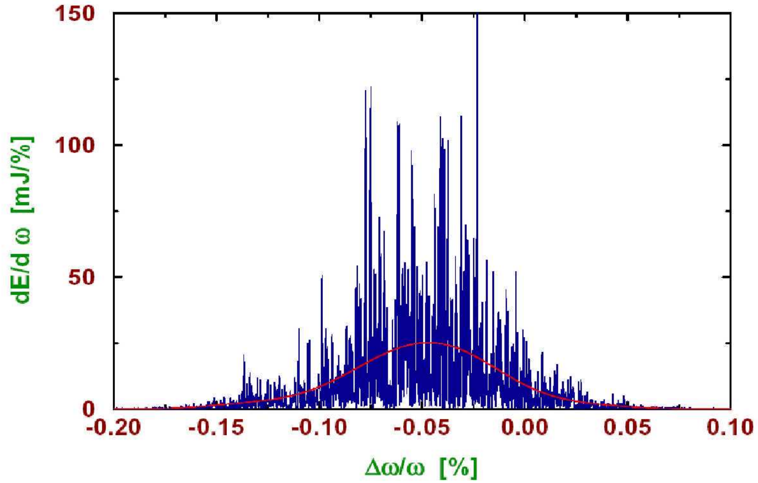

	Units	SASE 1
Wavelength*	Å	1–5
Peak power	GW	37
Average power	W	210
Photon beam size (FWHM)**	μm	100
Photon beam divergence (FWHM)***	μrad	0.8
Bandwidth (FWHM)	%	0.08
Coherence time	fs	0.3
Pulse duration (FWHM)	fs	100
Min. pulse separation****	ns	93
Max. number of pulses per train****	#	11500
Repetition rate****	Hz	5
Number of photons per pulse	#	1.8×10^{12}
Average flux of photons	#/sec	1.0×10^{17}
Peak brilliance	B*****	8.7×10^{33}
Average brilliance	B*****	4.9×10^{25}

*Parameters are given for the shortest wavelength.

** Value at the exit of the undulator.

*** Far field divergence.

**** Values determined by the time structure of the electron beam in the accelerator. The average parameters for the SASE-1 FEL are given for the ultimate case when only this beamline is in operation.

***** In units of photons/(sec $\cdot$ mrad^2 $\cdot$ mm^2 $\cdot$ 0.1 % bandwidth).

DESY

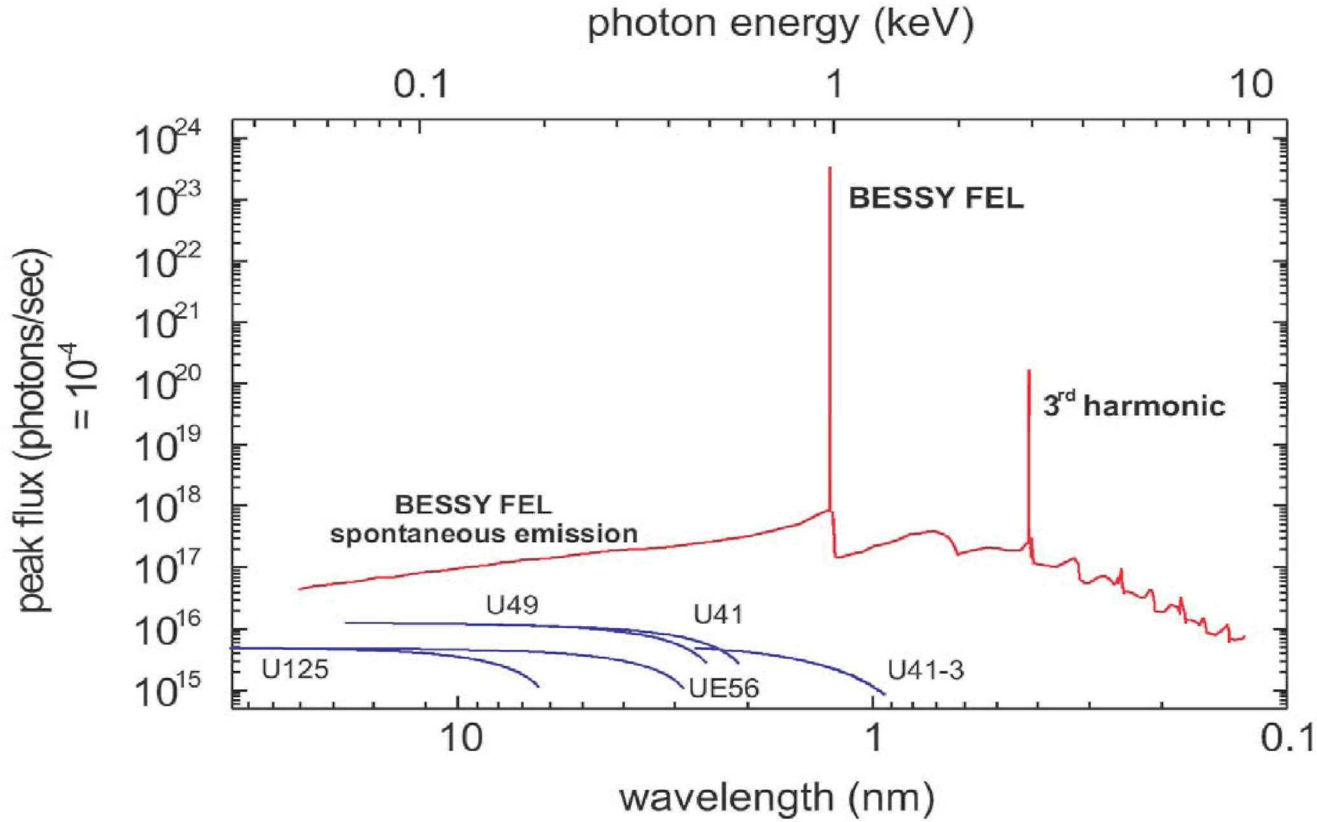

Spectrum of the BESSY SASE-FEL for a lasing photon energy of ħω = 1 keV compared to the BESSY II performance. BESSY II: single bunch operation with 10 mA of average beam current at E = 1.7 GeV. BESSY SASE-FEL: I = 5 kA, E = 2.25 GeV and a planar undulator with λ_u = 2.75 cm and N = 1450 periods. Spectra are calculated with a transmission efficiency of the monochromator of 5%.

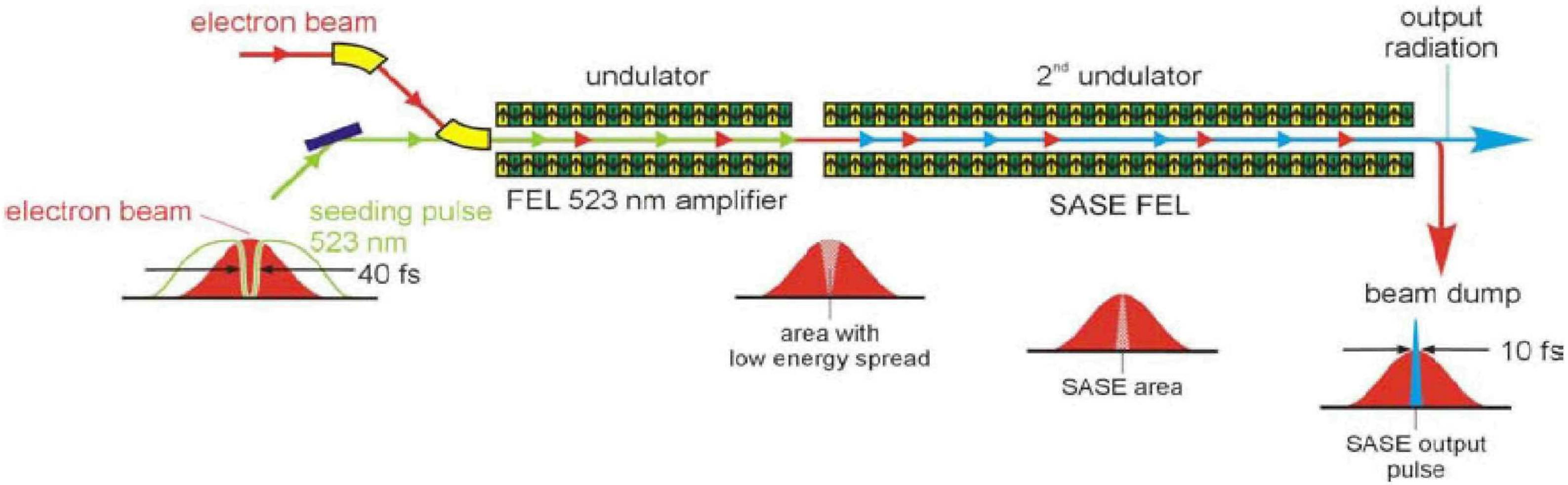
electron beam
undulator
2nd undulator
output radiation
electron beam
seeding pulse
523 nm
40 fs
FEL 523 nm amplifier
SASE FEL
area with
low energy spread
SASE area
beam dump
10 fs
SASE output
pulse

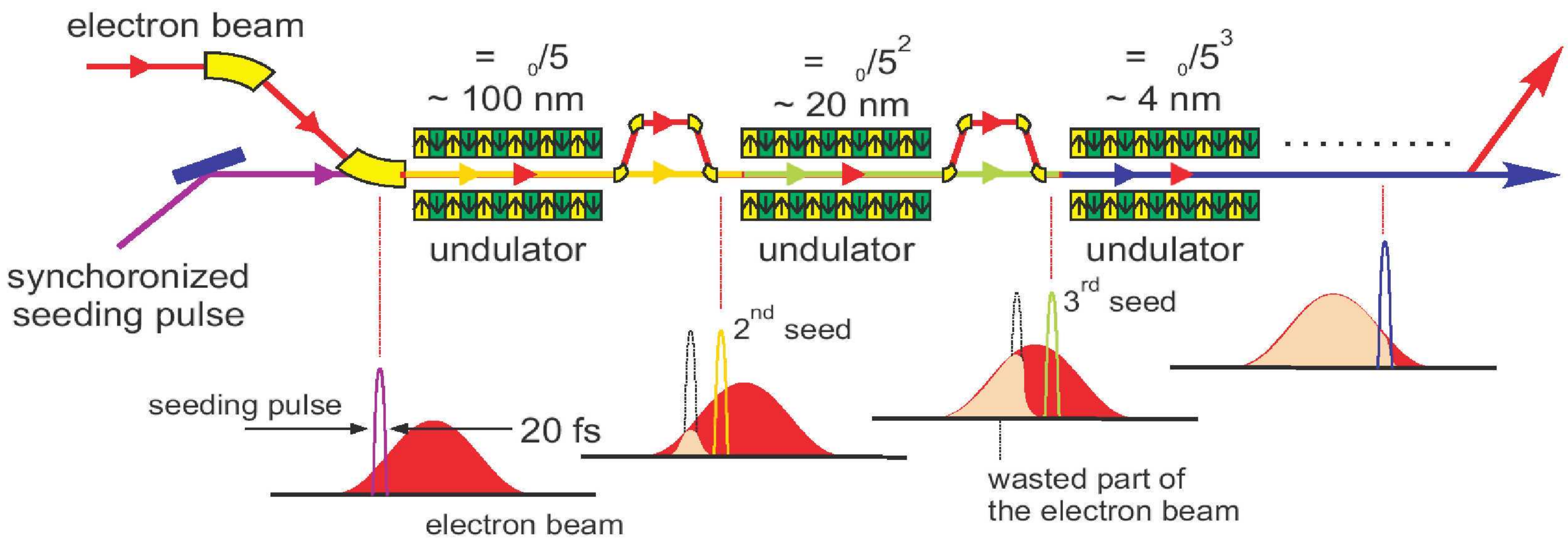
electron beam
= 0/5
~ 100 nm
= 0/5^2
~ 20 nm
= 0/5^3
~ 4 nm
undulator
undulator
undulator
synchoronized
seeding pulse
2nd seed
3rd seed
seeding pulse
20 fs
electron beam
wasted part of
the electron beam

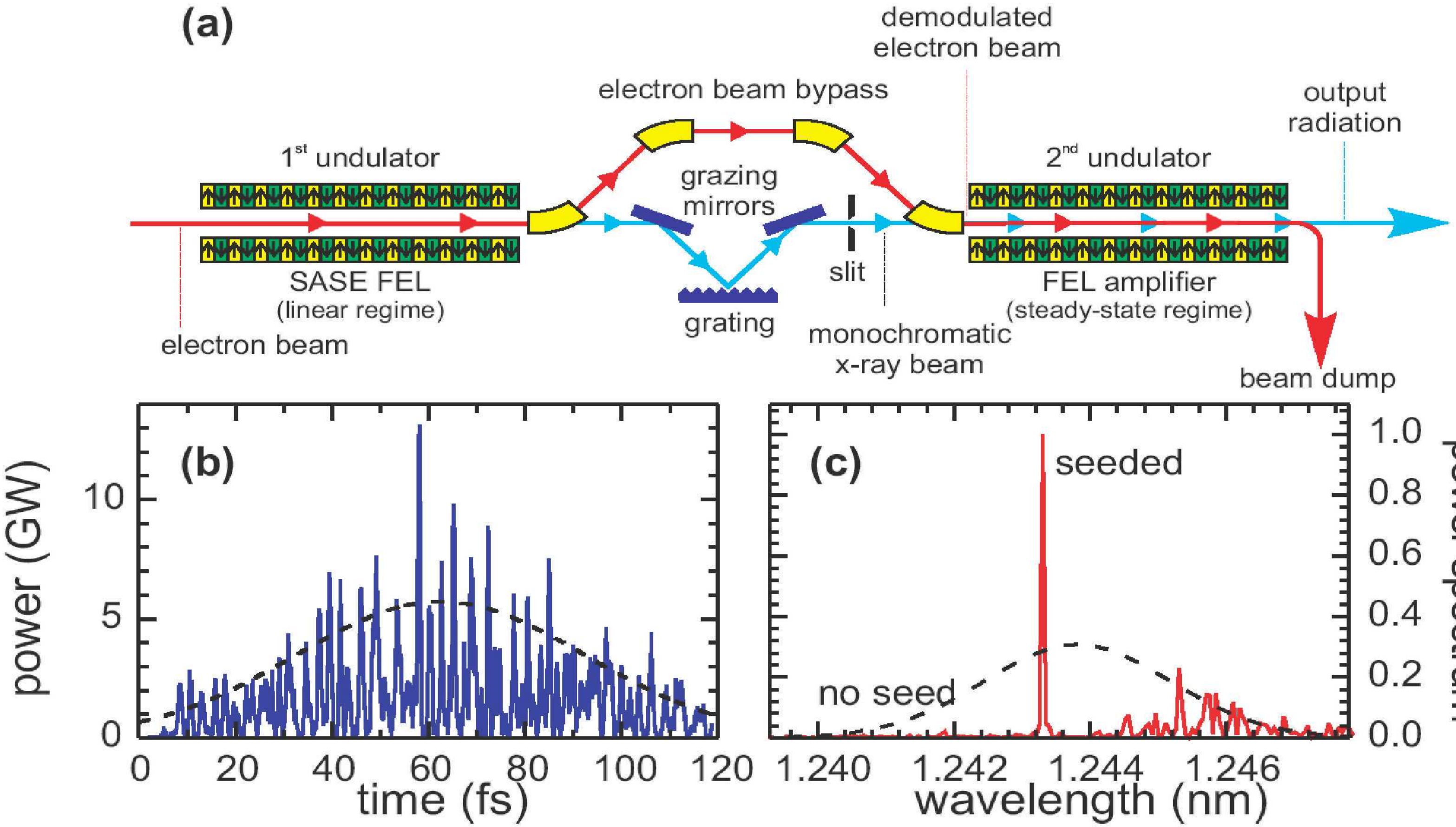

Top: Basic scheme of a two-stage FEL [16] providing full longitudinal and transverse coherent light, see text for details. Bottom: GENESIS simulation of the two-stage FEL employing a 3 kW seed in the second undulator.

First Ultraviolet High-Gain Harmonic-Generation Free-Electron Laser

L. H. Yu,* L. DiMauro, A. Doyuran, W. S. Graves,† E. D. Johnson, R. Heese, S. Krinsky, H. Loos, J. B. Murphy, G. Rakowsky, J. Rose, T. Shaftan, B. Sheehy, J. Skaritka, X. J. Wang, and Z. Wu

National Synchrotron Light Source, Brookhaven National Laboratory, Upton, New York 11973, USA

(Received 25 March 2003; published 14 August 2003)

We report the first experimental results on a high-gain harmonic-generation (HGHG) free-electron laser (FEL) operating in the ultraviolet. An 800 nm seed from a Ti:sapphire laser has been used to produce saturated amplified radiation at the 266 nm third harmonic. The results confirm the predictions for HGHG FEL operation: stable central wavelength, narrow bandwidth, and small pulse-energy fluctuation.

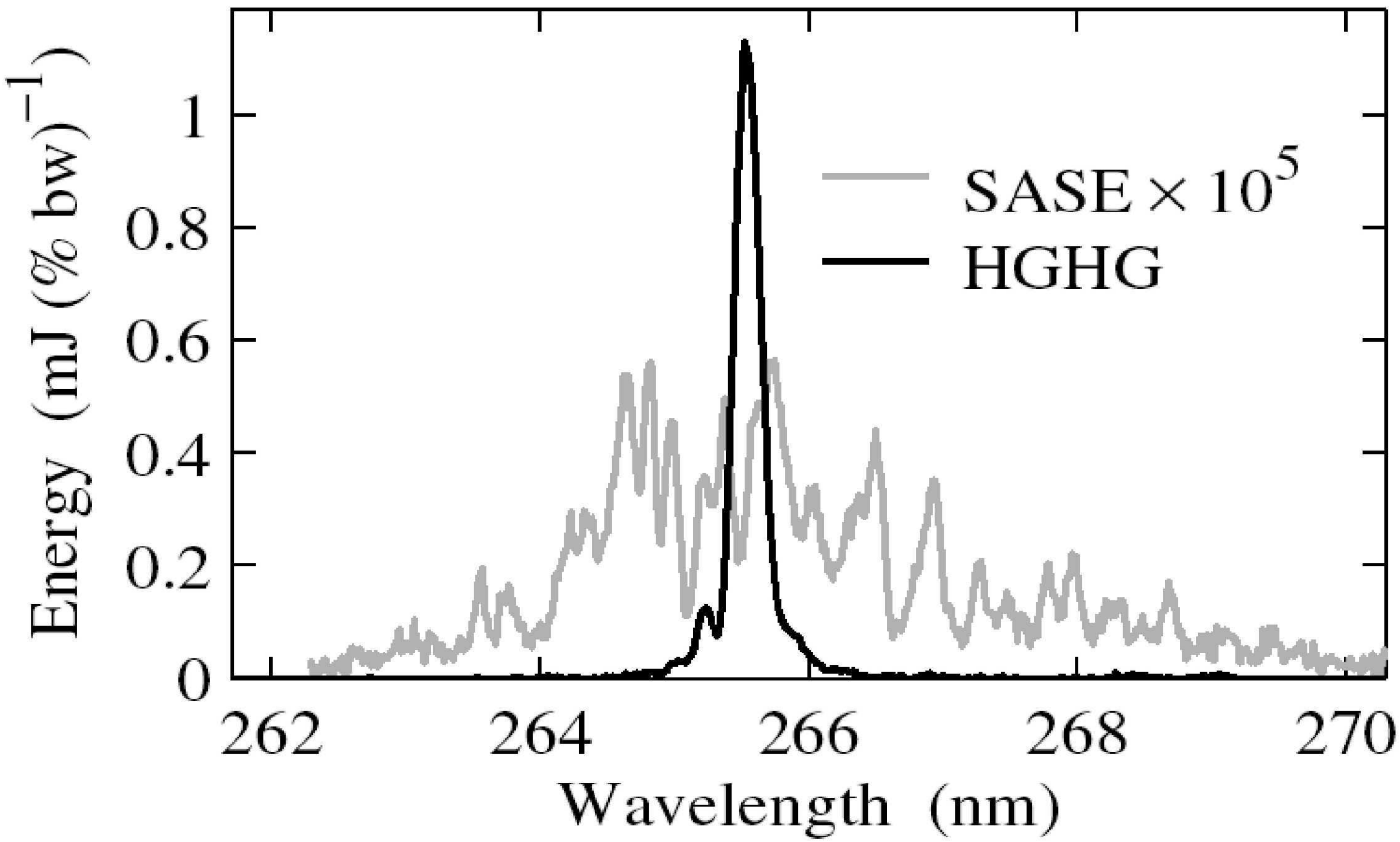

Performance

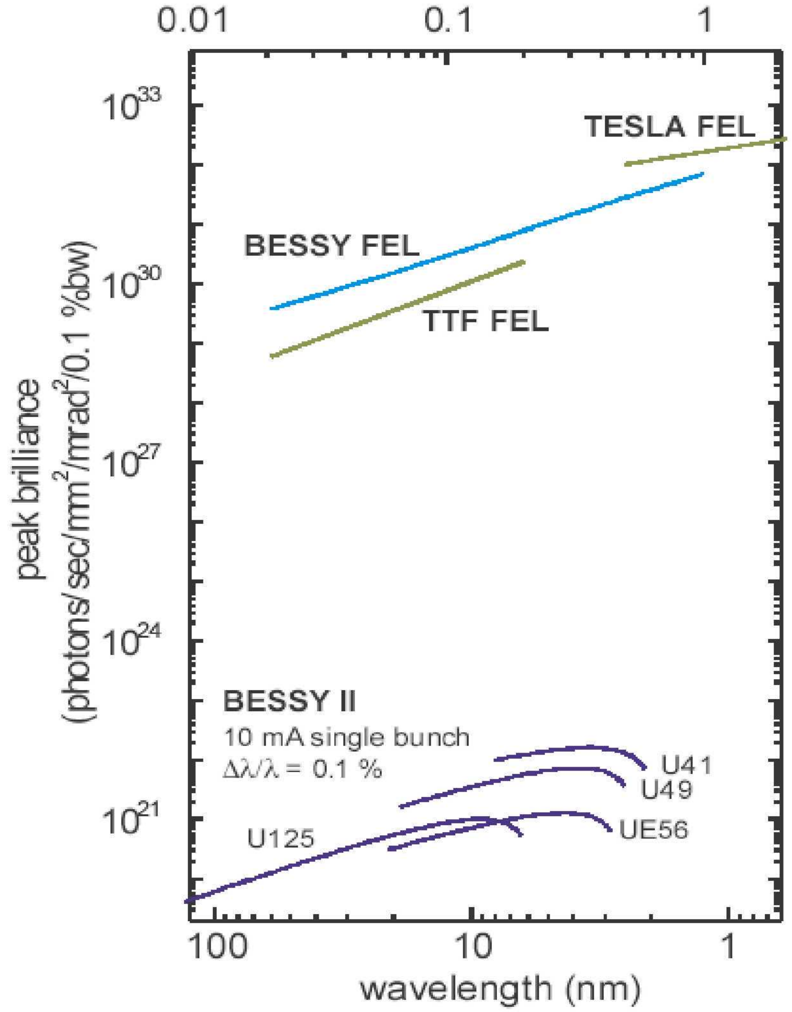

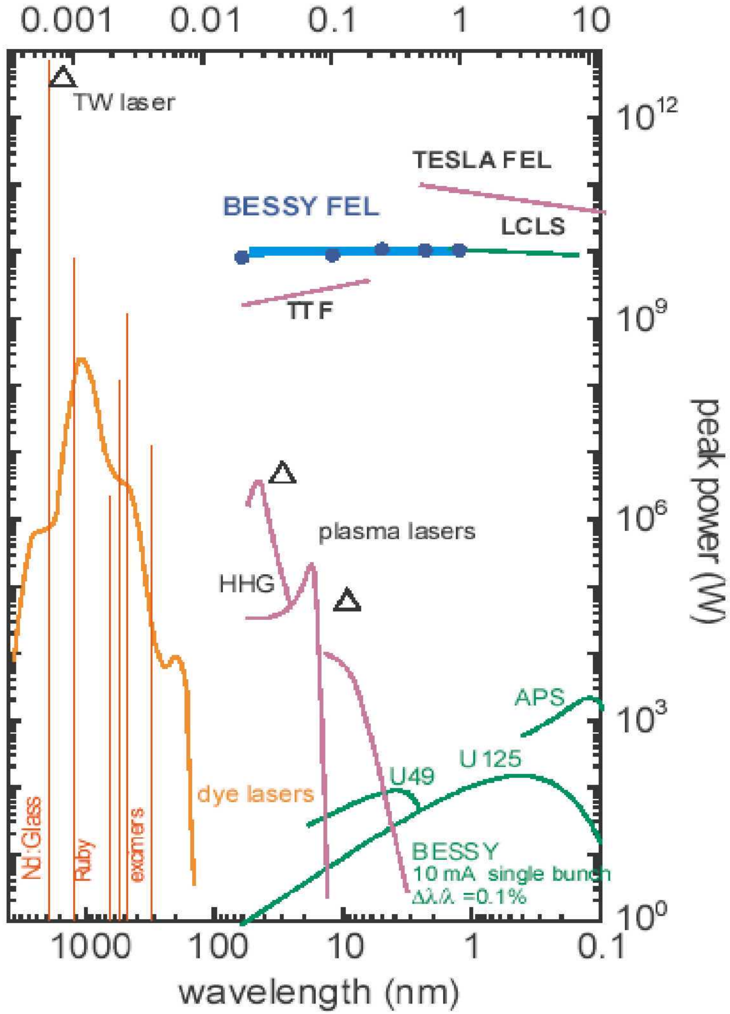

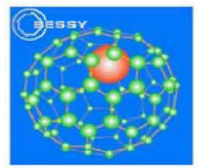

Peak Brightness Comparison

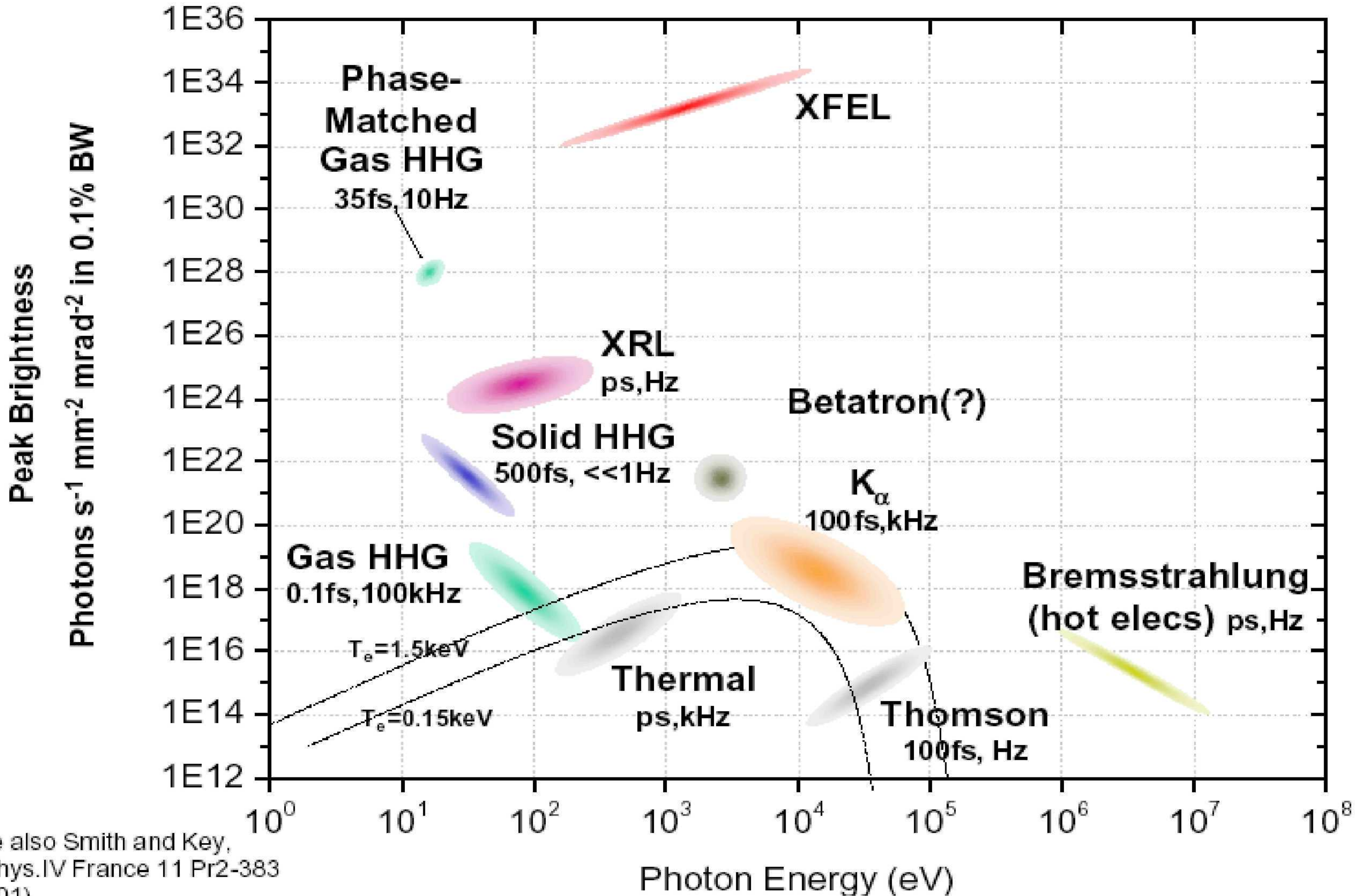

See also Smith and Key, J.Phys.IV France 11 Pr2-383 (2001)

Brilliance → **Microscopy**

- X-ray microscopy
- X-ray dichroic microscopy

Coherence → **X-ray scattering**

- X-ray elastic scattering (statistical optics)
- X-ray FT interferometry

Time structure → **Pump-Probe**

- Time resolved core level spectroscopy
- Time resolve spectroscopy zooming in the momentum space
- TR X-ray diffraction
- Dynamics of the phase transitions

Time structure

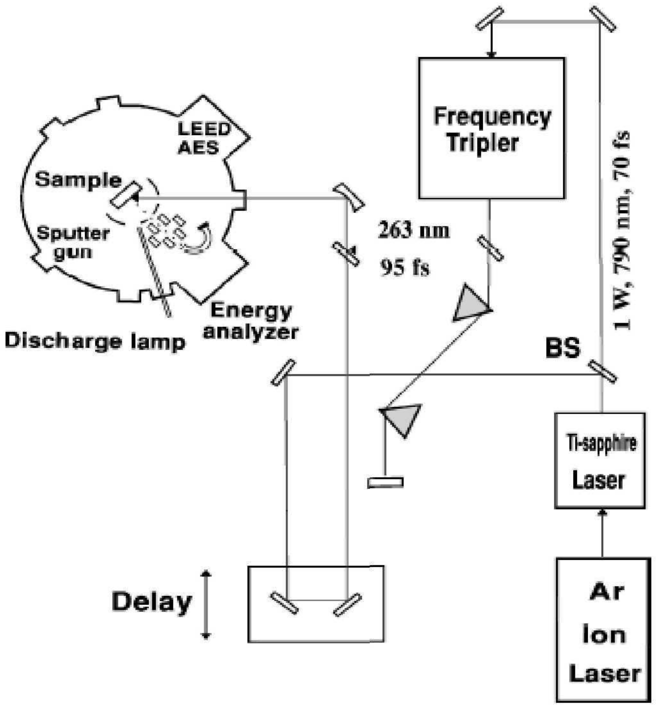

Pump - Probe setup

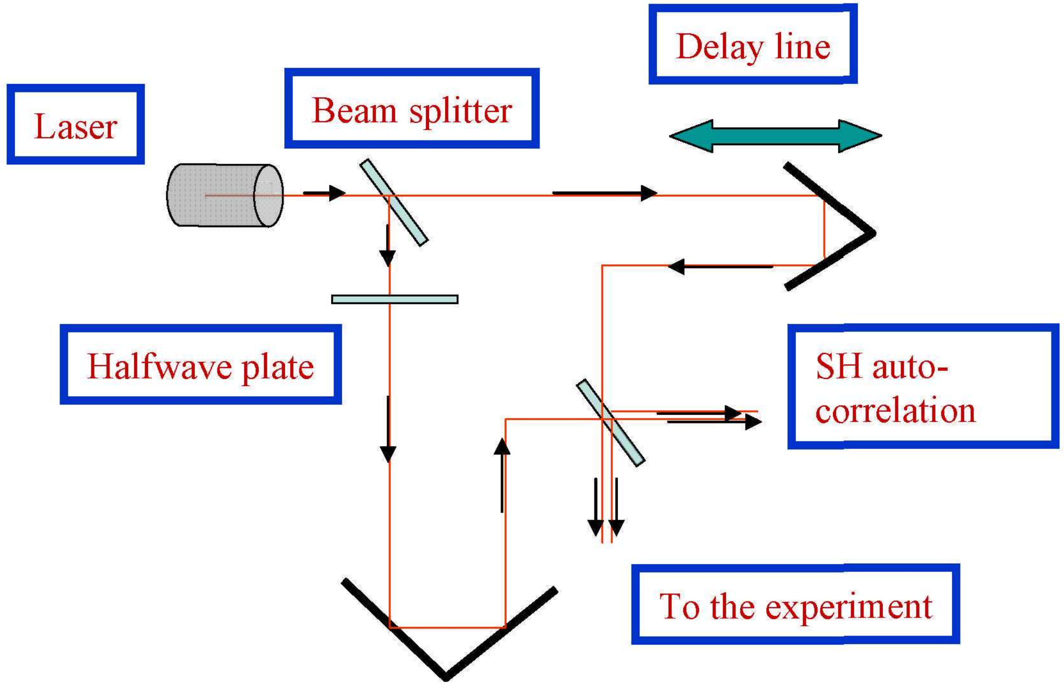

$$U_e(\tau) \propto \int_{-\infty}^{\infty} I_X(t) I_{IR}(t-\tau)\,dt$$

Mach Zehnder type interferometer

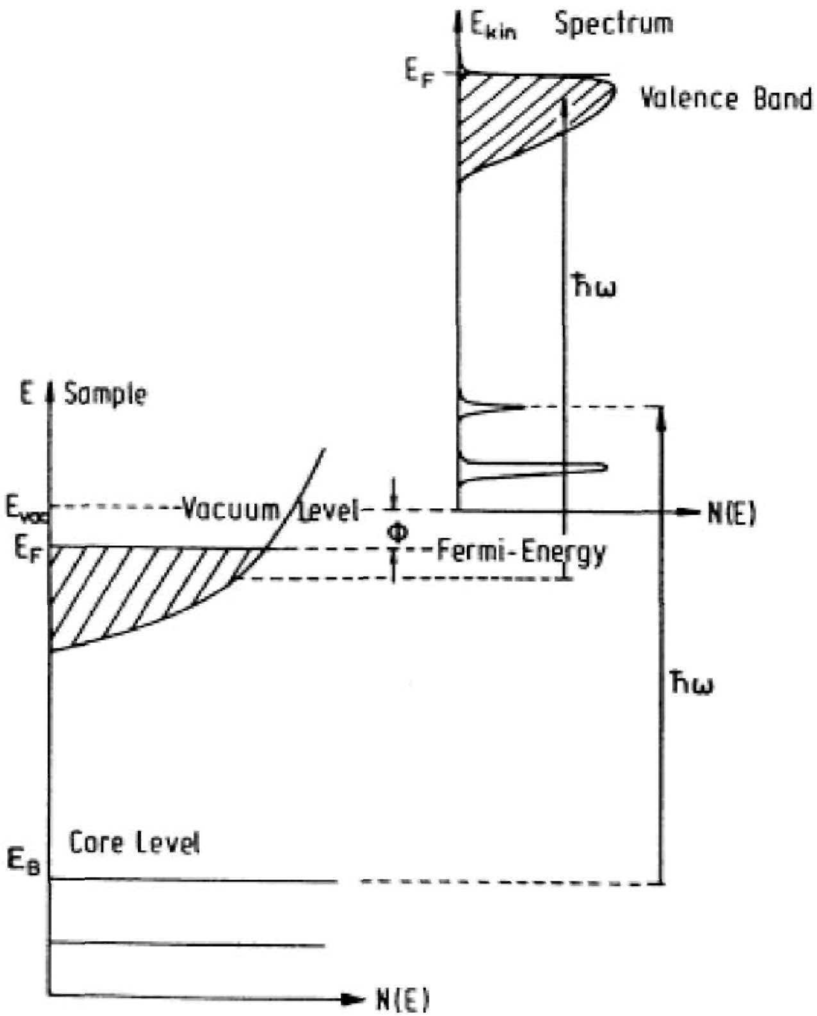

$$E_{kin} = \hbar\omega - \Phi \; - |E_B|$$

Measured Kinetic Energy

Measureed Photon Energy

Measured Work Function

Electron Binding Energy

150 fs Laser Pulse Measured by an Electron Time of Flight Spectrometer

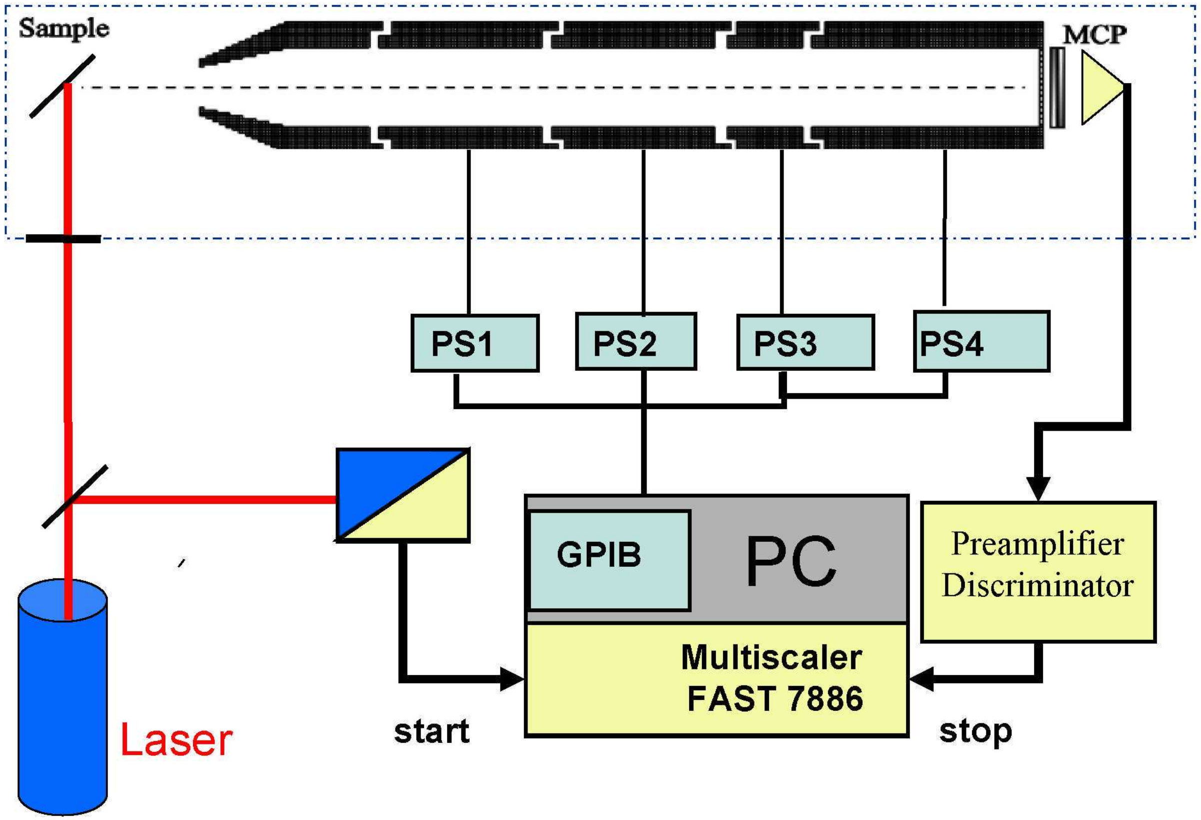

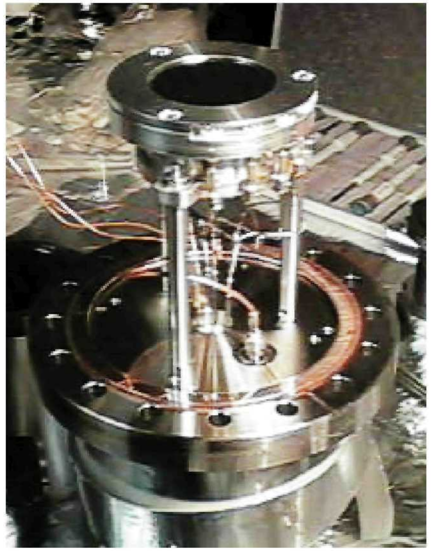

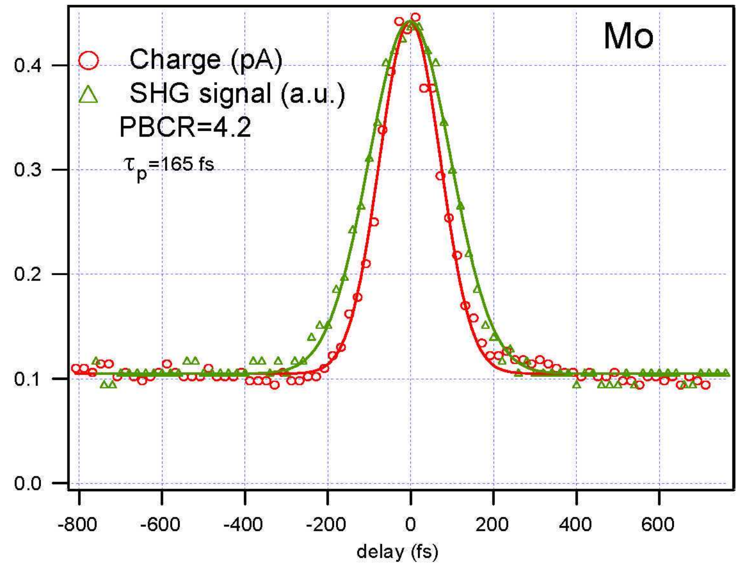

F.Parmigiani et al.

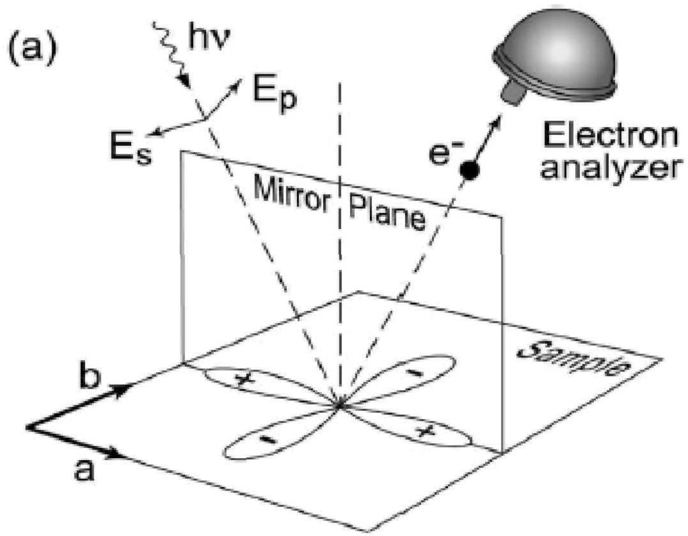

$$w_{fi}=\frac{2\pi}{\hbar}|\langle\Psi_f^N|H_{int}|\Psi_i^N\rangle|^2\,\delta(E_f^N-E_i^N-h\nu)$$

$$H_{int}=-\frac{e}{2mc}(\mathbf{A}\cdot\mathbf{p}+\mathbf{p}\cdot\mathbf{A})=-\frac{e}{mc}\mathbf{A}\cdot\mathbf{p}$$

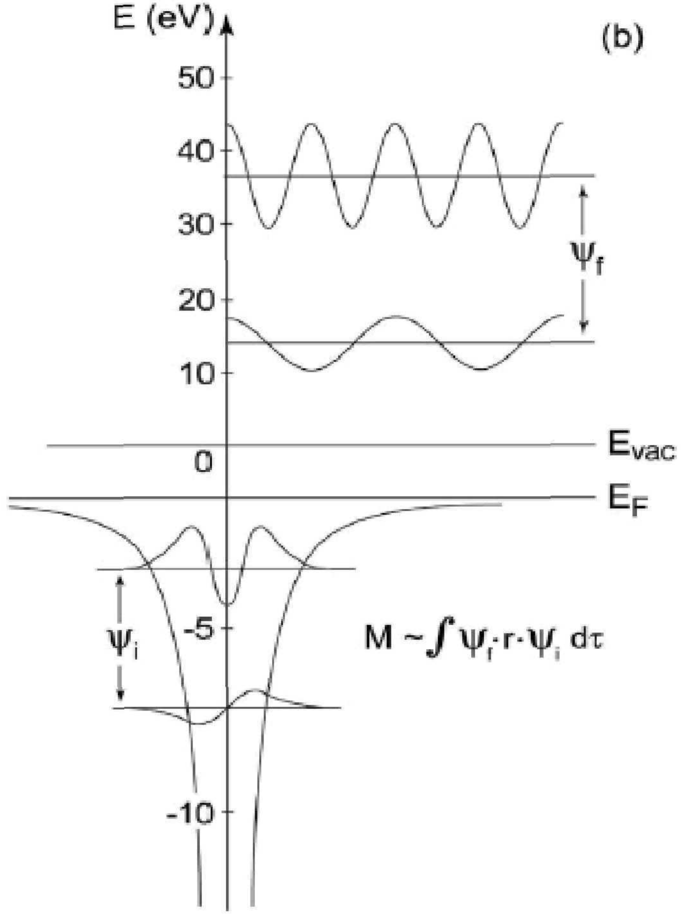

Time-Resolved Photoemission

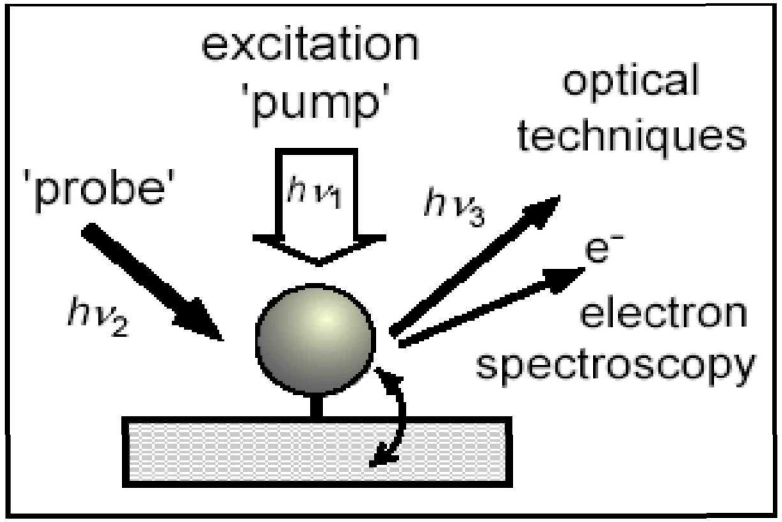

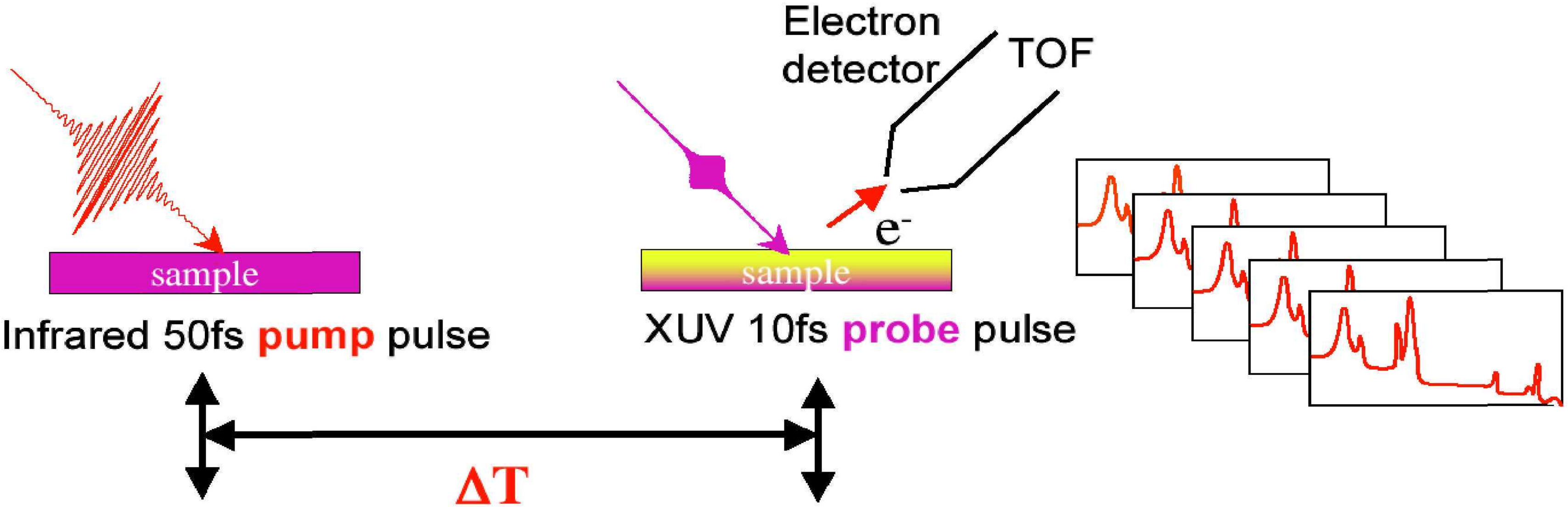

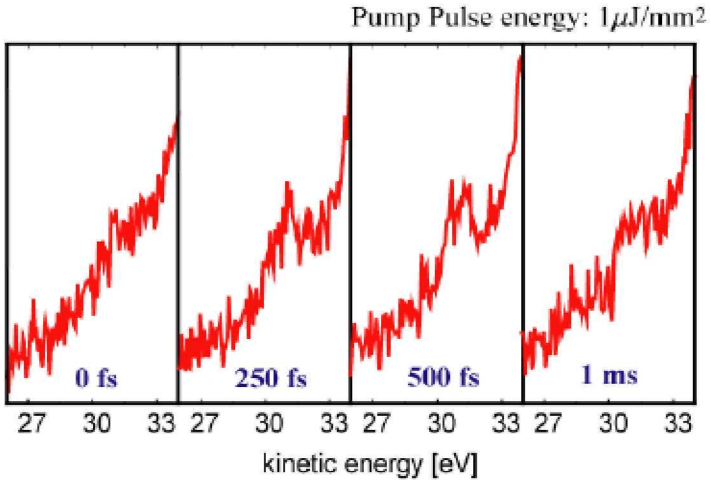

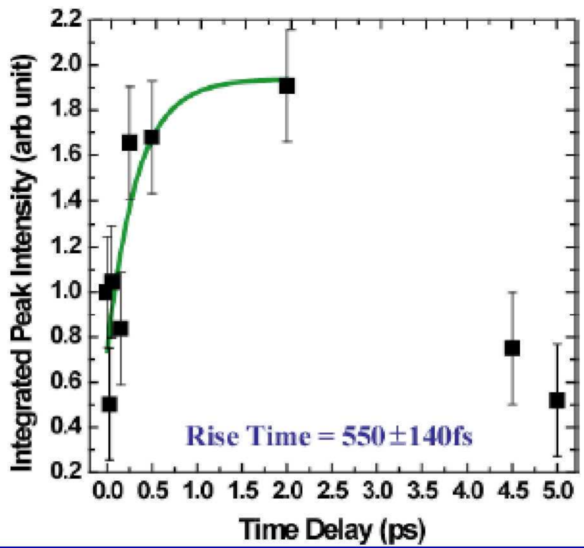

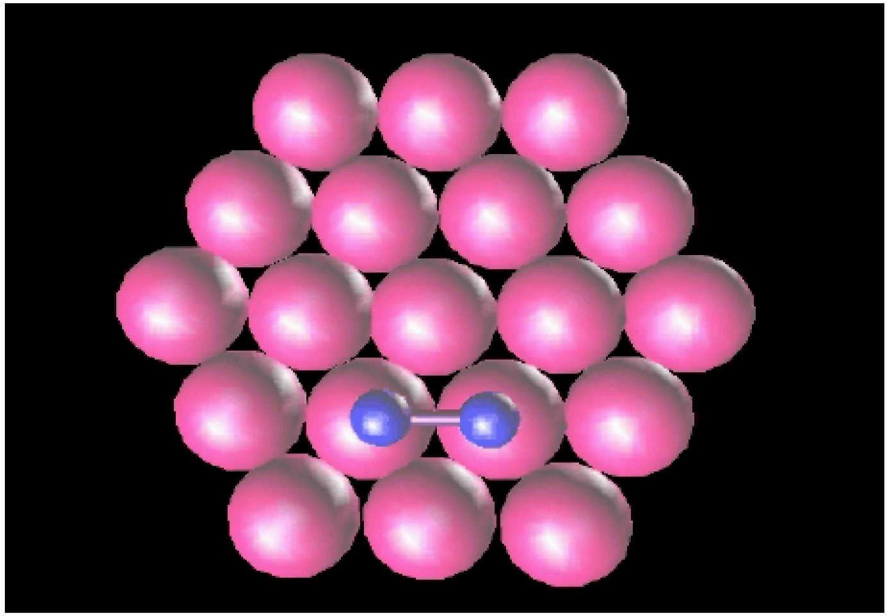

PRL 87, 25501 (2001)

Hot electron mediated surface charge transfer process on 100-500fs timescales

- **Perturbation Theory gives Fermi's Golden Rule for transition probability**

$$w = \frac{2\pi}{\hbar} \left| \left\langle \psi_f \middle| H_{\text{int}} \middle| \psi_i \right\rangle \right|^2 \delta(E_f - E_i - \hbar\omega)$$

- **For dipole allowed transitions,**

$$H_{\text{int}} = \frac{e}{mc} \mathbf{A} \cdot \mathbf{p}$$

Transmission absorption measurements

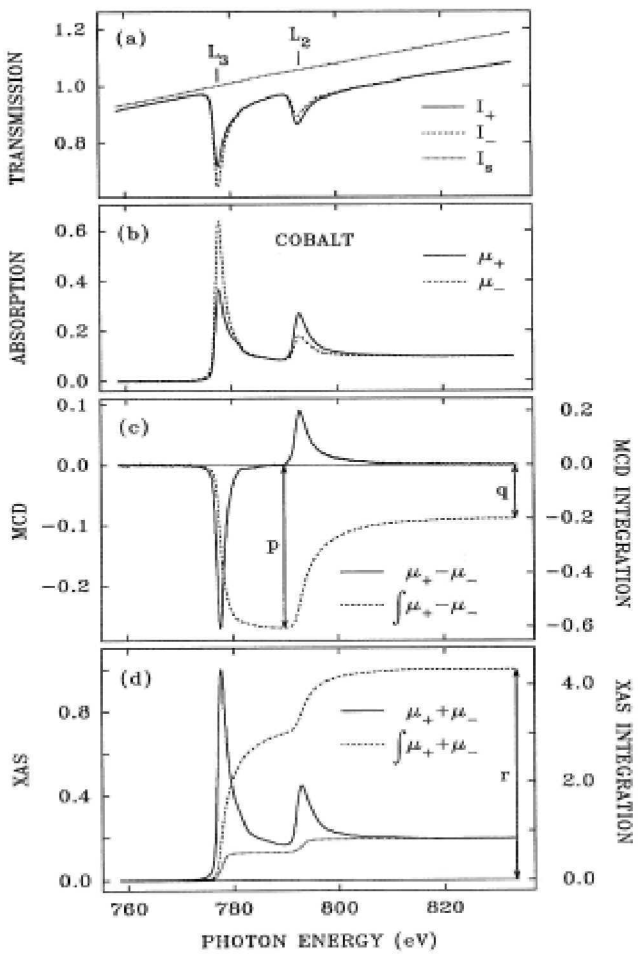

C.T.Chen et.al, PRL **75**, 152 (1995).

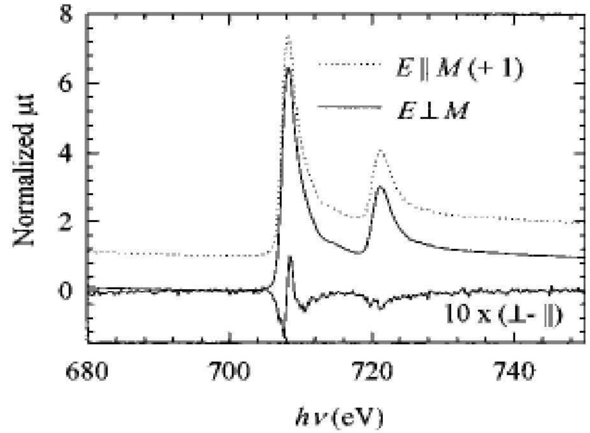

FIG. 5. Normalized transmission absorption spectra through a 32-nm Fe film at normal incidence with **E**⊥**M** and **E**∥**M** are offset by 1 in $\beta_\perp$ and $\beta_\parallel$, respectively. $\beta_\perp - \beta_\parallel$, multiplied by 10 and offset by 3 gives the MLD (Voigt effect).

Kortright & Kim, PRB **62**, 12216 (2000).

X-ray Fluorescence, Gd 2p3d and 2p 4d

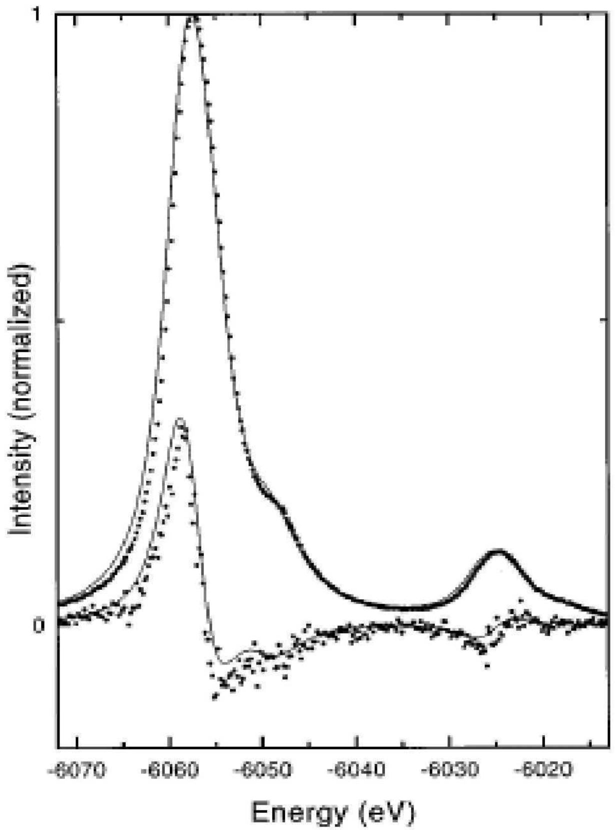

FIG. 3. Comparison of the calculated $2p3d$ x-ray emission spectral shape (solid line), with the $2p_{3/2}3d$ experimental results (points). The experimental curve is aligned and normalized to 1.0 at the peak position, with respect to the calculation. The theoretical MCD spectrum is given in the scale of the emission spectrum, and the experimental MCD has been normalized to it.

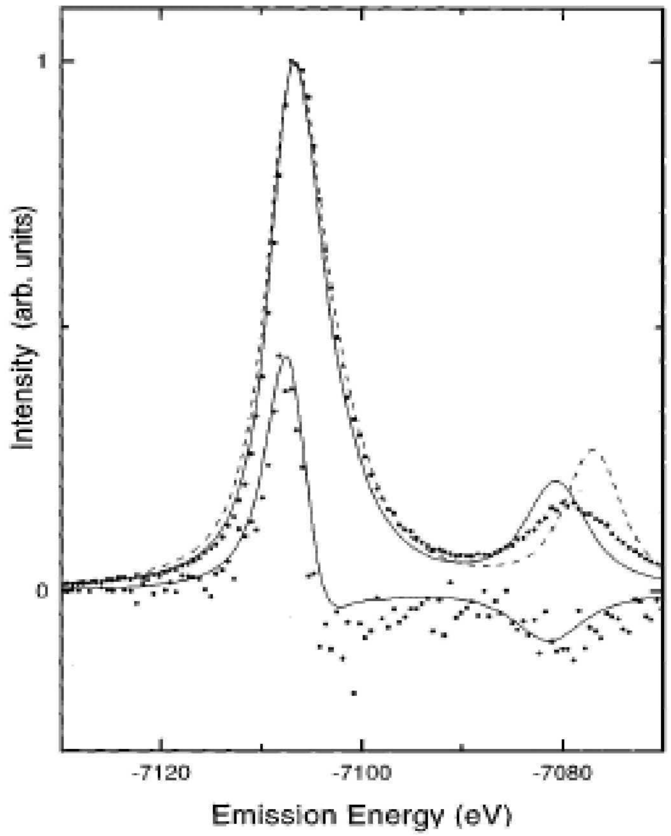

FIG. 4. Comparison of the calculated $2p4d$ x-ray emission spectral shape (dashed), with the $2p_{3/2}4d$ experimental results (points). The experimental curve is aligned and normalized to 1.0 at the peak position, with respect to the calculation. The solid line is the theoretical result with a reduction of the Slater integrals to 70% and a broadening as described in the text. The theoretical MCD spectrum is given in the scale of the emission spectrum, and the experimental MCD has been normalized to it.

de Groot et.al, PRB 56, 7625 (1997).

Microscopy by MXLD - MXCD: AF-FM interface coupling

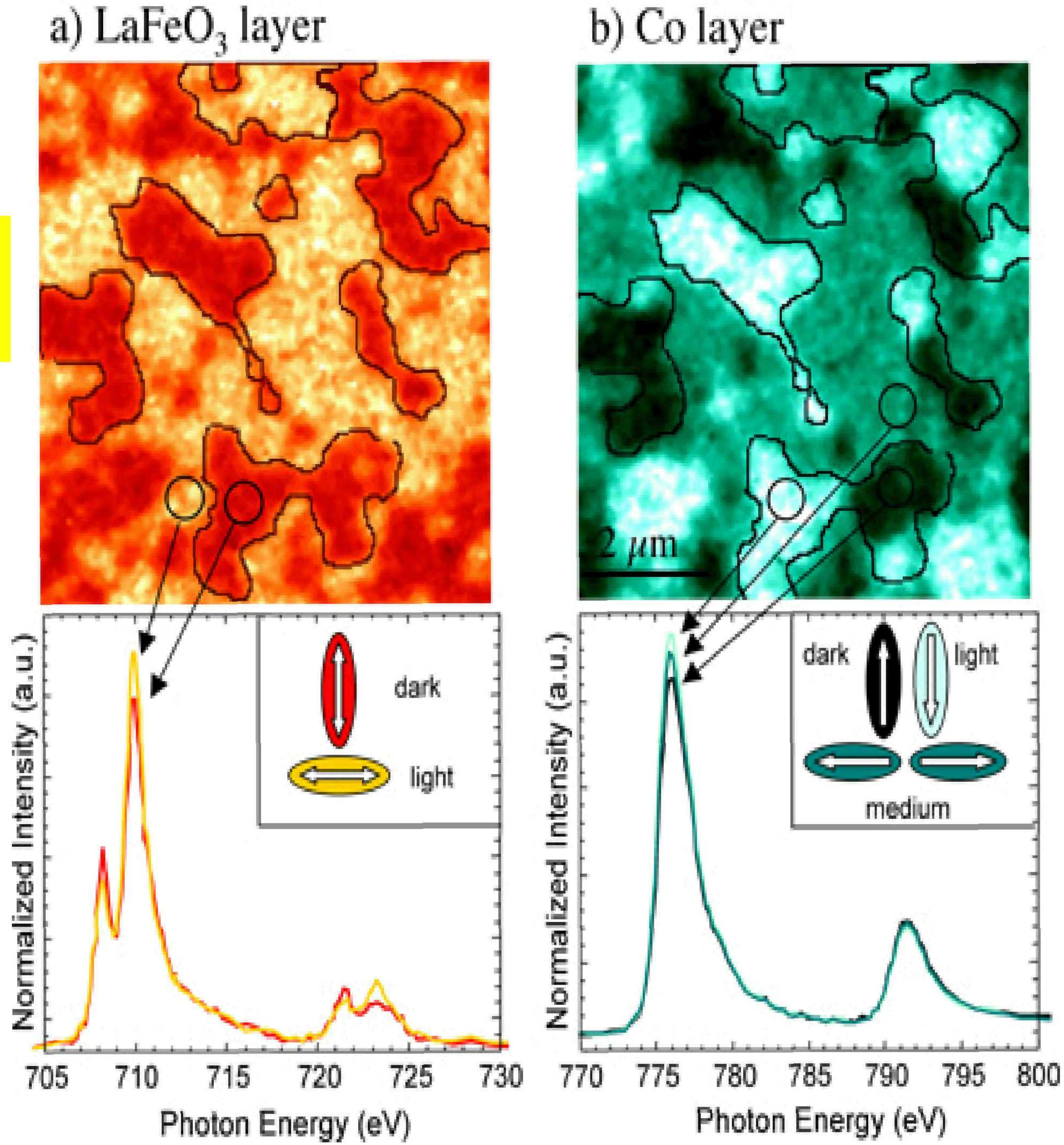

F. Nolting et al., Nature 405, 767 (2000)

Some preliminary considerations

• Type of experiments

Pump-probe

Single pulse

• Energy resolution / momentum resolution:

$\Delta E \times \Delta t \geq h/4\pi$

$\Delta \underline{\mathbf{p}} \times \Delta \underline{\mathbf{x}} \geq h/4\pi$

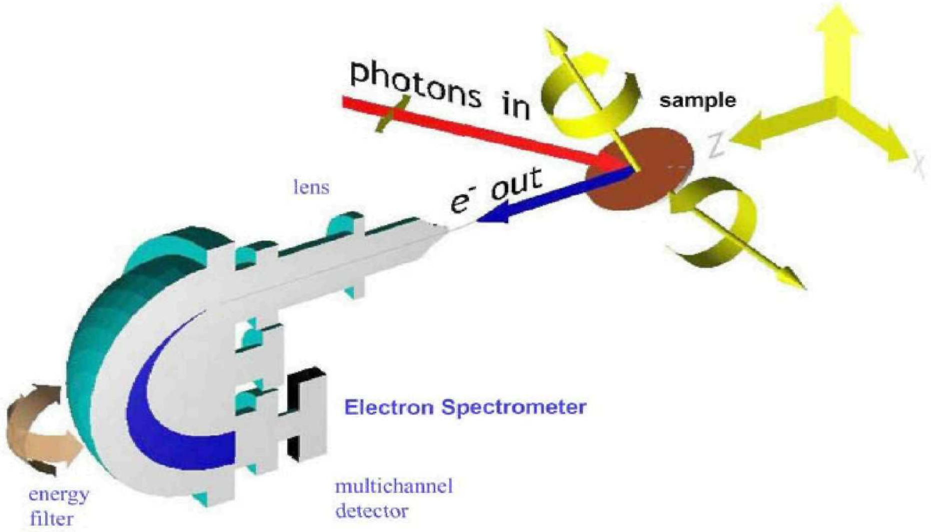

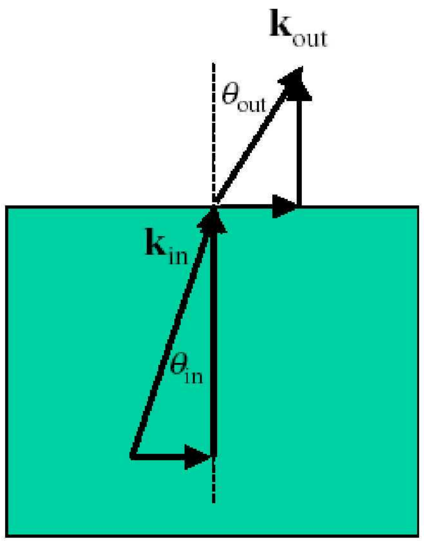

Kinematic relations

$$k_{out} = \sqrt{\frac{2m}{\hbar^2} E_{kin}}$$

$$k_{in} = \sqrt{\frac{2m}{\hbar^2}(E_{kin} + V_0)}$$

$$k_{out,\parallel} = k_{in,\parallel} \equiv k_{\parallel}$$

"Snell's Law"

$$k_{\parallel} = \sin\theta_{out}\sqrt{\frac{2m}{\hbar^2} E_{kin}} = \sin\theta_{in}\sqrt{\frac{2m}{\hbar^2}(E_{kin} + V_0)}$$

Critical angle for emission

$$(\sin\theta_{out})_{\max} = \sqrt{\frac{E_{kin}}{E_{kin} + V_0}}$$

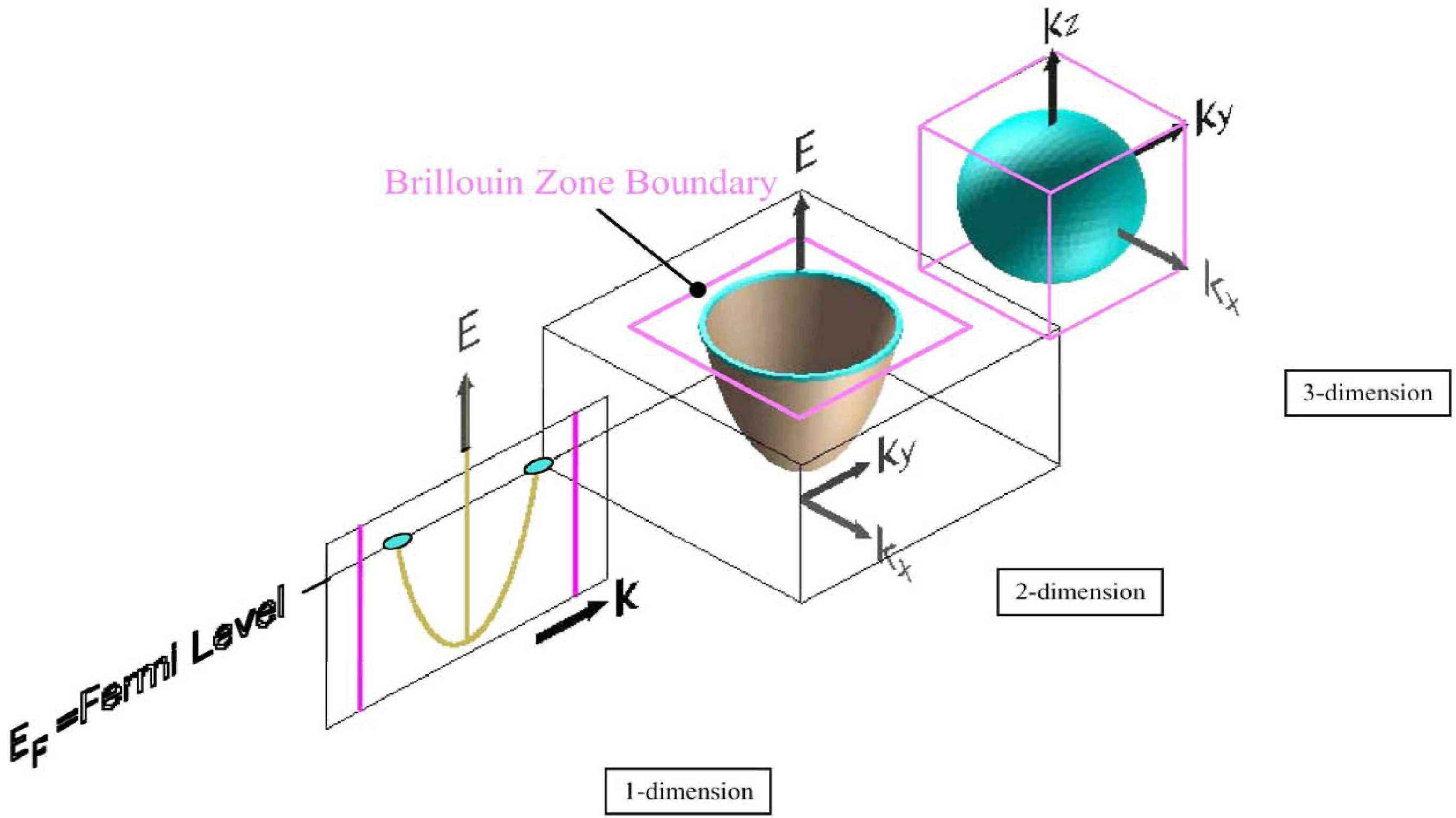

Brillouin Zone Boundary
E
E
Kz
Ky
Kx
Ky
Kx
K
E_F =Fermi Level
3-dimension
2-dimension
1-dimension

Time-Resolved and Angle Resolved Photoelectron Spectroscopy – TR-ARPES and Time-Resolved and Spin Resolved ARPES – TR-SR-ARPES (started 2006)

Objectives

Scope of the project is to design and built an angle resolved and time resolved photoemission system with a spin detector.

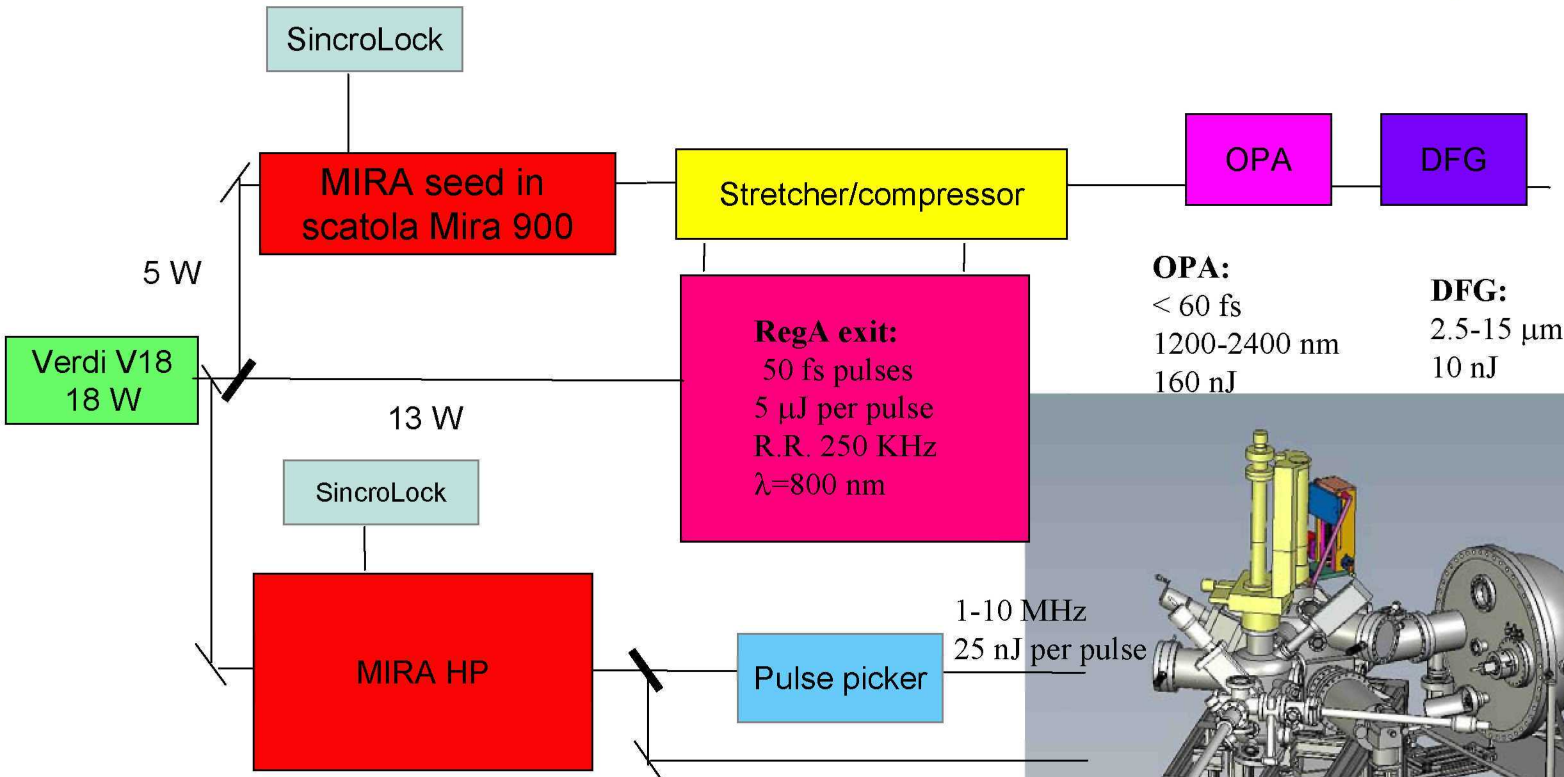

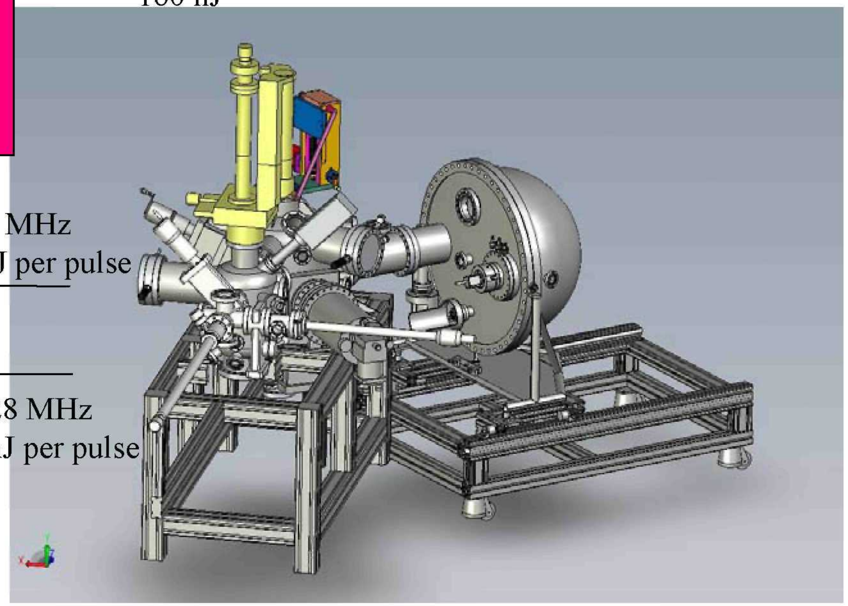

10 K Minimum Temperature on the Sample
6 degrees of Freedom motorized
sub meV Resolution
40 degrees Angular Acceptance
Max Ang Resolution 0.1 degrees
Plug and play upgradable for Spin detection

Band Mapping and Fermi Contours

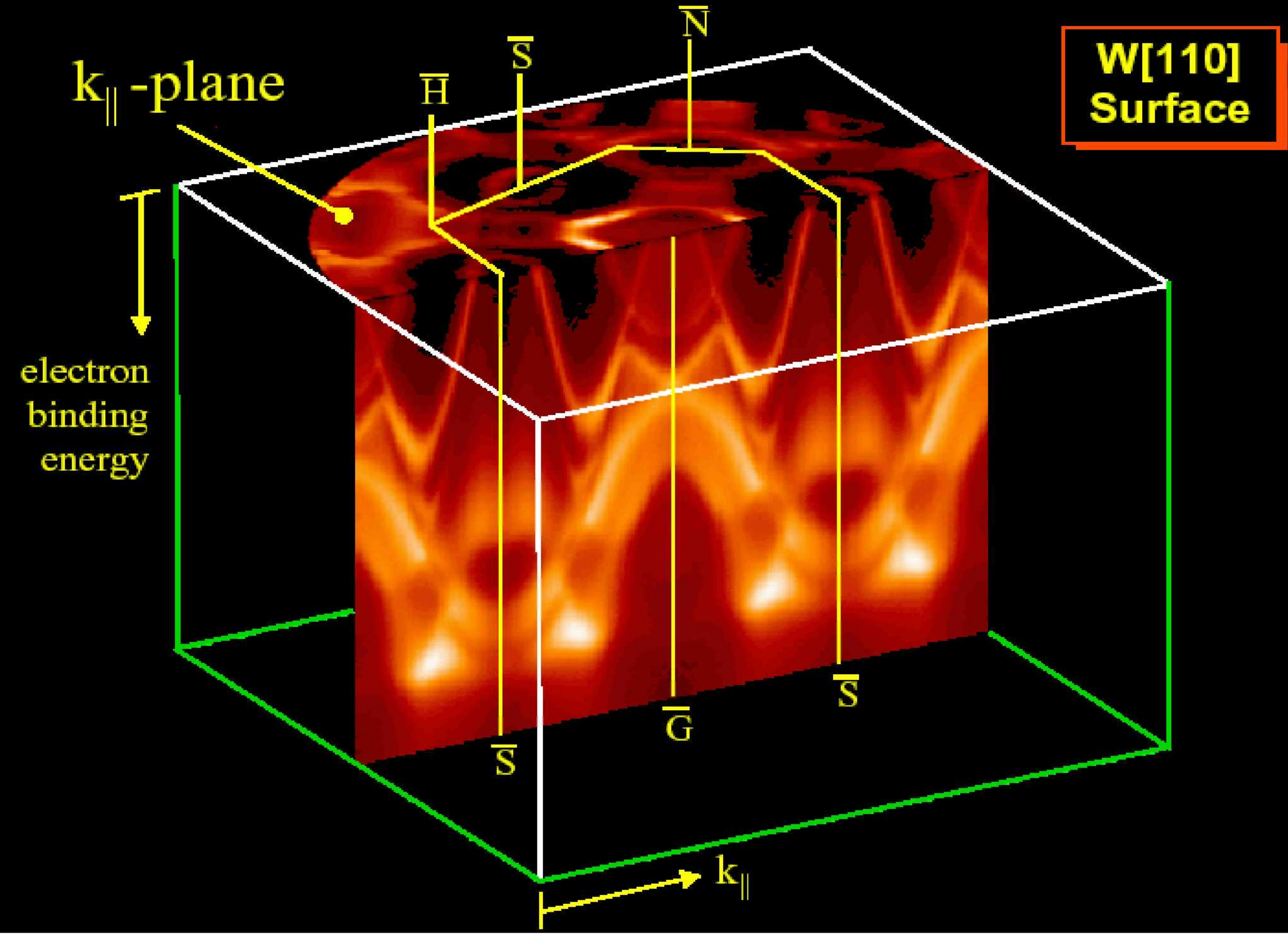

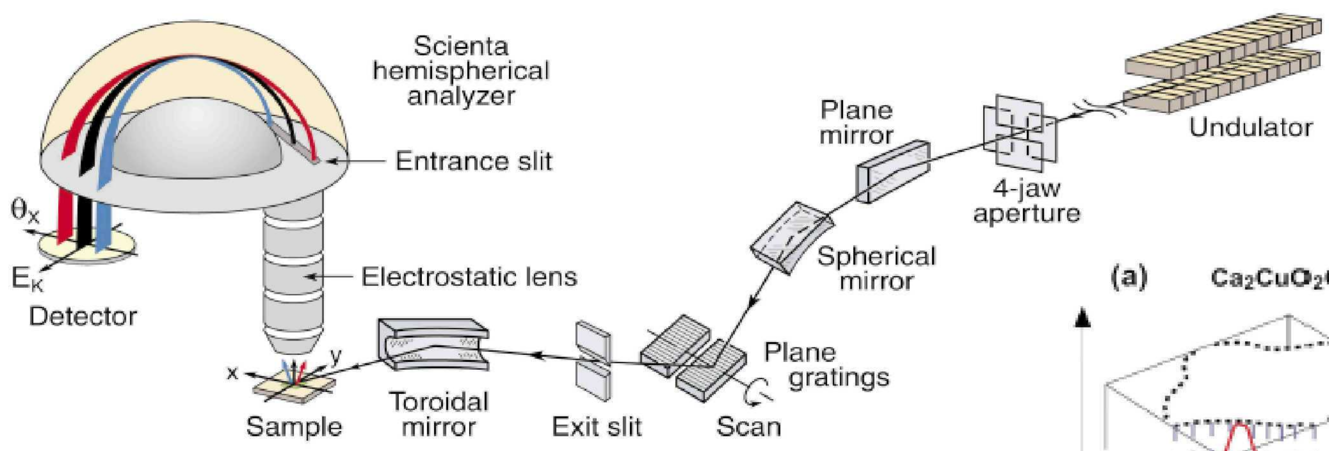

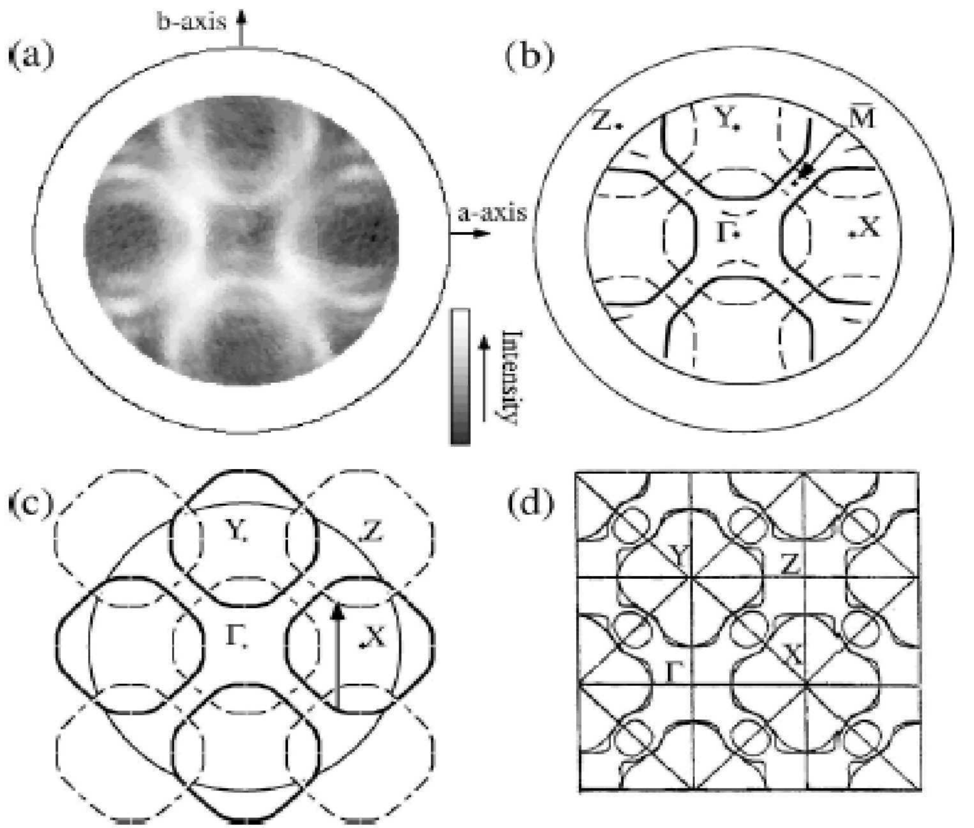

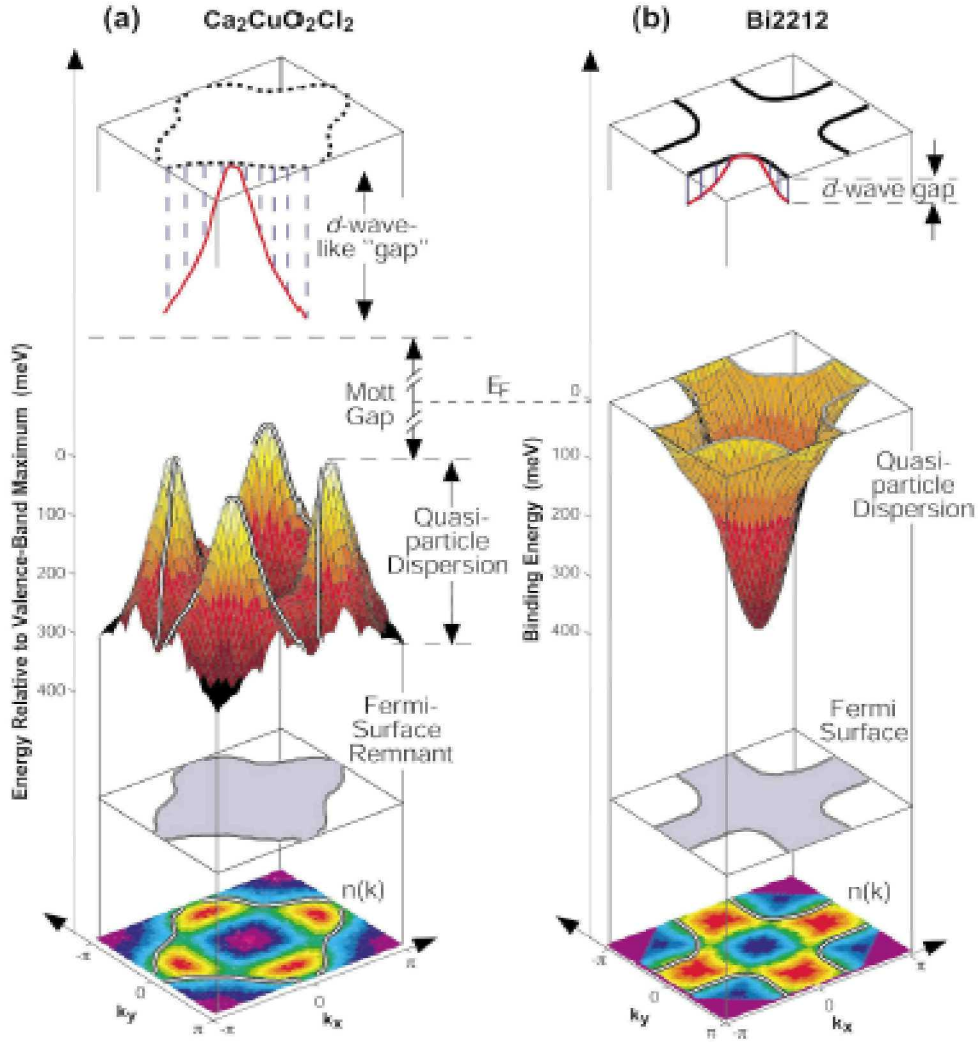

Damascelli, Hussain, and Shen: REVIEWS OF MODERN PHYSICS, VOLUME 75, APRIL 2003

FERMI Surface dynamics

In two recent papers has been shown that it is possible the control of the electronic phase of a manganite by mode-selective vibrational excitation [M. Rini et al., Nature **449**, 72 - 74 (2007)] and to measure the ultrafast electron relaxation in superconducting $Bi_2Sr_2CaCu_2O_{8+\delta}$ by time-resolved photoelectron spectroscopy [L. Perfetti et. al.,Phys. Rev. Lett. **99**, 197001 (2007)]. Our aim is to study the breathing of the Fermi surface in K_3C_{60} (Fig 4) and similar system by exciting the structure through selective mode vibrations [Science, **300**, 2003].

K_3C_{60}

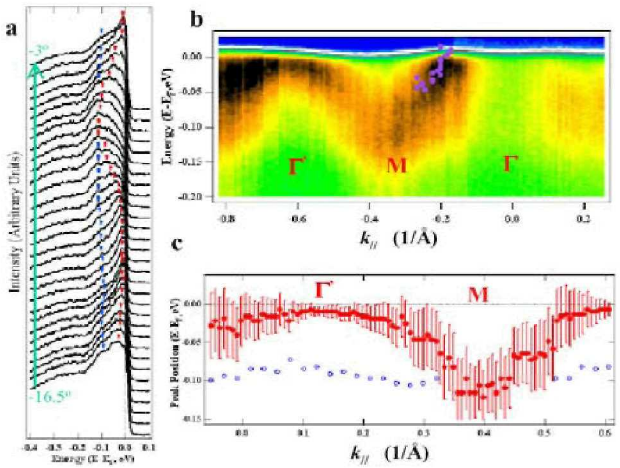

Science, 300, 2003

Cobaltites

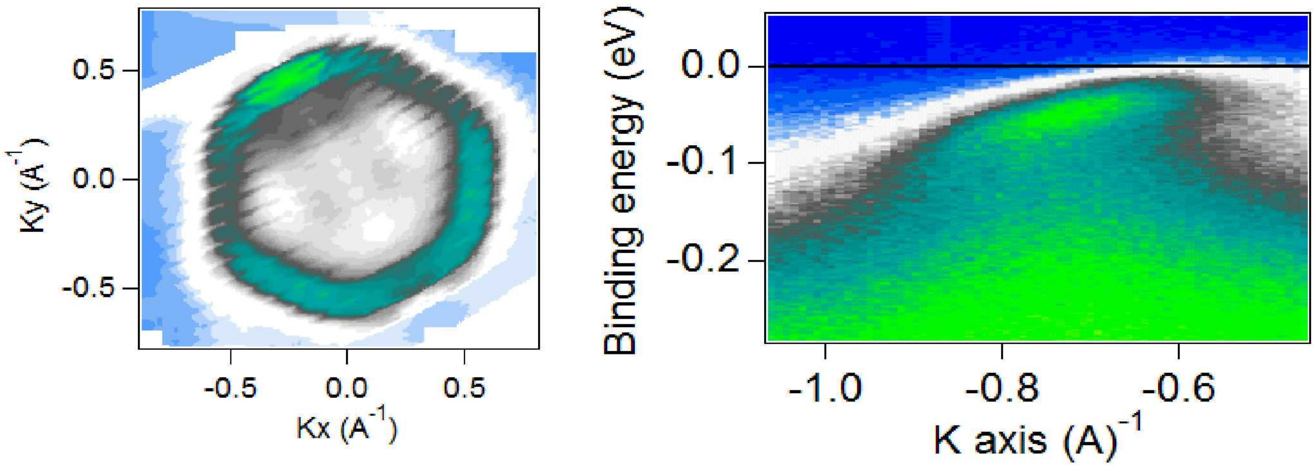

Brouet, Nicolaou, Zacchigna PRB 76, 100403 (07)

Spin states dynamics

Objective

The goal of this project is to measure the spin resolved band dispersion and spin dynamics in solid by harmonics and high harmonics generated from a 250 kHz Ti:SA amplified source

Time-of-Flight analyser
@ high operating frequency
(up to 5 MHz)

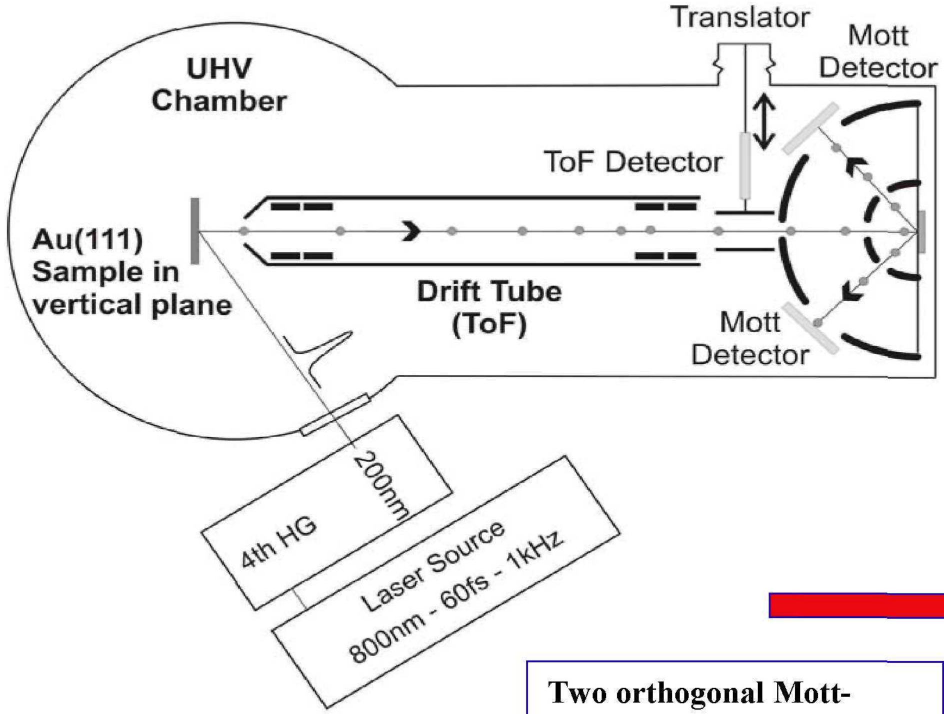

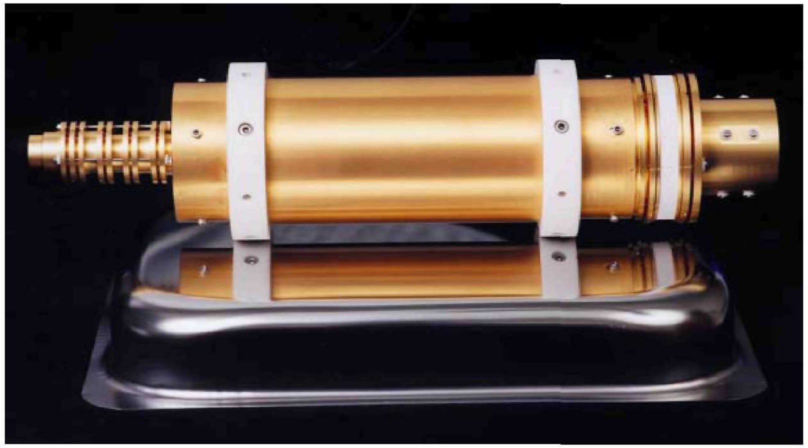

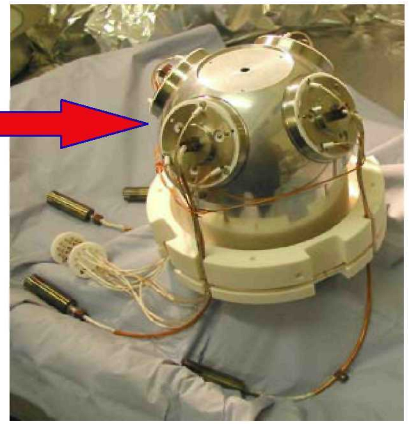

Two orthogonal Mott-detectors to measure V and H spin components

Electron detector

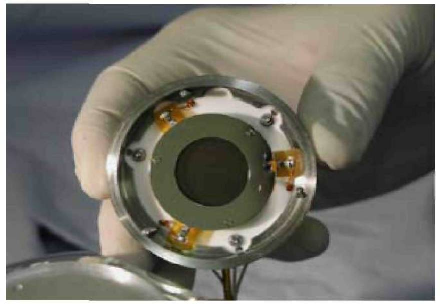

Mott polarimeter

Collaboration with 4GLS (E. Seddon and C. Cacho)

Test of the SR-TR ToF on the Au(111) surface states

- ✓TR- and AR-Photoemission
- ✓Time and Spin resolved experiments
- ✓Fermi surface mapping

Spin-orbit coupling $H_{SO} = \frac{1}{2c^2}\vec{S}\cdot(\vec{\nabla}V \times \vec{p})$

$$V(\vec{r}) = V_0(r,z) + V_3(r,z)\sin 3\varphi + V_6(r,z)\cos 6\varphi$$

$$\vec{\nabla}V = \alpha\,\vec{z} + \beta\,\vec{u}_\varphi \qquad \vec{p} = p\,\vec{u}_r$$

$$H_{SO} = \frac{p}{2c^2}(\alpha\vec{S}\cdot\vec{u}_\varphi + \beta\cos 3\varphi\,\vec{S}\cdot\vec{u}_z)$$

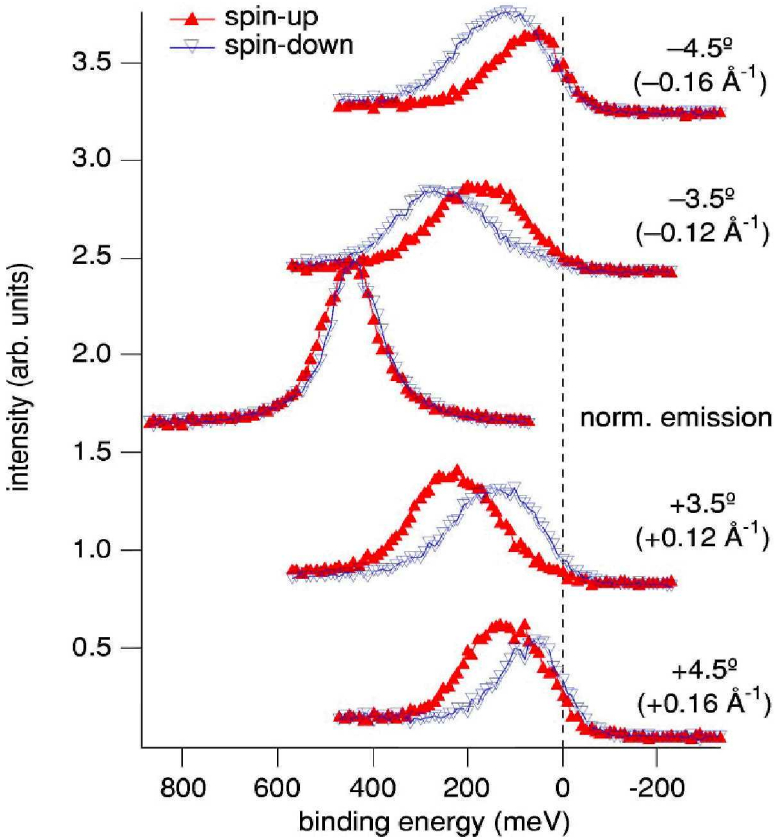

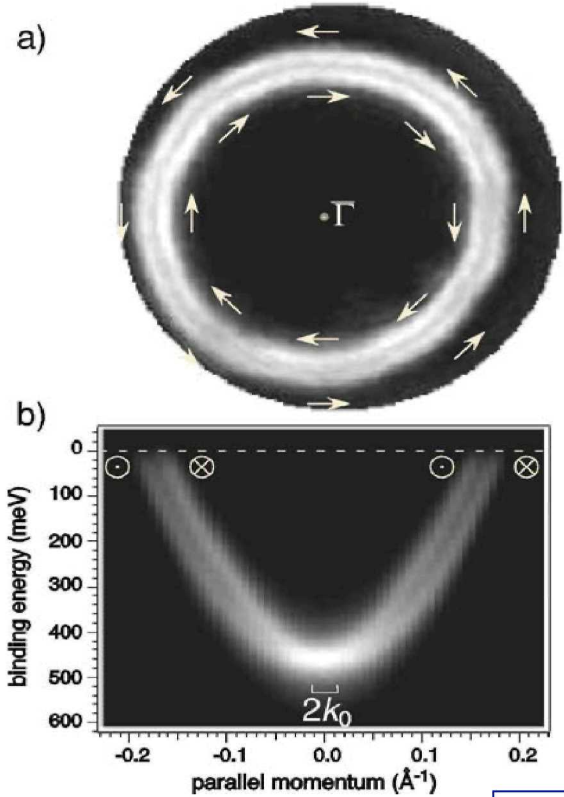

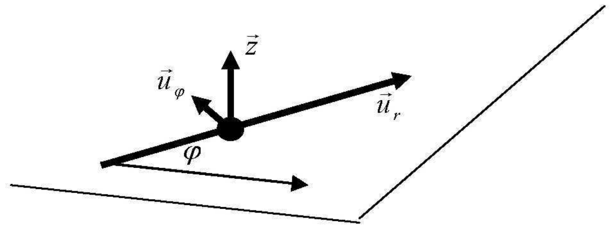

Osterwalder et al. PRB 69 pp.241401R, 2004)

Comparison between the 1kHz and 250kHz laser system

1kHz laser system
Total time = 4h
Total statistic = 4*23400 e-

250 kHz laser system
Total time = **1’ 20’’**
Total statistic = 4*22400 e-

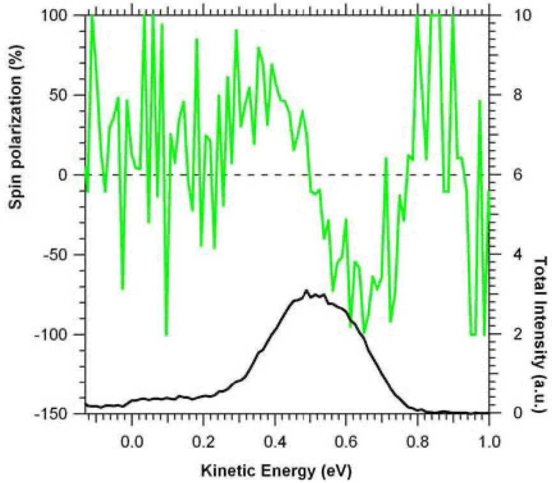

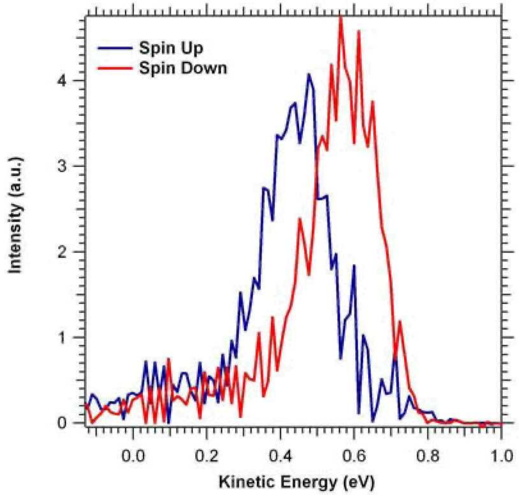

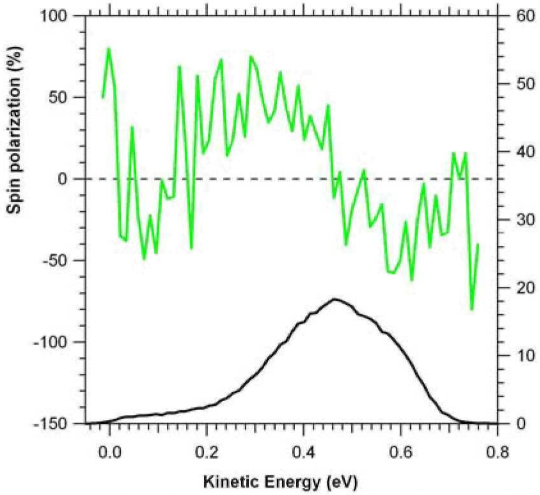

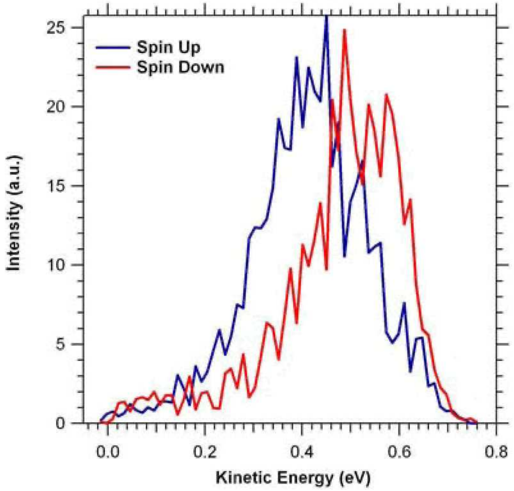

Space Charge Effects

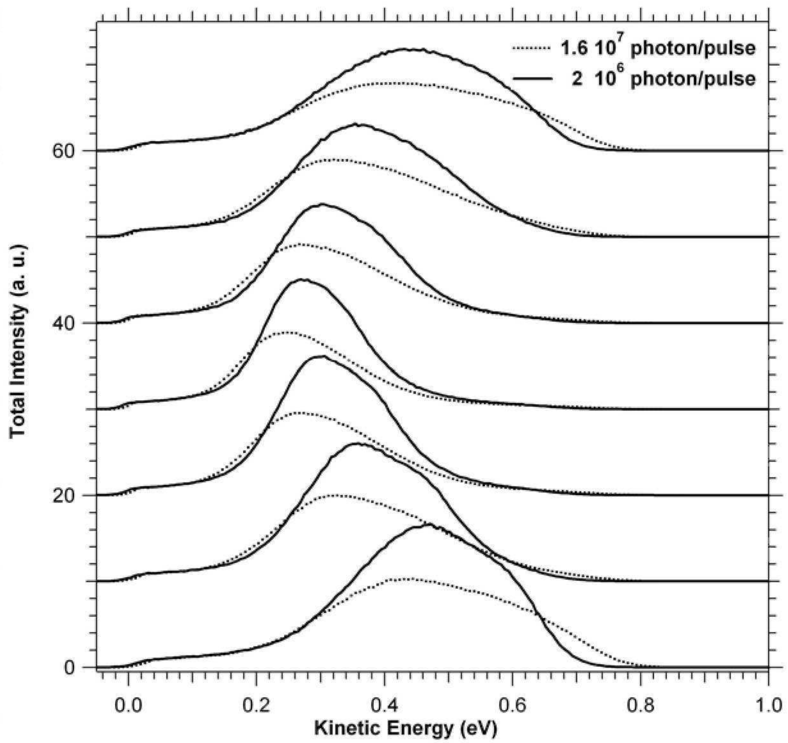

Ultrafast coherent imaging at Fermi

Spokesperson: H. Chapman (LLNL-CA) , J. Haidu (Stanford University and Uppsala University)

First EUV-FEL experiments show that structural information can be obtained before destruction

During 30 fs pulse (10^{14} W cm^{-2})
32 nm wavelength

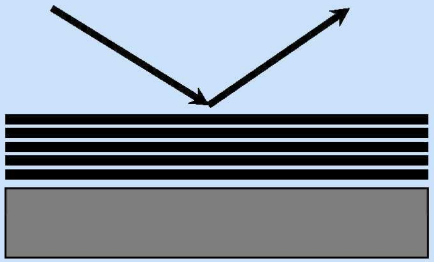

Reflectivity unchanged
Multilayer *d* spacing not changed by more than 0.3 nm

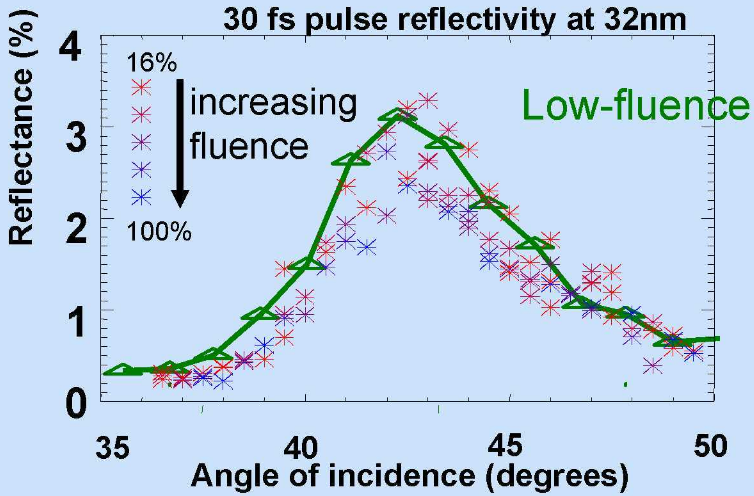

After pulse

Plasma forms, layers ablate

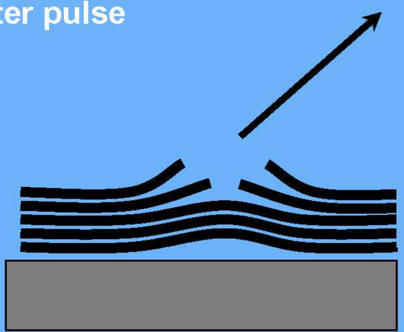

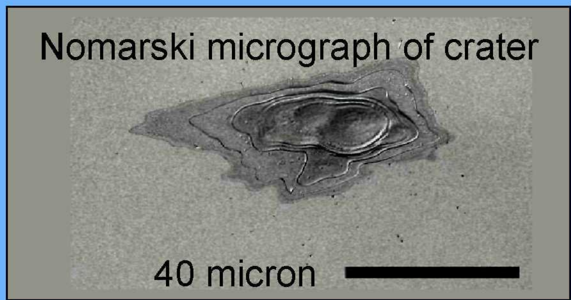

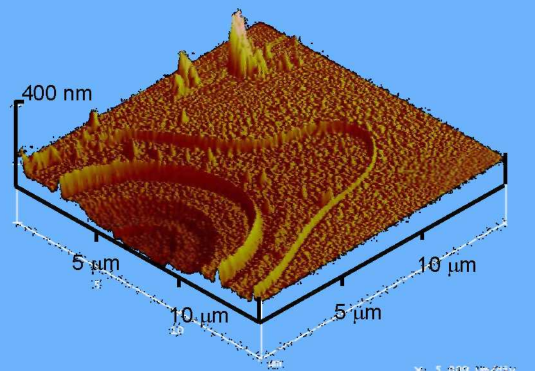

Peak Brightness Collaboration, R. Lee et al
J. Kryzwinski, R. Sobierajski, H. Chapman et al

Ultrafast coherent imaging at Fermi

Spokesperson: H. Chapman (LLNL-CA) , J. Haidu (Stanford University and Uppsala University)

Single-shot experiments

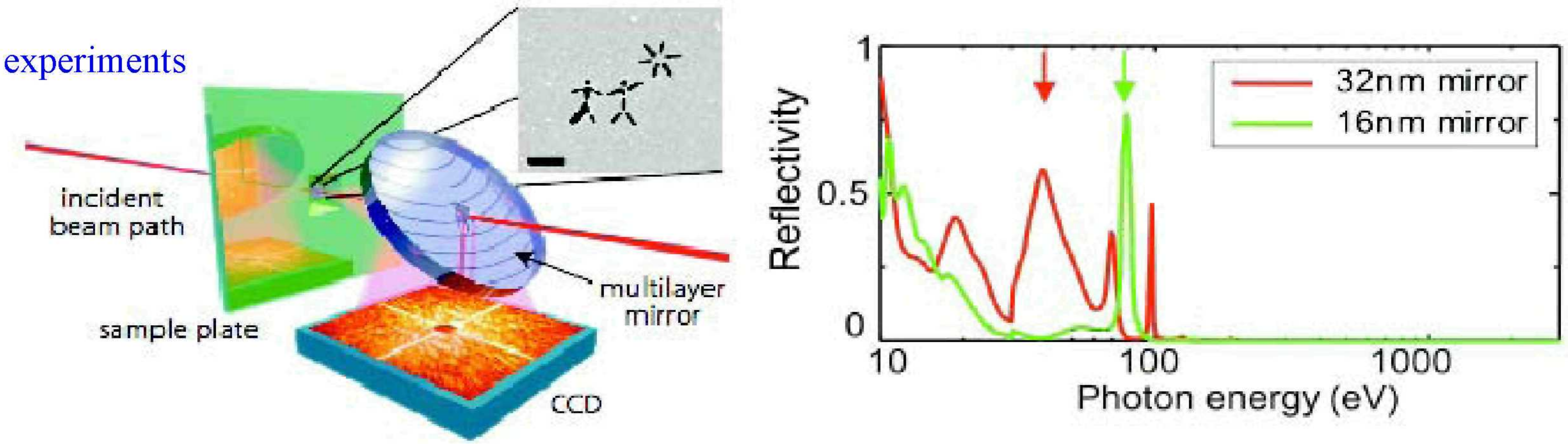

H.N. Chapman et al.; Nat. Phys. **2**, 839 (2006) and Physics Today, Jan 2007, pag. 19

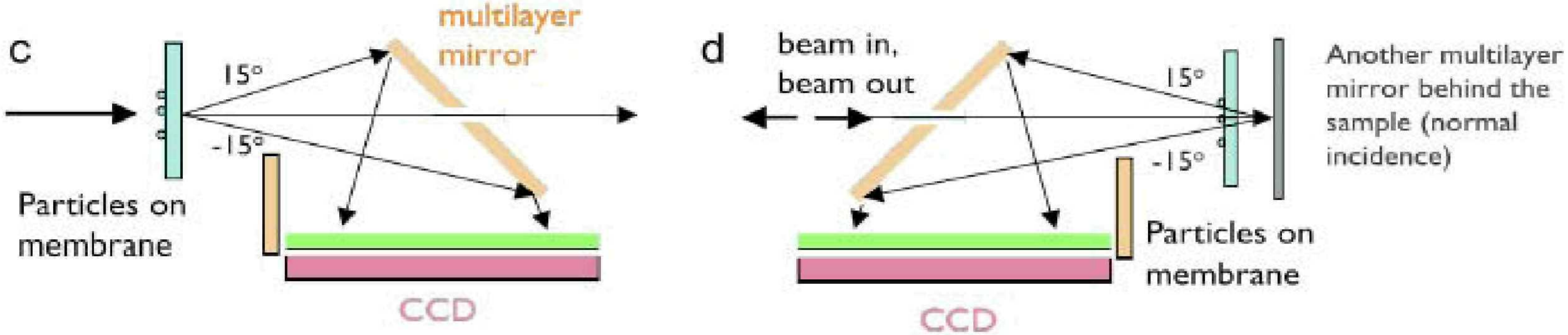

Fig. 1. Schematic of the diffraction camera for FLASH, which uses a multilayer-coated mirror to reflect the on pattern onto a CCD. (a) The configuration shown is for the measurement of diffraction from silicon nitride test objects. (b) Plots of the reflectivity of the mirror on axis, as a function of photon energy, for mirrors made for the first harmonic (32 nm) and second harmonic (16 nm). (c) Schematic for forward scattering, and (d) schematic for pump-probe imaging where the beam is reflected back onto the sample with a normal-incidence multilayer mirror. A foil filter (green) and light shield (beige) are also shown.

Ultrafast coherent imaging at Fermi

Spokesperson: H. Chapman (LLNL-CA) , J. Haidu (Stanford University and Uppsala University)

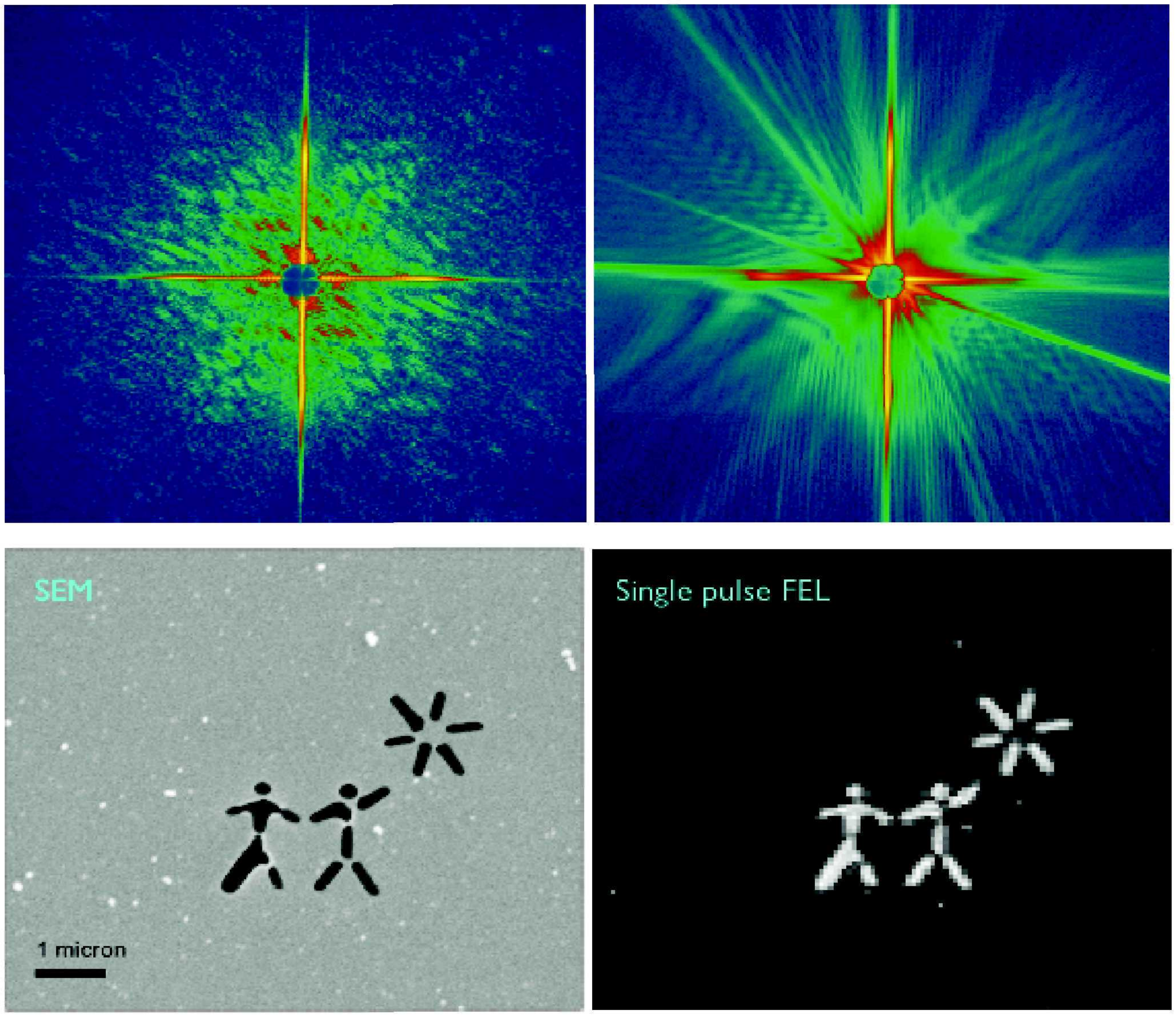

Defining the first experiments with FERMI@Elettra

CELLS INJECTED INTO THE FEL BEAM:
1st EXPERIMENTS ON LIVE PICOPLANKTON

J.Hajdu and H. Chapman

Procedure:

1. Take cells from solution
2. Introduce them into the beam
3. Hit them with the XFEL pulse and record diffraction pattern

Challenges:

1. Particle concentration
2. Keeping cells alive and in the “native” state
3. Diagnostics: How do we know if a hit was good?

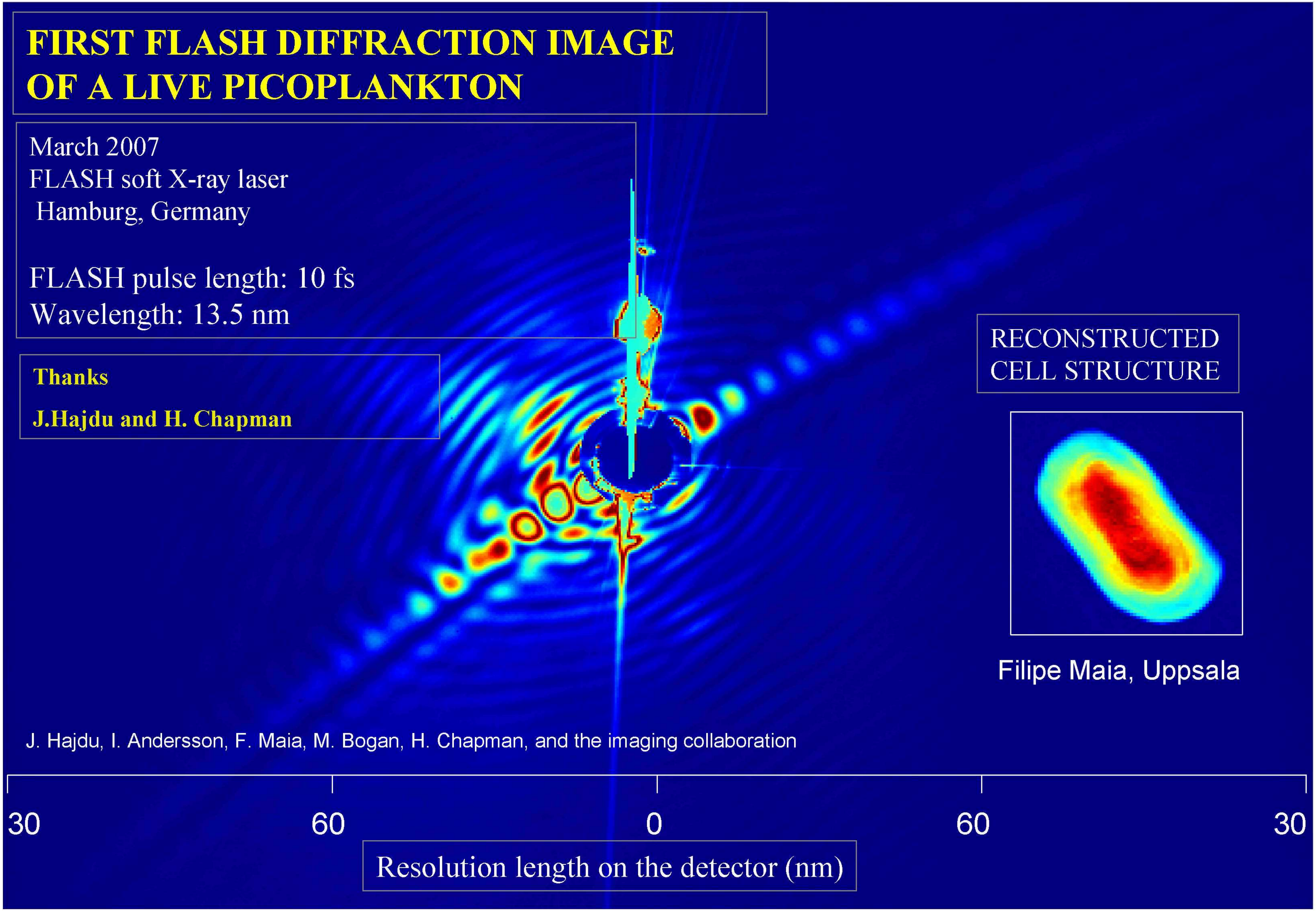
FIRST FLASH DIFFRACTION IMAGE
OF A LIVE PICOPLANKTON
March 2007
FLASH soft X-ray laser
Hamburg, Germany
FLASH pulse length: 10 fs
Wavelength: 13.5 nm
Thanks
J.Hajdu and H. Chapman
RECONSTRUCTED
CELL STRUCTURE
Filipe Maia, Uppsala
J. Hajdu, I. Andersson, F. Maia, M. Bogan, H. Chapman, and the imaging collaboration
30
60
0
60
30
Resolution length on the detector (nm)

FLASH-DIFFRACTIVE IMAGING - EXPECTED PRIMARY IMPACT

NON-CRYSTALLINE STRUCTURES IN THE MICROMETRE TO NANOMETRE SIZE DOMAIN

2D STRUCTURES FOR NON-REPRODUCIBLE OBJECTS

3D STRUCTURES FOR REPRODUCIBLE OBJECTS

4D STRUCTURES IN ATTOSECOND - FEMTOSECOND TIME-RESOLVED EXPERIMENTS

J.Hajdu and H. Chapman

Ultrafast processes and imaging of gas phase clusters and nanoparticles
Spokespersons: **T. Möller, C. Bostedt (TU-Berlin)**
Co-proponents: P. Milani, University of MilanoJ.
Hajdu, University of Stanford and University of Uppsala H.N. Chapman, LLNL, Livermore

Scattering and Imaging

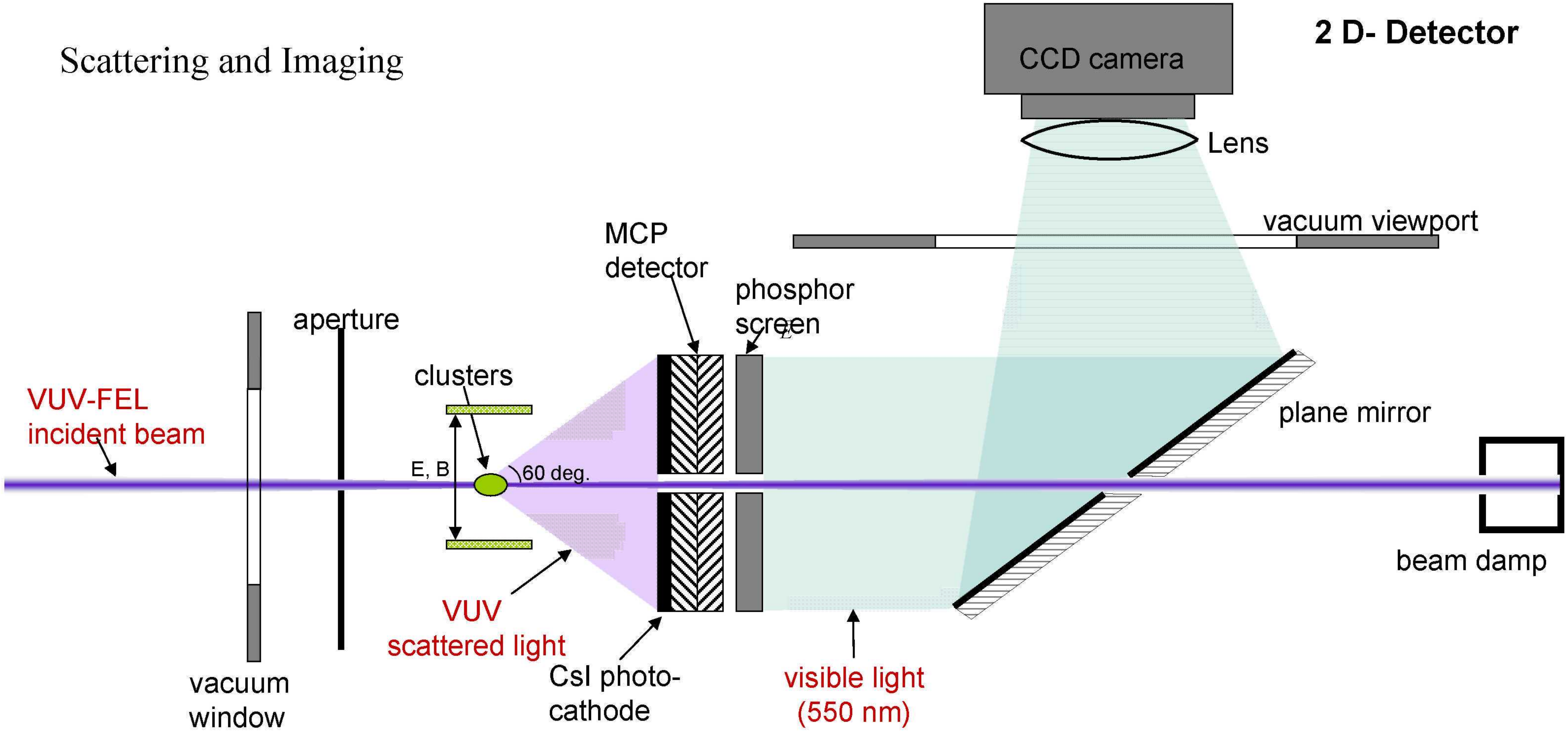

Ultrafast processes and imaging of gas phase clusters and nanoparticles
Spokespersons: **T. Möller, C. Bostedt (TU-Berlin)**
Co-proponents: P. Milani, University of MilanoJ.
Hajdu, University of Stanford and University of Uppsala H.N. Chapman, LLNL, Livermore

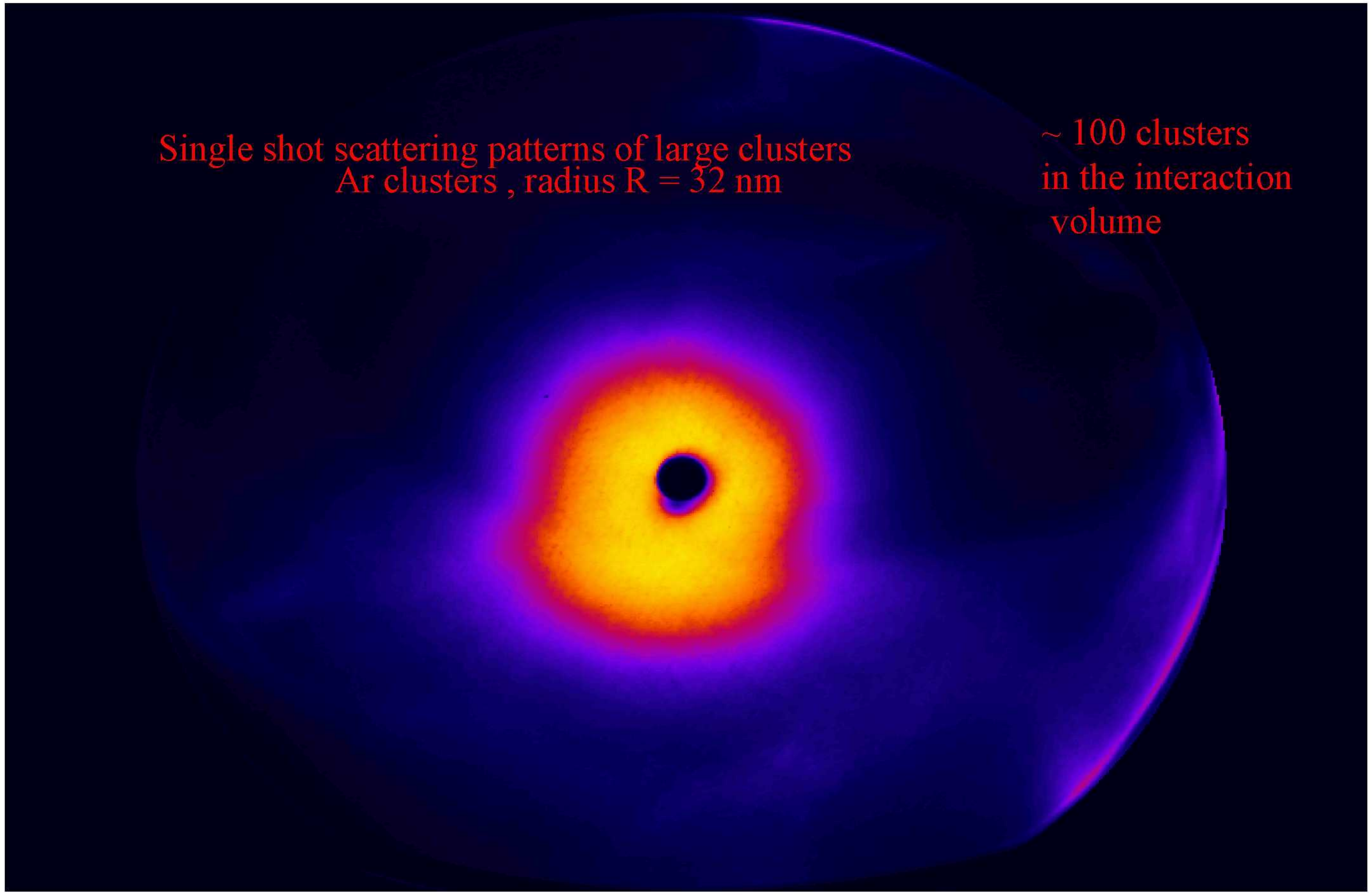

Clusters stay intact during exposure (30 fs), ΔR< 3Å

February 2006

Coherent scattering on FePd magnetic stripes

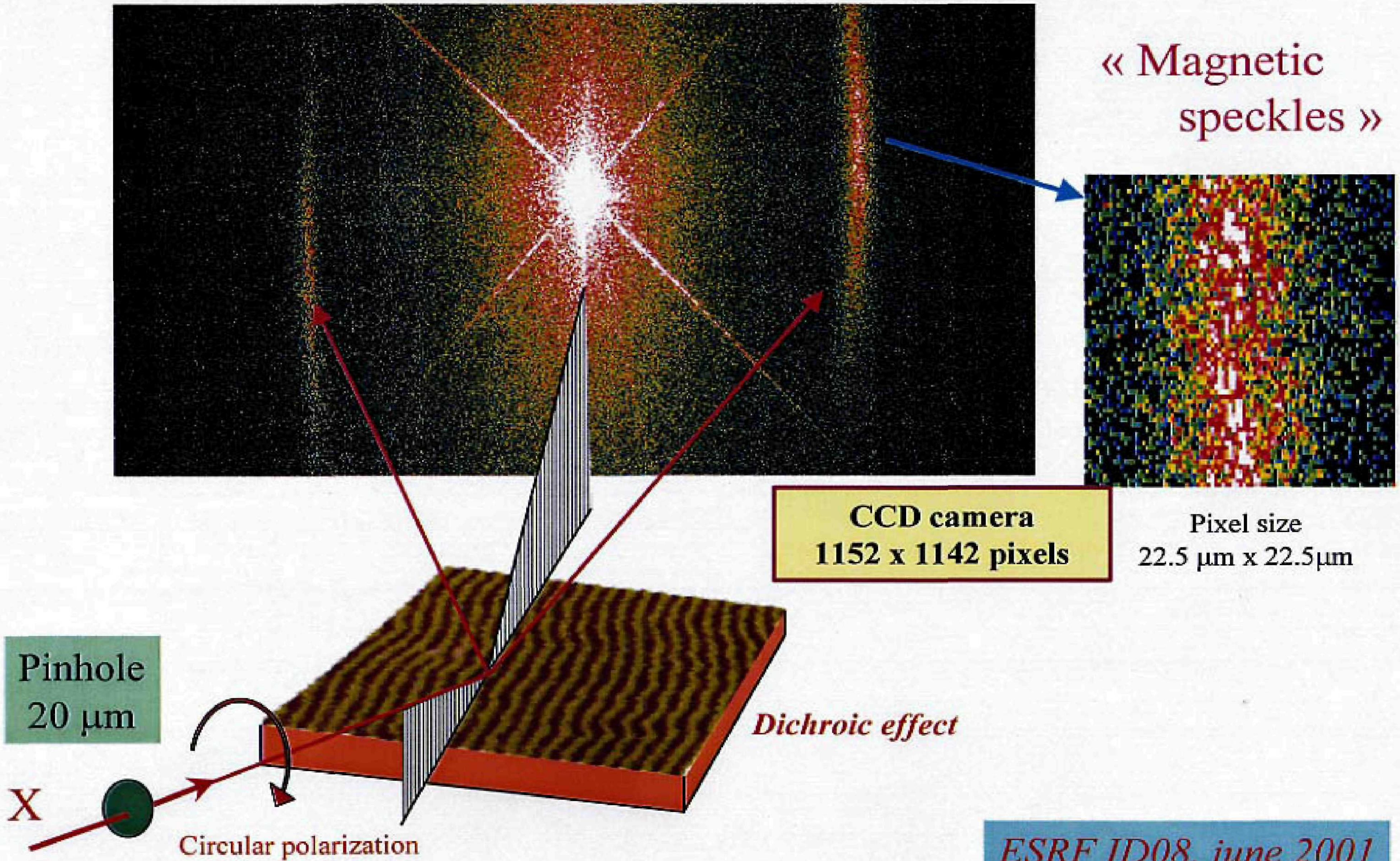

ESRF ID08, june 2001

Available Instruments to measure Collective Excitations

$S(Q,\omega) \rightarrow$ Dynamic Structure Factor

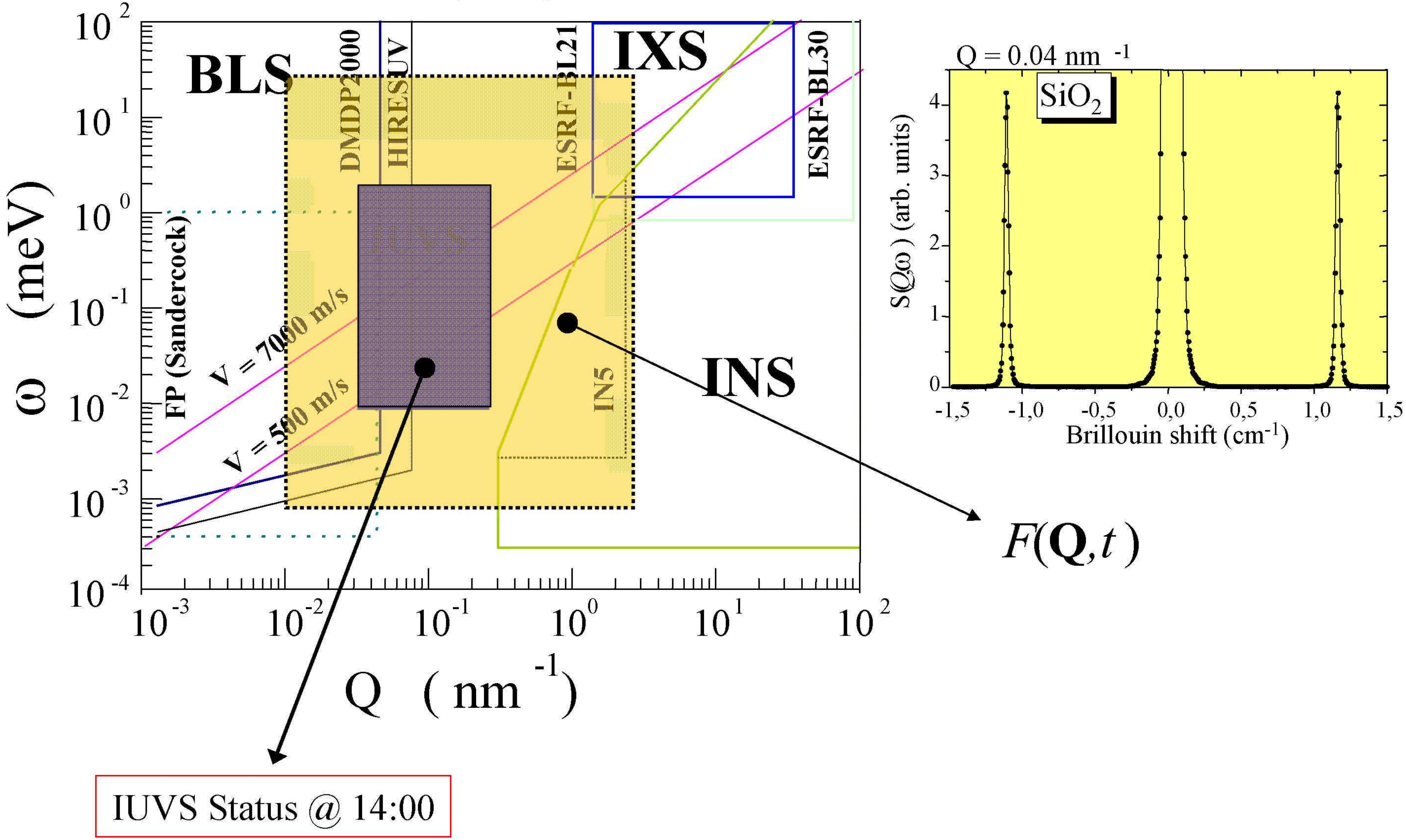

Transient Grating Spectroscopy at the Nanoscale

Liquids - Fluids

- Transition from the Hydrodynamic to the Kinetic regime in Simple liquids and fluids.
- Effect of the Local Structure on the Relaxation Dynamics of Molecular liquids and H-bonded liquids.
- Sound Bifurcation in Gas Mixtures
- Thermal Relaxation Dynamics in Liquid Metals.

Glasses

- Relaxational Processes in Super-Cooled liquids and their relation to the Glass Transition.
- Vibrational and Relaxational Low Temperature Properties of Fragile and Strong glasses.
- Characteristic Length of the Disorder

Surface Dynamics

- Transverse Dynamics in Liquids.
- Phase Transition in thin Films.

Polymers

- Structural Relaxations.
- Shear and Density Fluctuations.

R. I. Tobey et al., APL 2006

Cluster and nanoparticle spectroscopy

Spokespersons: **F. Stienkemeier, B. von Issendorff** (Univ. of Freiburg-D)
Co-proponents :K.Fauth (MPI- Stuttgart, D), M. Drabbels (EPFL- CH), M. Schmidt(CNRS –Orsay, Fr), U.Buck (MPI-Goettingen, D)

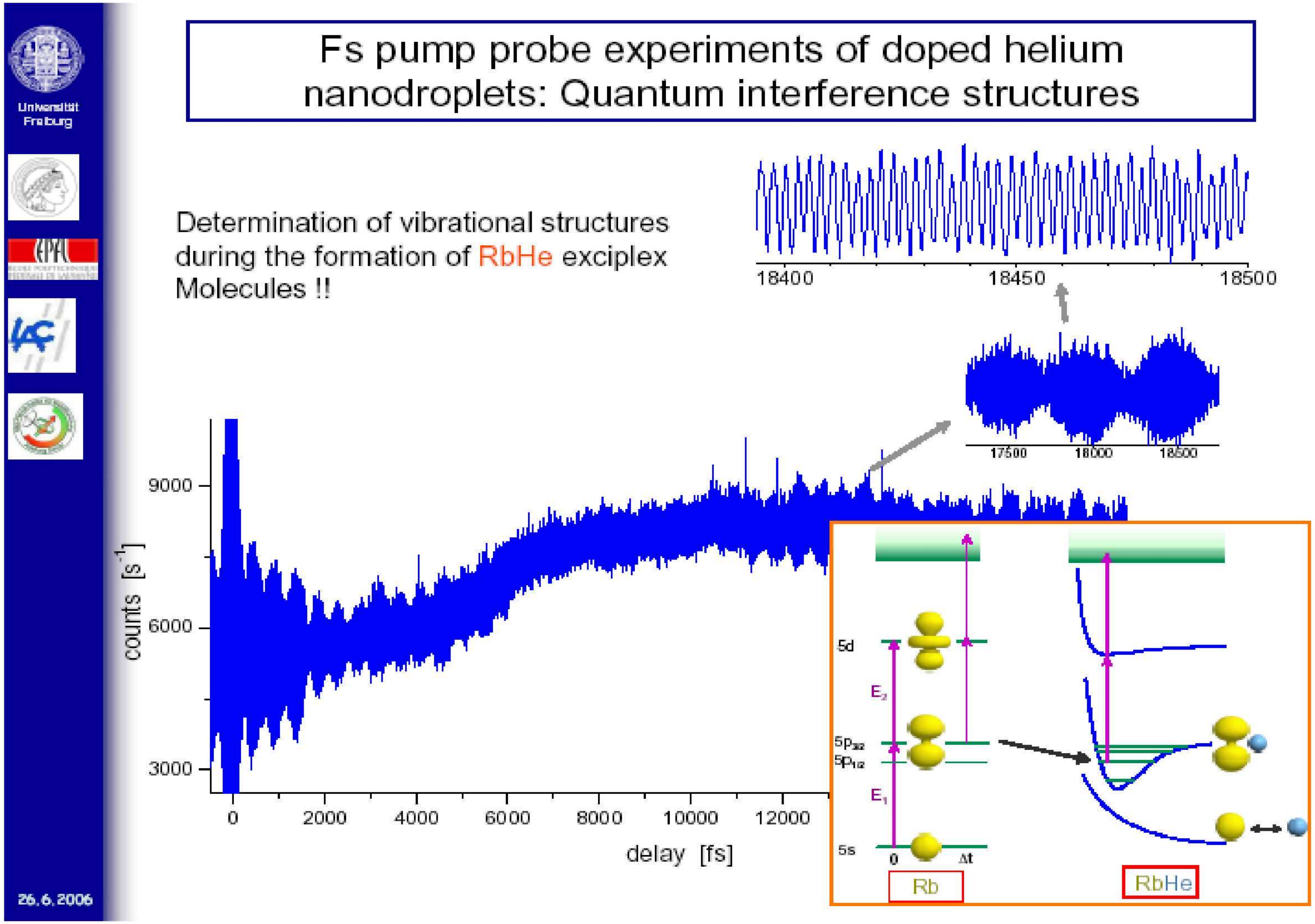

Cluster and nanoparticle spectroscopy

Spokespersons: **F. Stienkemeier, B. von Issendorff** (Univ. of Freiburg-D)
Co-proponents :K.Fauth (MPI- Stuttgart, D), M. Drabbels (EPFL- CH), M. Schmidt(CNRS –Orsay, Fr), U.Buck (MPI-Goettingen, D)

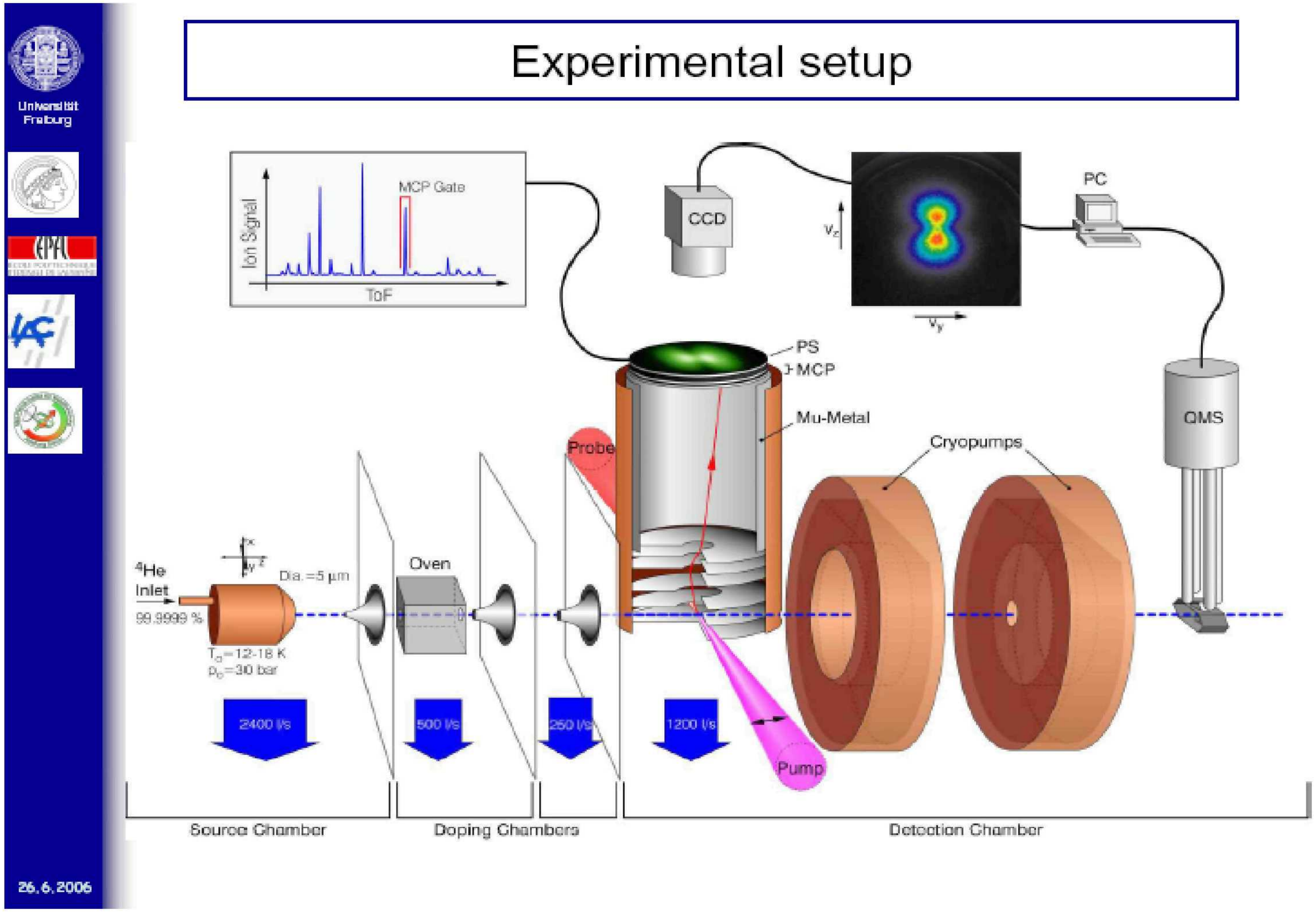

Selective excitations (CT and phonons) to study transient states and photo-induced phase transitions.
Superconductors (e-ph interactions, magnetism and superconductivity).
Magnetic materials (dynamics of the magnetic excitations).
Strong correlations in hard- and soft- condensed matter

(charge transfer and phonon assisted excitations).

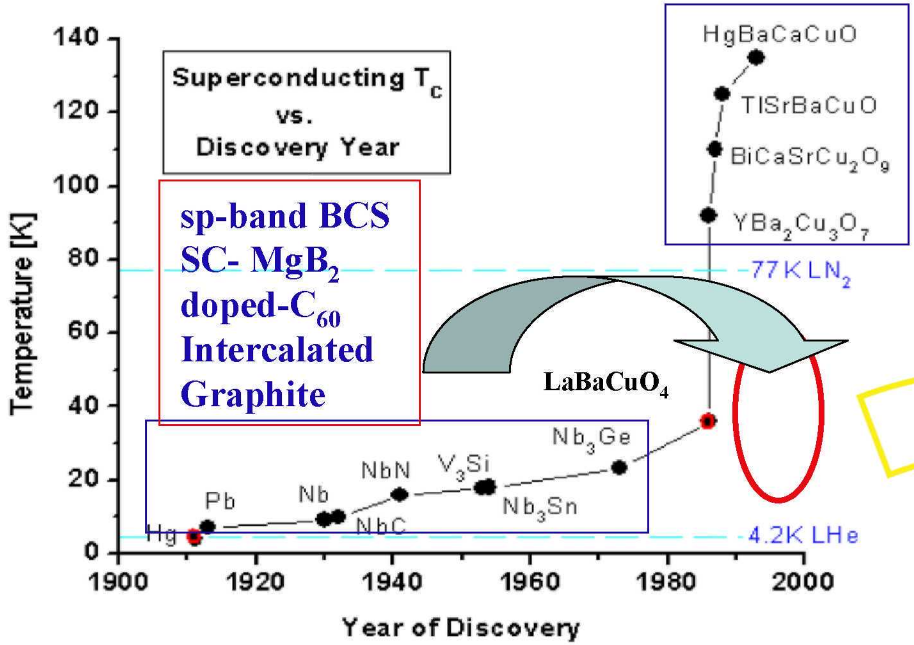

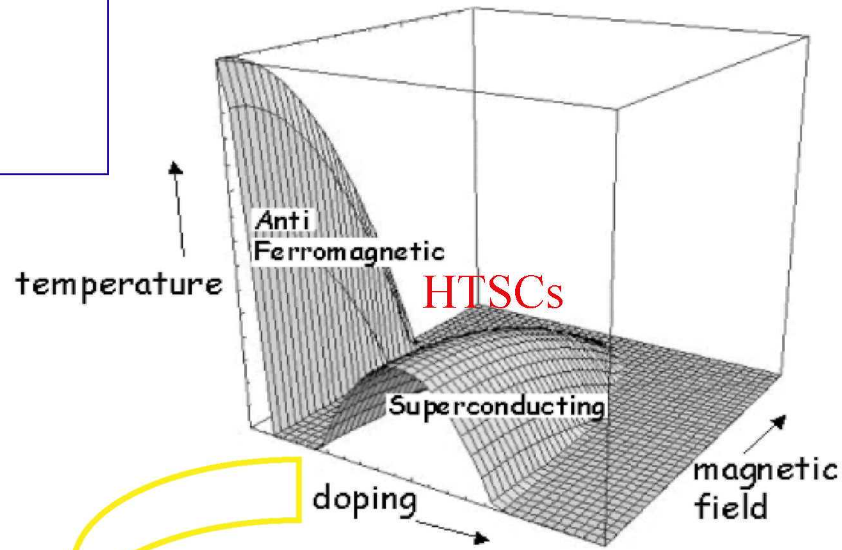

e-ph

?

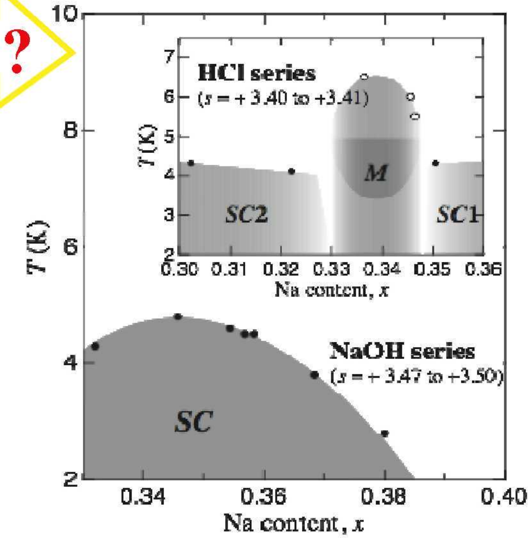

$$\lambda_{\nu\mathbf{q}} \equiv \frac{1}{\pi N(0)} \frac{\gamma_{\nu\mathbf{q}}}{\omega^2_{\nu\mathbf{q}}}. \qquad N_n(0) \equiv \sum_{\mathbf{k}} \delta(\varepsilon_{n\mathbf{k}})$$

$$\frac{\gamma_{\nu\mathbf{q}}}{\omega_{\nu\mathbf{q}}} = 2\pi \sum_{nm\mathbf{k}} |g_{\nu,\, n\mathbf{k},\, m(\mathbf{k}+\mathbf{q})}|^2 \delta(\varepsilon_{n\mathbf{k}}) \delta(\varepsilon_{m\mathbf{k}+\mathbf{q}}).$$

$$g_{\nu,n\mathbf{k},m(\mathbf{k}+\mathbf{q})} = \langle n\mathbf{k} | \delta V(\mathbf{r}) | m(\mathbf{k}+\mathbf{q}) \rangle / \delta Q_{\nu\mathbf{q}}$$

Photo-induced and Magnetic Field-Dependent X-Ray Emission in Magnanites

Photo-induced and magnetic field-induced insulator-to-metal transition

Photo-induced isothermal magneto-structural phase transition and magneto-resistance

For H>5 Tesla, T< 30 K

QuickTime™ and a

nature Vol 449|6 September 2007|doi:10.1038/nature06119

LETTERS

Control of the electronic phase of a manganite by mode-selective vibrational excitation

Matteo Rini[1], Ra'anan Tobey[2], Nicky Dean[2], Jiro Itatani[1,3], Yasuhide Tomioka[4], Yoshinori Tokura[4,5], Robert W. Schoenlein[1] & Andrea Cavalleri[2,6]

QuickTime™ and a
TIFF (LZW) decompressor
are needed to see this picture.

D Aoki *et al.* 2001 Coexistence of superconductivity and ferromagnetism in URhGe, *Nature* **413** 613-616

T R Kirkpatrick et al. 2001 Strong enhancement of superconducting *T*c in ferromagnetic phases *Phys. Rev. Lett.* **87** 127003

C Pfleiderer *et al.* 2001 Coexistence of superconductivity and ferromagnetism in d band metal ZrZn2 *Nature* **412** 58-61

Superconductivity and Ferromagnetism

H vs T phase diagram for (H_2O) Cobaltites.
Open and closed circles represent T_c and magnetic ordering Temperature

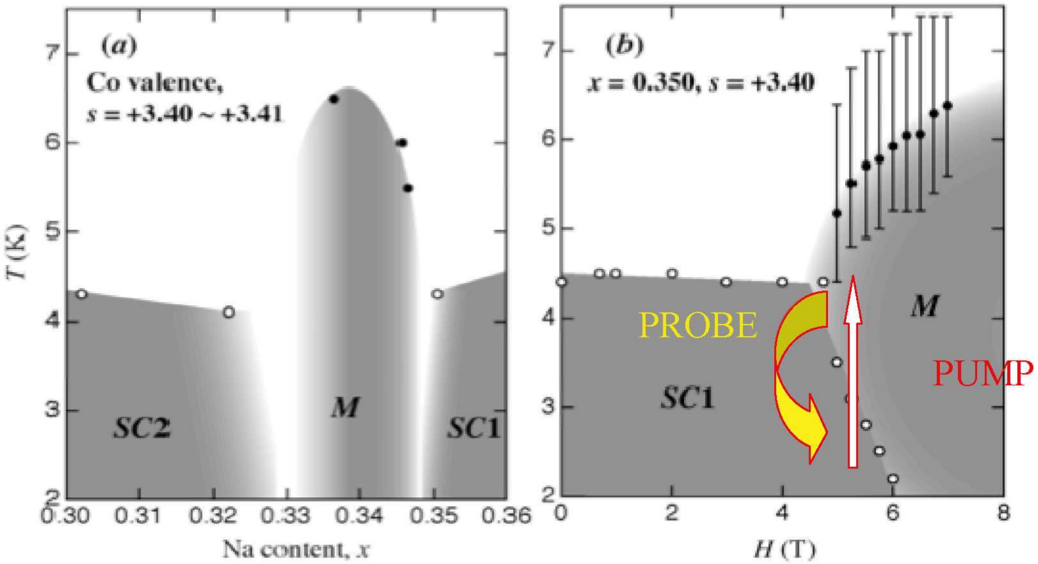

SUPERCONDUCTIVITY

A different class?

Coexisting superconductivity and ferromagnetism due to itinerant electrons is unusual, but even among them URhGe stands out. Its surprising behaviour could help reveal the underlying physics of ferromagnetic superconductors.

Gilbert G. Lonzarich
is in the Quantum Matter Group, Department of Physics, Cavendish Laboratory, J J Thomson Avenue, Cambridge CB3 0HE, UK.
e-mail: gl238@hermes.cam.ac.uk

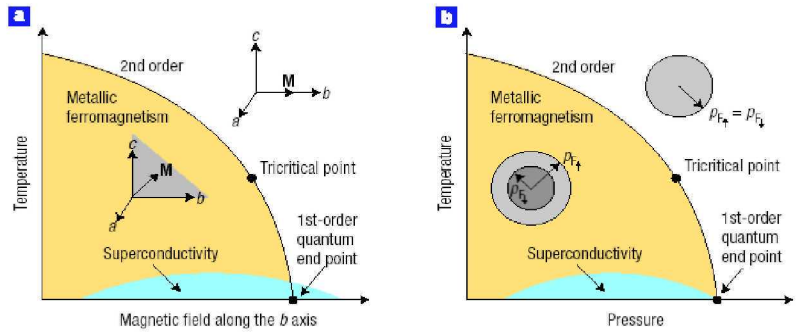

Figure 1 Schematic phase diagrams of the novel ferromagnetic superconductors URhGe, UGe_2 and UIr, close to first-order quantum end points. **a**, For URhGe, the solid line marks the magnetic transition between two spin-polarized states in which the magnetization **M** is aligned in different directions in the orthorhombic unit cell. The easy axis of magnetization is the *c* axis. The magnetic transition is second order (continuous) above the tricritical point and first order below the tricritical point. The value of the upper critical field along the *a* axis seems to diverge as the component of the magnetic field along the *b* axis is tuned towards the first-order quantum end point. This unprecedented behaviour is the key finding of Levy and colleagues[1]. **b**, The solid line in the temperature–pressure phase diagram marks a transition from a ferromagnetic state to a spin-unpolarized state (paramagnetic) in UGe_2 or UIr (metamagnetic transition lines are not shown). It is interesting that in all three itinerant-electron ferromagnets superconductivity is observed only in the spin-polarized state and electron pairing is therefore expected to be in spin-triplet *p*-wave states[5].

Nature, 2007

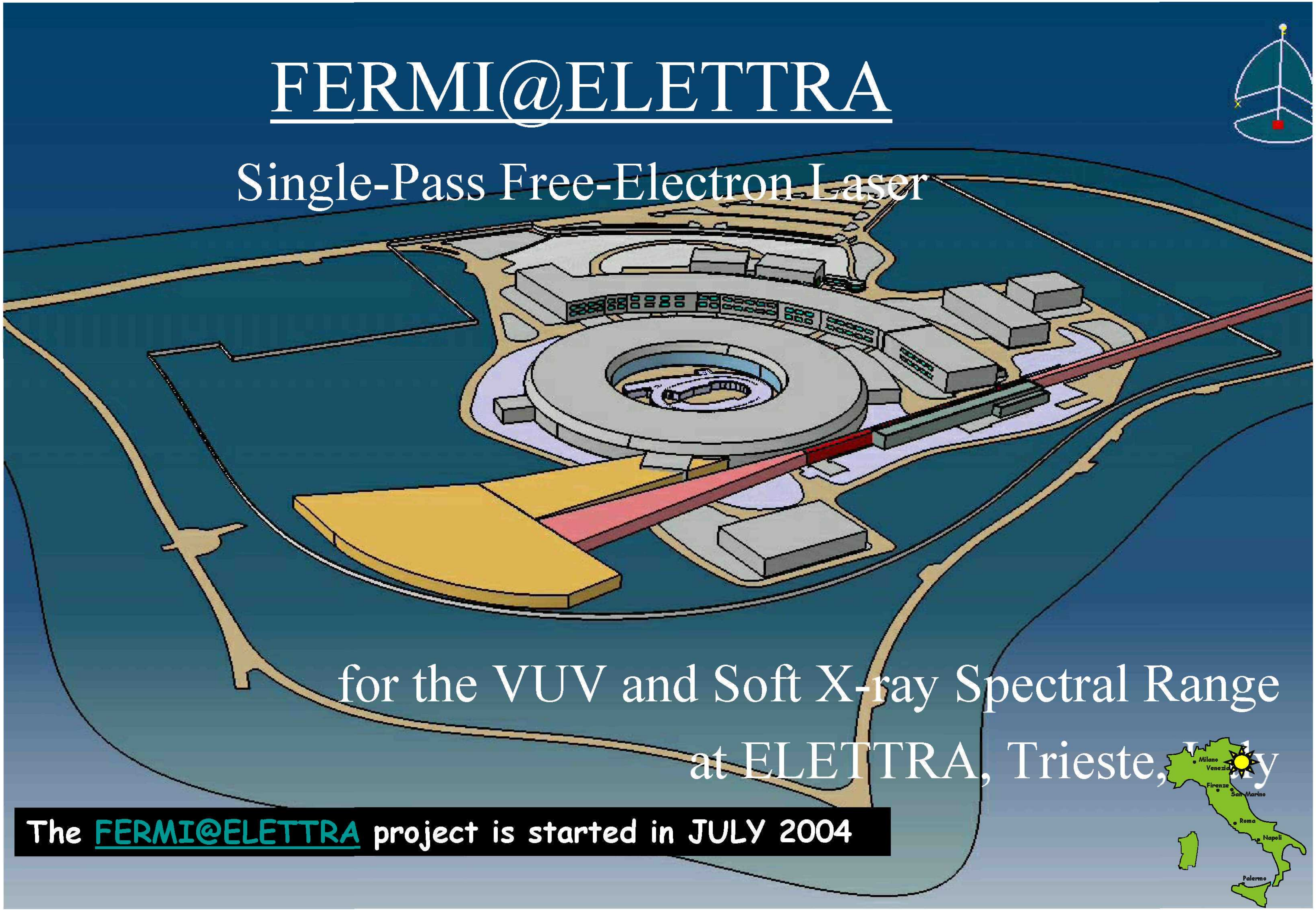
FERMI@ELETTRA
Single-Pass Free-Electron Laser
for the VUV and Soft X-ray Spectral Range
at ELETTRA, Trieste,
The FERMI@ELETTRA project is started in JULY 2004
Milano
Venezia
Firenze
San Marino
Roma
Napoli
Palermo

Joint Programme
for
Higher Education in Physics

University of Trieste - ICTP

The ICTP cooperates with the Faculty of Sciences of the University of Trieste in the education in physics of graduate students from Developing countries.

The cooperation concerns the "Laurea Magistralis in Fisica"

The "Laurea Magistralis in Fisica" can be compared to an advanced master in physics in the Anglo-Saxon system or to the last two years of the New European Educational System as fixed by the Bologna-Sorbonne agreement among the European Ministers of Education in the mid nineties.

ICTP announces that in 2008 a few scholarships and travel grants will be awarded to qualified, selected students from Developing countries in order to register and follow the training track in Condensed Matter Physics of the "Laurea Magistralis in Fisica" of the University of Trieste.

Each scholarship consists of: 800 Euro/month, travel grant, insurance and tuition fees.

The Programme covers two academic years

Courses are held in English

The minimum qualification for applicants is a degree equivalent to a M.Sc. (or an exceptionally good B.Sc.)

The selection of candidates will be based on their university record and academic recommendations.

More information at the web-page:

http://physics.units.it/didattica03/ICTPuniv.php